Neuroimaging Biomarkers in Paediatric Sickle Cell Disease

Jamie Michelle Kawadler, BA MSc

A thesis submitted to University College London

for the degree of

Doctor of Philosophy in Neuroimaging

Developmental Imaging & Biophysics Section

University College London Institute of Child Health

March 2015

I, Jamie M. Kawadler, confirm that the work presented in this thesis is my own. Any information derived from other sources has been indicated in the thesis.

_____

Acknowledgments

I would like to sincerely thank my supervisors, Chris Clark and Fenella Kirkham, who have guided me through the PhD with encouragement and enthusiasm. Both are equally brilliant academics – I couldn't say how much I have learned in the past three years!

More thanks go out to members past and present of the ICH Developmental Imaging & Biophysics Section for their unwavering support; in particular Jon Clayden for all the R tutorials and statistical advice, and Patrick Hales for the endless cups of tea.

I would like to thank the haematologists and neuroradiologists kind enough to collaborate with us during the project: Paul Telfer, Olu Wilkey, Andrew Robins, Simon Barker, Tim Cox and Dawn Saunders.

Very many thanks to Tina Banks and Wendy Norman, wonderful Great Ormond Street Hospital radiographers, who sacrificed their Saturdays with me to scan children who we did not want to miss school. Also thanks to fellow students Emma Seymour, Michelle Downes, Matt Hollocks, Rosy Edey and Olivia Wollenberg for their help with neuropsychological testing.

I would like to acknowledge studentship funding from UCL Grand Challenges.

I wish to thank the patients and their families who took part in the study, without whom this project would not have been possible.

Endless thanks to my family for supporting me through nearly a decade of education, and giving nothing but support and love even when I chose to live so far away from home.

Finally, thank you to James, for everything.

Abstract

Sickle Cell Disease (SCD) is a collection of genetic haemoglobinopathies, the most common and severe being homozygous sickle cell anaemia. In the UK, it has been estimated that 1 in 2000 children are born with SCD.

The disease is characterised by chronic anaemia, recurrent pain crises and vascular occlusion. Neurologically, there is a high incidence of stroke in childhood, as well as cognitive dysfunction. Newborn screening programmes and preventative treatments have allowed a much longer lifespan; however recently, neurological research has shifted to characterising subtler aspects of brain development and functioning that may be critically important to the individual's quality of life.

This thesis overviews the neurological and neurocognitive complications of SCD, and how magnetic resonance imaging (MRI) can provide biomarkers for severity of disease. During the PhD, retrospective and prospective cognitive and MRI data were collected and analysed. Diagnostic clinical MRI sequences and advanced MRI sequences were applied, as well as a neuropsychological test battery aimed at intelligence and executive function.

First, this thesis reviews the intelligence literature in SCD and includes previously unreported data, finding patients, regardless of abnormality seen on conventional MRI, have lowered full-scale intelligence quotient than controls. Then, to determine imaging biomarkers, volumetric differences and diffusion characteristics were identified. Patients were found to have decreased volumes of subcortical structures compared to controls, in groups corresponding to disease severity. Results from a three-year longitudinal clinical trial suggest evidence of atrophy in paediatric patients, with no apparent protective effect of treatment. Diffusion tensor imaging revealed reduced white matter integrity across the brain, correlating with recognised markers of disease severity (*i.e.* oxygen saturation and haemoglobin from a full blood count).

Overall, the four experiments bridge a gap in the cognitive and neuroimaging literature of the extent of neurological injury in children with SCD.

Table of Contents

List of Figures

List of Tables

Abbreviations

Sickle cell disease (SCD)

- **HbSS** or **SCA** – Homozygous sickle cell anaemia
- **Hb** – Haemoglobin
- **RBC** – Red blood cell
- **HbA** – Haemoglobin A (normal haemoglobin gene)
- **HbS** – Sickle haemoglobin (haemoglobin variant gene)
- **ISC** – Irreversible sickled cell
- **HbF** – Foetal haemoglobin
- **HbSC** – Haemoglobin C disease
- **HbAS** – Sickle cell trait (heterozygous inheritance genotype)
- **SCI** – Silent cerebral infarction
- **ASCIE** – Acute Silent Cerebral Ischaemic Event

Cohort Studies and Trials

- **CCSCD** – Cooperative Study in Sickle Cell Disease (USA)
- **STOP** – Stroke Prevention Trial in Sickle Cell Anemia (USA)
- **SIT** – Silent Infarct Transfusion trial (USA + Europe)
- **POMS** – Prevention of Morbidity in Sickle Cell Anemia
- **SAC** – Sleep Asthma Cohort (USA + UK)

Neuroimaging

- **MRI** – Magnetic resonance imaging
- **MRA** – Magnetic resonance angiography
- **TCD** – Transcranial Doppler ultrasound
- **T** – Tesla
- **RF** – Radiofrequency

- **TE** – echo time
- **TR** – repetition time
- **SE** – Spin-echo MRI sequence
- **GE** – Gradient-echo MRI sequence
- **FLASH** – Fast Low-Angle Shot (T1-weighted sequence)
- **FLAIR** – Fluid-attenuated inversion recovery (T2-weighted sequence)
- **DWI** – Diffusion-weighted Imaging
- **ADC** – Apparent Diffusion Coefficient
- **DTI** – Diffusion tensor imaging
- **FA** – Fractional Anisotropy
- **MD** – Mean Diffusivity
- **AD** – Axial Diffusivity
- **RD** – Radial Diffusivity
- **FSL** – Functional MRI of the Brain Software Library (Oxford, UK)
- **SIENA** – Structural Image Evaluation using Normalisation of Atrophy
- **CBF** – Cerebral blood flow
- **fMRI** – Functional MRI
- **BOLD** – Blood-oxygen level dependent (effect)

Neuropsychology

- **IQ** – Intelligent Quotient
- **FSIQ** – Full-Scale Intelligence Quotient
- **WASI** – Wechsler Abbreviated Scale of Intelligence
- **WISC** – Wechsler Intelligence Scale for Children
- **WAIS** – Wechsler Adult Intelligence Scale
- **D-KEFS** – Delis-Kaplan Executive Function System

Chapter 1. Introduction to Sickle Cell Disease

1.1 Key Triad of Clinical Manifestations

1.1.1 Irreversibly Sickled Cells

Haemoglobin is an iron-containing oxygen-transport protein in red blood cells (RBCs) of humans. Normal haemoglobin A (HbA) has a globular shape, and is formed from two α and two β globin protein chains together with four haem entities. The inherited sickle haemoglobin (HbS) gene is a variant of normal HbA, formed from a single amino acid point mutation (glutamic acid → valine) at position 6 of the β globin molecule[1]. Normal haemoglobin transports oxygen to the body's tissues; however, HbS has less affinity for oxygen than normal haemoglobin[2] and when oxygen is released in RBCs containing HbS, the haemoglobin molecules polymerise into dense, elongated sickled cells.

The process is irreversible, and even when re-exposed to oxygen, the membrane cannot return to normal shape[1]. The irreversible sickling cells (ISCs), after which the disease is named, is the essential underpinning of the sickle cell disease pathology – notably haemolytic anaemia, vaso-occlusion and recurrent pain crises (Figure 1-1).

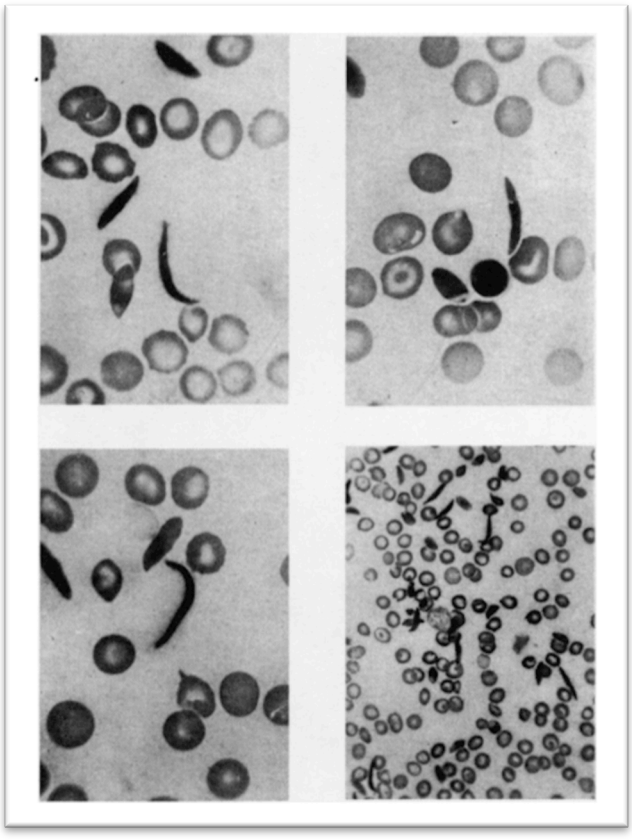

Figure 1-1. Blood sample photomicrographs from the first description of sickle cell disease in 1910, clearly showing elongated sickle-shaped red blood cells[3].

1.1.2 Vasoocclusion and Vasculopathy

Vaso-occlusion and chronically impaired blood flow constitute the basis for the most life-threatening clinical aspects of SCD, including overt and silent strokes, acute chest syndrome, pulmonary hypertension, kidney damage and the most frequent event, acute painful crises.

There is direct evidence that ISCs are responsible for vaso-occlusion; genotypes that have greater clinical severity (*i.e.* more vaso-occlusive events) also have higher intracellular concentrations of HbS, and HbS polymerisation is an integral risk for vaso-occlusion[4]. However, it is also clear that large vessels are involved in the process[5] and the pathogenesis of vaso-occlusion is most likely multifactorial. Under different circumstances, secondary mechanisms, such as inflammation and molecular factors affecting blood coagulation and RBC adherence to the endothelium, probably play a role. Figure 1-2 shows the mechanisms for a range of possible factors that may contribute to vascular occlusion in SCD, as well as potential outcomes due to chronic vaso-occlusion.

Vasculopathy is a prominent feature in SCD, involving several organs[6,7]. The most commonly affected areas are medium and large vessels of the spleen[8], umbilical vessels[9], pulmonary arterial tree[10] and circle of Willis[11], resulting in the following serious complications, respectively: autosplenectomy[12], growth restriction[13], pulmonary disease[14] and ischaemic stroke[15].

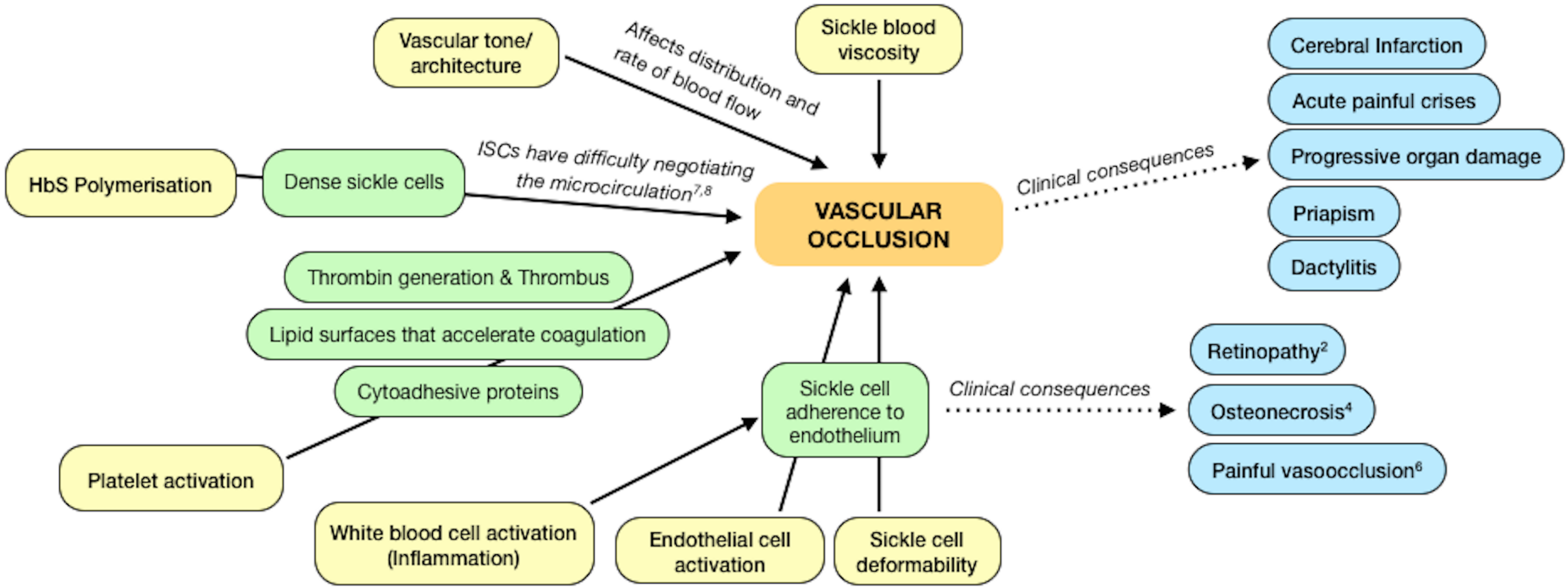

Figure 1-2. Physiological processes that lead to vascular occlusion and clinical outcomes. Although the β haemoglobin gene mutation directly affects HbS polymerisation, other molecular processes such as platelet activation and inflammatory responses can affect endothelial abnormalities and contribute to progressive vasculopathy. Vaso-occlusion can occur in other organs other than the brain, and some common clinical consequences of these events are retinopathy[16], osteonecrosis of the femoral head[17,18], and painful crises[19].

1.1.3 Haemolytic Anaemia

Haemolytic anaemia is a life-long condition in those with SCD. Haemolysis is the breakdown of RBCs; anaemia develops because the destruction of RBCs exceeds the rate of RBC production from bone marrow, and the manner in which the RBC disintegrates allows molecules containing iron into the bloodstream. Other features of haemolytic anaemia include decreased haemoglobin and haematocrit, increased reticulocyte (*i.e.* young RBC) count and decreased RBC life spans[20–22].

In those with SCD, anaemia is not present at birth, but develops as foetal haemoglobin (HbF) levels decrease and simultaneously HbS synthesis increases. HbS polymerises on de-oxygenation and initially may recover to a globular shape on re-oxygenation; but as the RBC containing HbS ages, the HbS remains in a polymerised state and the cell becomes irreversibly sickled. The RBC membrane is then more likely to break down so that the contents are released into the circulation and the RBC is broken down by the spleen.

The relationship between the amount of ISCs in the blood and the haemolytic rate has been found to be significant[23,24]. The percentage of ISCs does correlate with the degree of haemolysis and the level of anaemia in general; however, the degree of anaemia is not consistent among individuals of the same genotype. Even within the same individual, anaemia severity will vary, suggesting that other mechanisms are involved in mediating the production of reticulocytes as well as the degree of haemolysis. Aplastic crises, due to a temporary cessation in RBC production (*e.g.* secondary to infection with parvovirus), and acute splenic sequestration crises, due to acute intrasplenic trapping of blood, are the most common triggers to exacerbate chronic anaemia with an acute fall in haemoglobin[25].

1.1.4 Recurrent Painful Episodes

The acute painful crisis is the third of the cardinal clinical manifestations of SCD, and also the most frequent reason for hospital admission[26,27]. The only reliable characteristic of sickle cell recurrent pain is its variability. The frequency, location, duration, severity and character of pain is unpredictable and variable within and among patients[27]. The pain spectrum is vast; in regard to location, it may be localised, migratory or diffuse[1], could last hours to weeks, and anywhere from mild to excruciating in intensity[28]. One study reported that a typical crisis in an adult is approximately 10.3 days[29]. Children and families are taught to manage mild pain with rest, hydration and prescribed analgesics, as well as to recognise signs of an upcoming crisis that requires hospitalisation.

It is thought that vaso-occlusive ischaemia, inflammation and infarction are responsible for initiation of a painful crisis[30] on the background of chronic haemoglobin oxygen

desaturation[31]. The combination of hypoxia, reperfusion injury and the cycle of ischaemic tissue damage and inflammation makes sickle cell pain unique[32]. Relative anaemia may predict pain in children; however in adults the frequency of painful crises varies directly with haemoglobin level and inversely with percentage of HbF[19]. In fact, babies as young as 6 months may experience this pain in the context of HbF decline[1].

Chronic pain in SCD can result from a number of conditions, including bone infarction, avascular necrosis of joints, leg ulcers and chronic osteomyelitis; like other chronic pain conditions, sickle cell pain associated with distress and reduced quality of life[33]. In children, frequent hospitalisations result in school absences, notably affecting academic achievement[34]. Post-traumatic stress has been described in children with history of frequent painful crises and their parents[35]. Treatment with hydroxyurea reduces the frequency of painful episodes in children[36] as well as adults[37], and cognitive and behavioural therapies, as well as early detection of school difficulties, have shown potential in children to improve ability to cope with pain[38] and improve quality of life.

1.1.5 Other Complications

SCD manifests as a diverse multisystem disorder. Chronic effects of the three hallmarks of SCD have a major impact on childhood mortality rate in developed[39] as well as developing countries[40], and affects lifelong health. The median age of death is in middle age in the developed world, but even now, mortality in childhood is around 7% in the USA[39] although it appears to be lower (around 1%) in the UK[41].

Exacerbations of the chronic anaemia can affect not only the brain[42], but also may be involved in chronic renal insufficiency[43] and in rare cases, liver function[44]. The spleen functions poorly in SCD; splenic enlargement may follow sequestration and splenic infarction secondary to vaso-occlusion typically occurs in early life. Pulmonary abnormalities can also lead to serious illness and death, and include recurrent acute chest syndrome, occurring in 15-43% of patients[45], sickle cell chronic lung disease[46] and pulmonary hypertension[10,14]. Priapism, or persistent, painful swelling of the penis, is also common in males[47]. Dactylitis, or painful inflammation of a digit occurs in infants[48], and is often a prequel to recurrent painful episodes, although whether it predicts severe disease is controversial[49]. Microvascular vaso-occlusion and blockage of microcirculation can, in addition to causing pain directly, affect bone marrow, leading to bone infarction and predisposition to osteomyelitis[50–52]. Often the long bones, ribs, sternum, vertebrae and pelvic bones are affected; a common clinical feature is osteonecrosis of the femoral heads of the hips and humeral heads of the shoulders[17,18].

1.2 Epidemiology

SCD was familiar to people living in Africa long before the first documented patient in 1910[3]. It was called by different ancient tribal names[53] and perhaps with different semantic denominations attributed to wide variety of symptoms, rather than a single entity[54]. The Igbo of southeastern Nigeria believed that children who suffered poor health and died typically before 5 years were later reborn to the same family and destined to die again, repeating the cycle. These 'reincarnate children' were described as having suffered growth retardation, recurrent febrile illnesses, convulsions, body aches and pains, protuberant abdomen and yellow eyes – most likely caused by sickle cell anaemia[55].

1949 was an important milestone in SCD research. In a seminal paper, Pauling and colleagues[56] were the first to demonstrate chemical differences and the presence of HbS in healthy people, carriers and patients, deeming SCA the first molecular disease. Also in that year, Neel described the homozygous Mendelian inheritance pattern in the disease[57] after much uncertainty of the link between sickle cell trait (one copy of HbS gene) and sickle cell anaemia (two copies of HbS gene). Not until 1957 was the mutant HbS gene identified on a molecular basis and sequenced[58].

HbS is most extensively distributed in equatorial regions of the developing world. The umbrella term of sickle cell disease includes the most prevalent genotype HbSS, or homozygous sickle cell anaemia, but also includes genotypes in which HbS is inherited with other haemoglobin variants: haemoglobin C (HbSC), HbS-thalassaemias (*e.g.* HbSβ^0-thalassaemia and HbSβ^+-thalassaemia) and other much rarer genotypes such as hereditary persistence of foetal haemoglobin, O Arab, D Punjab, and S Antilles. SCA and HbSβ^0-thalassaemia are the most clinically severe genotypes, while HbSC disease and HbSβ^+-thalassaemia, although relatively common in some parts of the World (West Africa and Greece, respectively), are usually milder in children[59].

1.2.1 Connection with Malaria

In the 1950s, reports of populations with high HbS frequencies in Africa observed strikingly fewer numbers of people homozygous for HbS (HbSS) than heterozygous for HbS, or those that carry one normal haemoglobin A gene and one sickle haemoglobin S gene (HbAS)[60,61]. Those who were heterozygous for HbS (*i.e.* with HbAS, commonly called sickle cell trait) appeared to have some sort of protection against malaria, and had some selective survival advantage[1,62].

The 'malaria hypothesis' was recently strengthened[63] by showing a strong geographical link on a global scale between frequencies of HbS alleles in the population and high malaria endemicity (Figure 1-3). Evidence has been established for partial resistance for haemoglobin variant carriers, specifically sickle cell trait, to *Plasmodium falciparum* malaria[64,65]. The mechanism of the protective effect of sickle cell trait against malaria has been widely debated. However, several epidemiological studies support the hypothesis that HbS is protective by restricting disease progression, so that parasitic infections less often progress to evident symptoms because HbS cells limit ability of parasites to grow and multiply[66,67], or by early parasitic removal from the circulation[64].

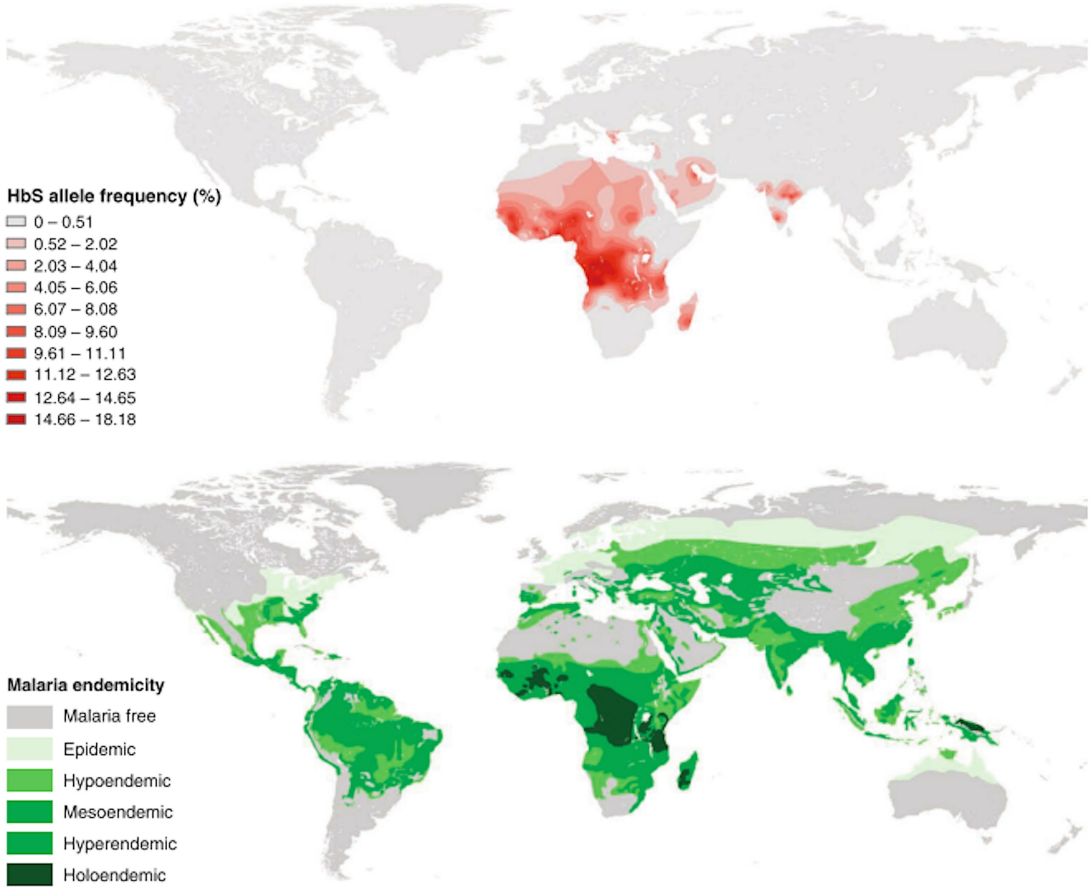

Figure 1-3. Global distribution of the HbS gene. Piel and colleagues[63] provide evidence for the 'malaria hypothesis' by linking the frequency of HbS allele (top panel) and historical map of malaria endemicity[68] and classes of parasite infection rates in children aged 2-10 years (bottom panel).

1.2.2 Prevalence

Because of the link to regions of high malaria prevalence, many people carrying the sickle gene live in countries on or near the equator or are descendants of those populations but living in other regions around the globe. In the Africa, more than 20% have sickle cell trait and the prevalence is as high as 45% in areas such as western Uganda, while SCD affects approximately 2% of the population[69,70]. It has been reported that between 120,000 and 200,000 babies are born with SCD each year in Africa[70–73].

SCD is commonly screened for in newborns, affecting 1/1800 births and 1/400 African-American infants[74], with 1/600 African-American births affected with homozygous SCA[75]. Similarly, results from the UK National Health Service screening programme covering a two-year period from 2005-2007 report a national birth prevalence of 1 in 2000, with half of all those who carry the gene identified as living in London[76]. This secures SCD as the most common serious inherited disorder in England[76].

1.3 Cerebral Ischaemic Events

1.3.1 Overt Stroke

Clinical stroke is defined as a focal neurological event lasting more than 24 hours and is usually permanent, while transient ischaemic events are focal neurological events lasting less than 24 hours (*i.e.* there is a full clinical recovery)[77]. Reversible ischaemic neurological deficits last more than 24 hours, but recover fully. None of these clinical definitions require neuroimaging confirmation.

Overt stroke is part of the natural history in children with SCD[78,79]. Those with HbSS and HbSβ^0-thalassaemia genotypes are at highest risk, although stroke has been documented in children with HbSC and HbSβ^+-thalassaemia genotypes[79]. Stroke can occur as early as 6-12 months[80] when HbF decreases and HbS begins to be synthesised; the first decade of life, when the onset of strokes typically occur, appears to constitute a 'critical period' for neurologic complications and subsequent neurocognitive morbidity[79,81]. It has been reported, without prophylactic blood transfusions (see below), that between 5-11% of children will experience a clinical stroke during childhood[79,82].

Strokes can be classified into infarction due to cerebral ischaemia from arterial or venous compromise, or haemorrhage. Ischaemic stroke accounts for 70-80% of all cerebrovascular episodes, and nearly all episodes in children younger than 15 years and adults older than 30 years. Intracranial haemorrhage typically occurs between 20 and 30 years of age[79,83,84].

Death from a haemorrhagic event is more common than with ischaemic infarction, as high as 50%[15], because of the associated intracranial hypertension and cerebral herniation.

Overt stroke is usually associated with large vessel arterial disease, with evidence of stenosis, or narrowing, of internal carotid arteries and anterior cerebral and middle cerebral arteries of the circle of Willis[5,85,86]. Other abnormalities seen on arterial imaging, either contrast angiography[5] or magnetic resonance angiography (MRA) include moyamoya syndrome[87], and occlusion. Venous sinus thrombosis has also been documented[88].

The pathophysiology of arterial vasculopathy is multifactorial. The body responds to anaemia by elevating cerebral blood flow velocity that can cause injury to the endothelial cells lining the vascular wall[89,90]. Increased cerebral blood flow velocity results from adaptive vasodilation of vessels to match metabolic demand, causing a reduction in cerebrovascular reserve[91]. Further demand when metabolic rate is high (*e.g.* fever) or when there is a decrease in oxygen delivery (*e.g.* from worsening anaemia) could cause large and small vessel injury/ischaemia[92]. Occlusion of small vessels by ISCs can produce microcirculatory ischaemia, especially in "borderzones", where blood flow may be lower[93] in the context of large vessel disease and relative hypotension[78].

Low haemoglobin, high white blood cell count, previous transient ischaemic attack, hypertension, history of acute chest syndrome, high TCD velocities and low haemoglobin oxygen saturation[94–96] are recognised risk factors for ischaemic stroke in SCD[79]. Other precipitators for infarction include a painful or acute chest crisis, infection or systemic illness[84,97] short-term acute severe anaemia[15] and obstructive sleep apnoea (sleep-disordered breathing)[98].

The most common neurological symptom following a cerebrovascular event is the onset of hemiparesis[84,90], along with dysphasia and difficulty walking. Visual field deficits and ataxia may be detected after posterior circulation territory infarction. In 10-33% of cases, focal seizures also can be seen with the onset of symptoms relating to ischaemic infarction[97,99,100]. 'Soft neurological signs'[101] may be detected by careful neurological examination in those with and without a history of previous clinical stroke or seizures. Although most patients typically make a good recovery of motor function following stroke[84,99,102], many show lasting cognitive deficits in other domains such as intelligence and executive functioning[103,104], which will be discussed later.

1.3.2 Silent Cerebral Infarction

More common than overt stroke, up to 35% of children will show evidence of silent cerebral infarction (SCI)[105], diagnosed using MRI as a lesion is seen in two planes of a scan with no

focal neurological deficit lasting more than 24 hours[78,82,106,107]. In children with evidence of SCI on MRI, there is a fourteen fold increase in the risk of clinical stroke[108] and further lesions seen on MRI[109]. Known risk factors for SCI are lower rate for pain crises, history of seizures, increased leukocyte count and Senegal beta-globin haplotype[110], but also low baseline haemoglobin[49], male sex and higher baseline systolic blood pressure[111].

SCI by definition are clinically silent, so timing is unknown; however, it has been postulated that brain damage is the result of recurrent micro-infarctions and recurrent acute hypoxic damage[42,96,112] secondary to severe anaemia, diminished pulmonary function, splenic sequestration, aplastic crisis and acute chest syndrome[104,113]. Presence of SCI is also associated with poor cognitive outcome[114,115], which will be discussed later.

1.4 Treatments and Management

A patient with SCD typically requires a lifetime of treatment and management of symptoms. In the UK, there is a national screening programme for infants and established standards of medical treatments; however, like any chronic disease, it is very important for families and children to get involved in their management of the disease to sustain a high quality of life.

1.4.1 Screening Programmes

In developing countries in Africa where health care facilities are insufficient and treatments are limited, it has been reported that of approximately 50-80% of babies born will die before 5 years[70]. In developed countries, mortality for children with SCD was also high in the 20th century before treatments became available[116]. Therefore, newborn screening programmes are crucial to identify patients early in order to receive the best care possible.

In the UK, newborn screening diagnostic programmes have been put into place prevent life-threatening bacterial infection. The spleen, which destroys encapsulated bacterium such as *Streptococcus pneumoniae,* functions poorly and often infarcts in infancy. Pneumococcal infection is the most common cause of death in infants; daily prophylactic penicillin is frequently administered, as a randomised trial published in 1986 showed a reduction in mortality[117,118]. Screening also allows for early monitoring for acute splenic sequestration events and dactylitis, as well as identification of other hemoglobinopathies. Folic acid is prescribed in view of the high haemolytic rate. Many studies have since shown that neonatal screening, careful follow-up and relatively simple interventions significantly reduce morbidity and mortality[81,117,119].

1.4.2 Red Blood Cell Transfusions

Transfusion is now widely used in the short-term management of acute complications of SCD and has a role in the prevention of chronic complications, specifically stroke[120–123]. Transfusions improve the flow properties of the blood by either lowering the fraction of HbS via dilution or "replacing" HbS with HbA. The clinical standard is to maintain an HbS level less than 30%, reducing the incidence of recurrent stroke from rates ranging from 65-90%[85,99] to 10%[124,125]. Transfusions increase the oxygen-carrying capacity of the blood to prevent cerebrovascular events[126] by minimising viscosity of the blood, increasing haematocrit and improving large vessel stenosis[85].

Although blood transfusions are standard in clinical practice in developed countries, there are also complications. Iron can accumulate in the liver[127] and heart[128], usually monitored using MRI of the liver[129] and heart[130], and treated with iron chelation therapies. The possibility that there is an accumulation of iron in the brain is still under active investigation[131]. Hyperviscosity of the blood can occur following over-transfusion[132]. Transfusion reactions, possibility-contaminated blood with viruses such as HIV or hepatitis C, and alloimmunisation[133], where there is sensitisation of RBC antigens, are also possible complications[132].

1.4.3 Hydroxycarbamide

Children with SCD who cannot receive regular blood transfusions for any reason may be treated with the drug hydroxycarbamide[134] (also known as hydroxyurea). The drug acts to inhibit polymerisation of HbS, by increasing percentage of HbF[135] and decreasing cellular dehydration[136], both helping to improve red blood cell survival. The risk of stroke is lowered by increased levels of HbF[137,138], and also by a reduction in white blood cell count and expression of cell-adhesion molecules associated with vasoocclusion[139]. Controlled trials have shown hydroxycarbamide can ameliorate disease severity[140] (*i.e.* decrease frequency of painful crises, acute chest syndrome and the need for blood transfusion[37,134,141]), and reduce the risk of first stroke[142].

1.4.4 Bone Marrow Transplantations

The only cure so far described in SCD is bone marrow transplantation[143], which can be an option for children with a matched sibling donor[144]. This therapy is considered when there are severe complications (*e.g.* stroke) where there is dependence on blood transfusions. Data suggests 92-94% survival overall, with 82-86% event-free rate post-transplantation[145].

Induced pluripotent stem cells[146], as well as gene therapy[147,148], currently in pre-clinical research can offer promise for the future of SCD treatment[149].

1.4.5 Psychosocial Interventions

Another advantage of newborn screening is the involvement of parents very early on as care partners with clinicians in managing complications of SCD. Parents and children can sometimes have considerable on-going fear of hospital visits and painful crises; post-traumatic stress disorder in children with SCD often mirrors parents' worries, and has been reported to adversely affect recovery[35]. Early family education of the aspects of the disease, (*e.g.* learning how to palpate the spleen to feel for enlargement) and identifying lifestyle factors (*e.g.* reduced fluid intake) that increase risk of vaso-occlusive episodes, is critical to achieve the best possible comprehensive care.

Although child survival rate is high in developed countries[41], adolescence is a critical period, associated with increased mortality risk[39] as young adults transition from paediatric to adult clinics. It is of crucial importance to educate adolescents about the potential severity of their disease and how to manage their chronic illness as they start living independently from relatives. The transition from paediatric to adult care has been under scrutiny[150], calling for 'uninterrupted, coordinated, appropriate care'[151] and for healthcare providers to establish multidisciplinary teams offering education, psychosocial support and vocational training[152,153].

1.5 Stroke Prevention & Clinical Trials

1.5.1 Primary stroke prevention

Transcranial Doppler (TCD) ultrasound screening, as well as prophylactic blood transfusion in those with high stroke risk from high TCD findings, has become an established and effective method of primary stroke prevention (*i.e.* reducing the risk of first stroke). TCD is a safe, non-invasive and well-tolerated procedure which measures the blood flow velocity in the intracranial vessels[124] (Figure 1-4). Three groups have been identified: those with normal TCD velocities (<170cm/sec), those with conditionally abnormal TCD velocities (between 170cm/sec and 200cm/sec) and those with abnormal velocities (>200cm/sec)[154]. In children, high cerebral blood flow velocities greater than 200cm/sec in the internal carotid and middle cerebral arteries are associated with a 40% risk of stroke over the subsequent 3 years[155], while those with conditionally abnormal velocities have a 7% stroke risk over the same period. It has become standard care to prevent stroke by transfusing patients with

velocities >200cm/sec and to monitor closely those with conditional velocities between 170-200cm/sec to make sure that they do not cross into the abnormal range.

Figure 1-4. A child with SCD being screened with Transcranial Doppler ultrasound. Image courtesy of Fenella Kirkham; originally published in The Times with parental consent.

1.5.2 Secondary stroke prevention

As mentioned previously, regular blood transfusions have reportedly reduced the risk of recurrent stroke from 66-90% to 10-27%[85,87,99,124,156]. Although these treatments have lessened the risk of stroke, approximately 20% of children with a history of stroke who receive transfusion therapy will have a second stroke, and approximately 30% will have a third stroke[157]. There is currently no other evidence-based secondary stroke prevention strategy, but many children are treated with hydroxyurea or aspirin, in addition to or instead of blood transfusion, after recurrent stroke, or if blood transfusion is impossible. Those with moyamoya pattern of occlusion with collateral vessels (see next chapter) may be candidates for revascularisation[158].

1.5.3 STOP

The Stroke Prevention Trial in Sickle Cell Anemia (STOP) randomised children with abnormal TCD velocities (>200cm/s) to regular transfusion in additional to standard care or to standard care alone. There was a 92% reduction in the risk of clinical or overt stroke in the transfused arm[123,155]. The study was discontinued early because of this clear benefit in transfusing children to prevent first stroke[123].

STOP II followed, recruiting children with abnormal TCD and 30 months or more of regular transfusion, who had converted from high-risk to low-risk TCD. The children were randomly allocated to continue or discontinue transfusion. Again, the study was halted early because too many children reverted to high-risk TCD. From these two clinical trials, the US National Heart, Lung, and Blood Institute recommended all children should have TCD screening and be transfused if their velocities are greater than 200cm/sec[159] and those children should be transfused indefinitely[156]. Transcranial Doppler screening and transfusion for velocities greater than 200cm/sec is now standard National Health Service practice.

1.5.4 SIT

The Silent Infarct Transfusion (SIT) trial included only children with evidence of SCI and normal TCD measurements, and again used blood transfusion as therapeutic intervention. If the child's TCD was greater than 200cm/sec, blood transfusions were given as standard care. The primary hypothesis of the SIT trial was that transfusion therapy would reduce occurrence of new clinical stroke and SCI by 86% and that therapy will limit further decline of general intellectual ability when compared with observation arm. Additionally, the overall benefit of treatment would outweigh the risk associated with the treatment.

Primary results from the trial indicated that those receiving regular blood transfusion therapy had have a 58% relative risk reduction in the recurrence of clinical stroke or SCI[160]. This was lower than that predicted as well as the reported risk reduction of blood transfusion therapy to prevent clinical stroke in the STOP trial, but still clinically and statistically significant[123]. Trial investigators suggest blood transfusion therapy possibly corrects for anaemia, known to be temporally associated with subclinical ischaemic injury[112], by improving cerebrovascular reserve[160]. Data from this trial, which includes children from sites in London, will be discussed in this thesis.

1.5.5 POMS

Cohort studies have highlighted the high prevalence of sleep-related breathing disorders and nocturnal oxygen desaturation in children with SCD[161] and provided evidence for an

association with central nervous system complications, including stroke[94] and cognitive dysfunction[162]. In the Prevention of Morbidity in Sickle Cell Disease (POMS) study phase 1 randomised controlled trial, children were randomised for six weeks to either standard care or auto-adjusting continuous positive airways pressure (auto-CPAP), triggered when breathing was obstructed. After two weeks, overnight haemoglobin oxygen saturation monitoring was undertaken and if needed, an oxygen concentrator was added to the auto-CPAP to deliver oxygen to keep oxygen saturation above 94%. The aims of the study were to test whether reversing nocturnal oxyhaemoglobin desaturation would prevent cognitive morbidity associated with the disease. Results from the pilot study showed improved processing speed and attention in the treatment group[163].

Currently, a second POMS pilot study is in progress to assess whether auto-adjusting continuous positive pressure therapy or oxygen therapy is more acceptable to patients, leading to a larger proof-of-concept trial in 2015, funded by the National Institutes for Health Research/Research for Patient Benefit stream. The proposed outcome measures for the larger trial are to reduce frequency and severity of pain symptoms, quality of life and cognition. The trial will also explore potential reversibility of hypoxic damage to the brain.

1.6 Conclusion

This chapter overviewed the main clinical complications of SCD, its prevalence in society, treatments and why it is a public health concern. This thesis will focus on the neurological aspects, discussed in the following chapters.

Chapter 2. Neuroimaging in Sickle Cell Disease

Successful medical interventions have allowed the childhood mortality rate of SCD to decrease and life expectancy to increase. However, cerebrovascular events in childhood are relatively common and can significantly limit the full potential of a developing child, adolescent or adult.

MRI is a safe, non-invasive, useful technique for diagnosis and management of SCD-related cerebral infarction, cerebrovascular disease and other neurological abnormalities. Conventional structural MRI sequences are routinely used in hospital settings, while more advanced MRI sequences are becoming more commonplace in research institutes. For section 2.1, principles of MRI physics are referenced from selected textbooks[164,165].

2.1 Basics of conventional MRI

2.1.1 Origin of the MR signal

In a magnetic field (B_0), hydrogen protons found in water content of tissue are aligned in the direction of the magnetic field in two possible states: spin-up or spin-down. The strength of the magnetic field, as measured in Teslas (T) determines the amount of magnetisation when there is thermodynamic equilibrium. The sum of the spins in B_0 amounts to the net magnetisation aligned with B_0.

Spinning nuclei precess around B_0 at Larmor frequency:

$$\omega = \gamma B_0$$

where ω is the angular frequency of the spins, γ is the gyromagnetic ratio (an intrinsic property of hydrogen protons set at 42.56 mHzT-1), and B_0 is the magnitude of the magnetic field strength. This equation implies that changes in the magnetic fields will proportionately affect precession frequencies. Figure 2-1 shows precession frequencies at various magnetic strengths. At 1.5T, a common field strength for a clinical MR scanner, protons precess around the main magnetic field at 64MHz.

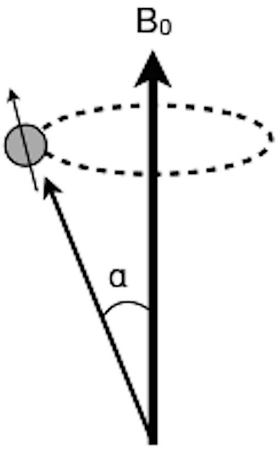

T	MHz
0.5T	21
1.0T	42
1.5T	64
3.0T	127

Figure 2-1. Proton precession. Protons precess around the axis of the main magnetic field (B_0) at the Larmor frequency, which at 1.5T scanner is 64MHz.

A coil is used to produce an oscillating magnetic field, called a radiofrequency (RF) pulse, which precisely matches the natural precession frequency. This causes a torque that is orthogonal to the main magnetic field, which tips the magnetisation out of equilibrium into the transverse plane. Over time, the transverse magnetisation decays away exponentially as the spins dephase with respect to each other and return to equilibrium, restoring the magnetisation along the direction of the main magnetic field B_0.

To achieve maximum signal, it is best to apply an oscillating magnetic field that tips the magnetisation into the transverse plane. The desired flip angle (α) depends on the amount of time the RF pulse is applied. The RF pulse oscillates at the Larmor frequency, and it creates a magnetic field that is perpendicular and orthogonal to B_0. This new magnetic field (B_1) is static when perceived in a rotating frame of reference. The equation that describes RF pulses is:

$$\text{flip angle } (\alpha) = \gamma B_1 \, tp$$

where B_1 is the strength of the RF magnetic field and tp is the duration of the pulse. With this equation, one can change the strength of the pulse to create different flip angles. When the excess energy is re-emitted, that is when the MR signal can be collected.

When an RF pulse that matches the precession frequency of the spins is applied, this affects spin equilibrium because of an exchange of energy. Absorption of electromagnetic energy will only happen when protons spin at the same frequency as the RF pulse. The term relaxation is used to describe when the system returns to thermal equilibrium, or their

original energy state, and there is an emission of electromagnetic energy back into the environment – this is the signal that is measured in MRI.

2.1.2 Relaxation Times

Relaxation times are fundamental parameters that reflect the tissue 'environment', both due to the nature of the spins themselves or due to the magnetic field. There are two main features of relaxation: realignment of the spins along the transverse plane as they lose the energy they absorbed from the RF pulse, and dephasing of spins following the RF pulse.

T1 relaxation, also known as 'spin-lattice relaxation' or longitudinal relaxation, refers to an exponential growth of longitudinal magnetisation, where the spins return to a thermal equilibrium state in the main magnetic field B_0. It is called longitudinal relaxation because the spins return to the longitudinal plane.

T2 relaxation, also called 'spin-spin relaxation' or transverse relaxation, is a process that causes spins to get out of phase with each other. It causes a loss of magnetisation in the transverse plane. T2 is governed by an exponential decay, and can be described as a time constant of the transverse magnetisation after an RF pulse in a homogeneous static magnetic field. The contrast obtained in a spin-echo sequence, where the effects of magnetic field inhomogeneity are reversed are, in part, dependent on T2.

T2* is also a time constant for the transverse magnetisation decay, but where the effects of an inhomogeneous field are not compensated, as is the case for a gradient-echo sequence. It is described as the combined effect of T2 decay plus the decay due to local inhomogeneities in the main magnetic field B_0.

T2* and T2 dephasing happens within a few hundred milliseconds (T2* is shorter than T2). T1 is slower, taking several seconds before the net magnetization is restored along the transverse plane.

2.1.3 Contrast

Other important parameters that describe pulse sequences are echo time (TE), the time between the first excitation RF pulse and when the 'echo' signal is formed, and repetition time (TR), the time between subsequent excitation RF pulses. These two parameters determine the contrast in image, and different combinations will produce different degrees of contrast between tissues. Proton density (PD) is a characteristic of tissue describing the number of spins absorbing and emitting energy. Each tissue has a specific PD, T1 and T2 time, and the signal depends on these three factors (Figure 2-2).

Changing TR will affect the contrast between tissues with different T1 relaxation times and changing TE will affect contrast between tissues with different T2 relaxation times. For example, a tissue with a long TE and TR, such as CSF, will be dark in a T1-weighted image (that has a short TE and short TR), but bright in a T2-weighted image (that has a long TE and long TR).

at 1.5T	PD	T1	T2
Fat	-	260	60
Grey Matter	0.69	760	77
White Matter	0.61	510	67
Cerebrospinal Fluid	1	2500	280
Oedema	0.86	900	126

	TE	TR
PD	short	long
T1	short	short
T2/T2*	long	long

Figure 2-2. Relaxation times of various tissues at 1.5T[166]. Right panel: Contrast in PD-, T1- and T2/T2*-weighted images depends on combinations of TE and TR.

2.1.4 Spin echo and Gradient echo sequences

Both spin echo (SE) and gradient echo (GE) sequences start with an initial 90° RF excitation pulse which produces magnetisation in the transverse plane. In a SE sequence, after the initial RF pulse and the magnetisation decays away, a 180° RF pulse is then applied. This pulse flips the magnetisation vectors, so they precess in the same direction and at the same speed as before (*i.e.* the protons that are moving faster move towards the back and those that are moving slower move towards the front so they all end up in phase). In this way the transverse magnetisation is refocused to form an echo.

GE imaging utilises a negative field gradient applied just after the initial 90° RF pulse, which causes deliberate rapid dephasing of the spins. A positive gradient is then applied to reverse the previous magnetic field gradient that rephases the spins (*i.e.* spins that were precessing at a low frequency due to position along the gradient direction will now precess at a higher frequency and vice versa).

One way to represent a pulse sequence is through a diagram that gives the relative timing as well as the amplitude of each pulse (Figure 2-3).

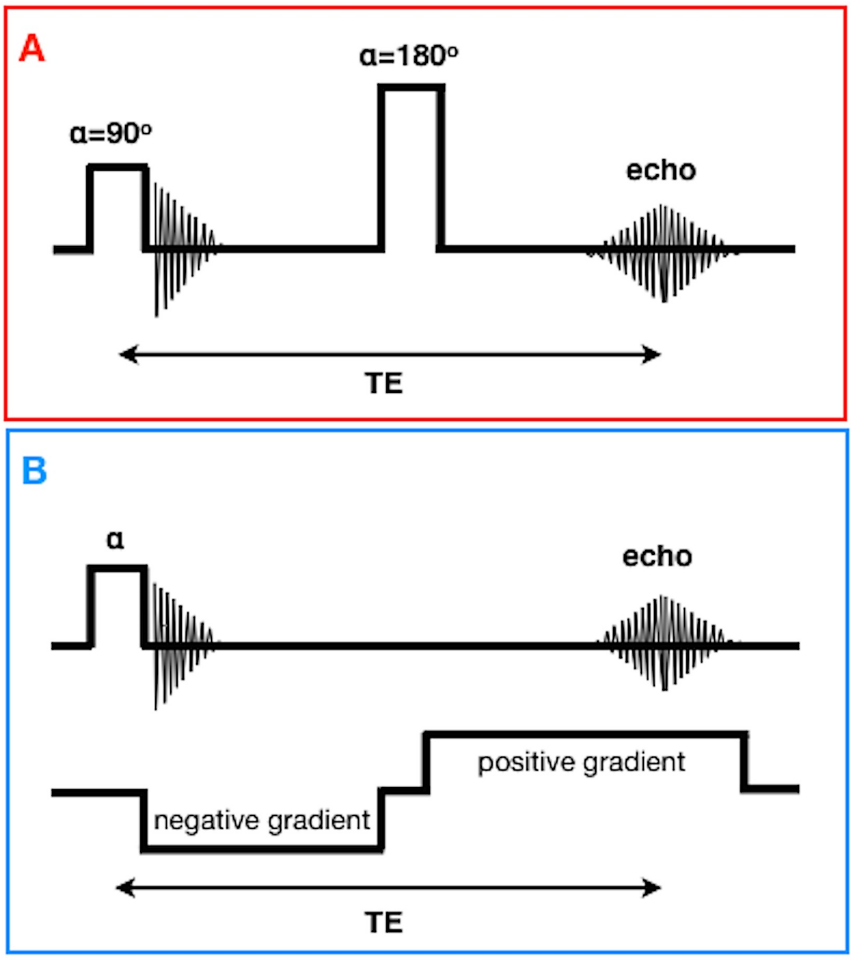

Figure 2-3. Pulse sequence diagrams for spin echo and gradient echo sequences. A (red): Spin echo sequence uses an initial 90° pulse, then an 180° refocusing pulse to rephase the spins. B (blue): Gradient echo sequence uses an initial pulse (flip angles can vary), followed by negative and positive gradients to rephase the spins.

T1-weighted GE images are often used anatomically, because contrast between different tissue types is high: water-based tissues (*i.e.* grey matter) appear mid-grey and fat-based tissues (*i.e.* white matter) are brighter. T2-weighted SE images are generally used for clinical diagnosis of pathology, because tissues with the longest T2-relaxation times (*i.e.* cerebrospinal fluid, oedema and lesions) appear bright (Figure 2-4).

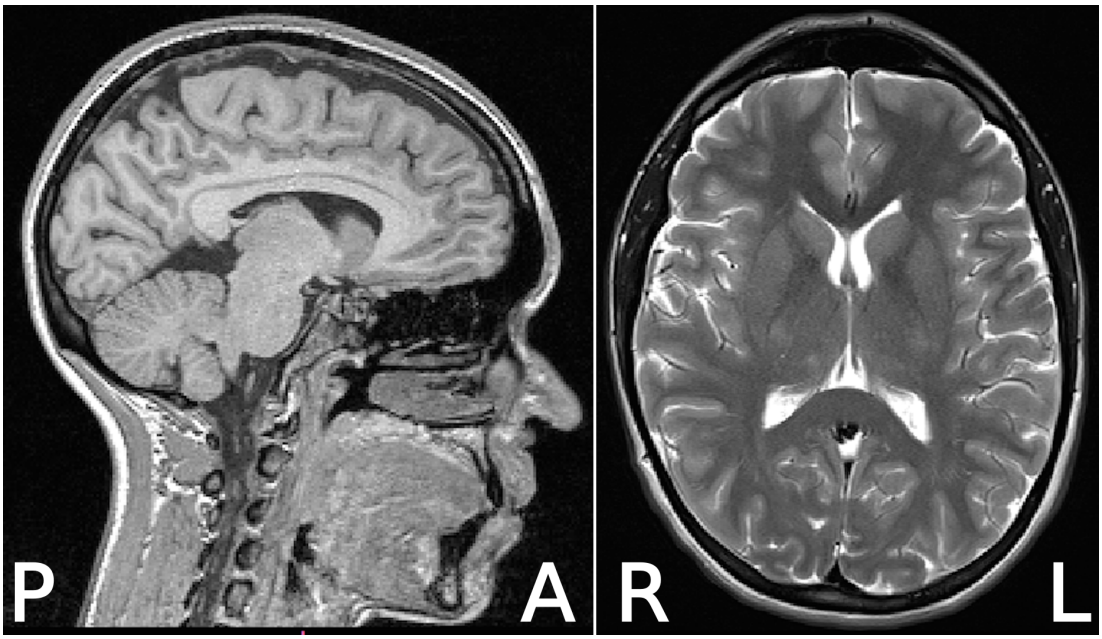

Figure 2-4. T1- and T2-weighted images of a healthy 24-year-old female. Left panel shows a T1-weighted (Fast Low-Angle Shot; FLASH) spoiled gradient echo sequence. Right panel shows a T2-weighted (turbo spin echo sequence).

2.2 Diffusion MRI

Diffusion MRI utilises the concept of water displacement in brain tissues that allows for *in vivo* analysis of white matter microstructural integrity.

In water, molecules move with a kinetic energy in a random fashion, called Brownian motion or random translational motion. The mean squared displacement of water molecules $\langle r^2 \rangle$ is proportional to the diffusion coefficient (D) and time (t) over which the diffusion process is observed, and can be accurately described by Einstein's equation:

$$\langle r^2 \rangle = 6Dt$$

D is dependent on temperature, but at normal body temperature (37°C), diffusivity of water is approximately 3.0×10^{-3} mm^2/s. The displacement of water molecules is also governed by Fick's law: $Jx = -D(dC/dX)$, which states that the diffusive flux of concentration will go from regions of high concentrations to low concentrations. In the case of water, from which the MR signal is concerned, the diffusive process is referred to as self-diffusion.

2.2.1 Diffusion-Weighted Imaging

In the human brain, there is not only water, but also microscopic structures such as axons, myelin and glial cells that affect the mobility of water molecules. The displacement is different in various tissues. In diffusion imaging, the 'apparent' diffusion coefficient (ADC)[167] is measured within each volume pixel element (voxel), which represents an index of the mobility of water molecules inside biological tissues.

Where there is little hindrance to diffusion, water has an isotropic diffusion profile in accordance to Einstein and Fick's principles. In isotropic diffusion, the net direction of diffusion is 0 since it is uniform in all directions. Diffusion is isotropic in cerebrospinal fluid, where there is also high diffusivity, and in grey matter where there is low diffusivity. White matter however, displays an anisotropic diffusion profile. Water molecules are constrained in white matter, where the presence of cell membranes, myelin, axons and other 'biological barriers'[167,168] hinder diffusion so that diffusion is greatest along specific directions (Figure 2-5).

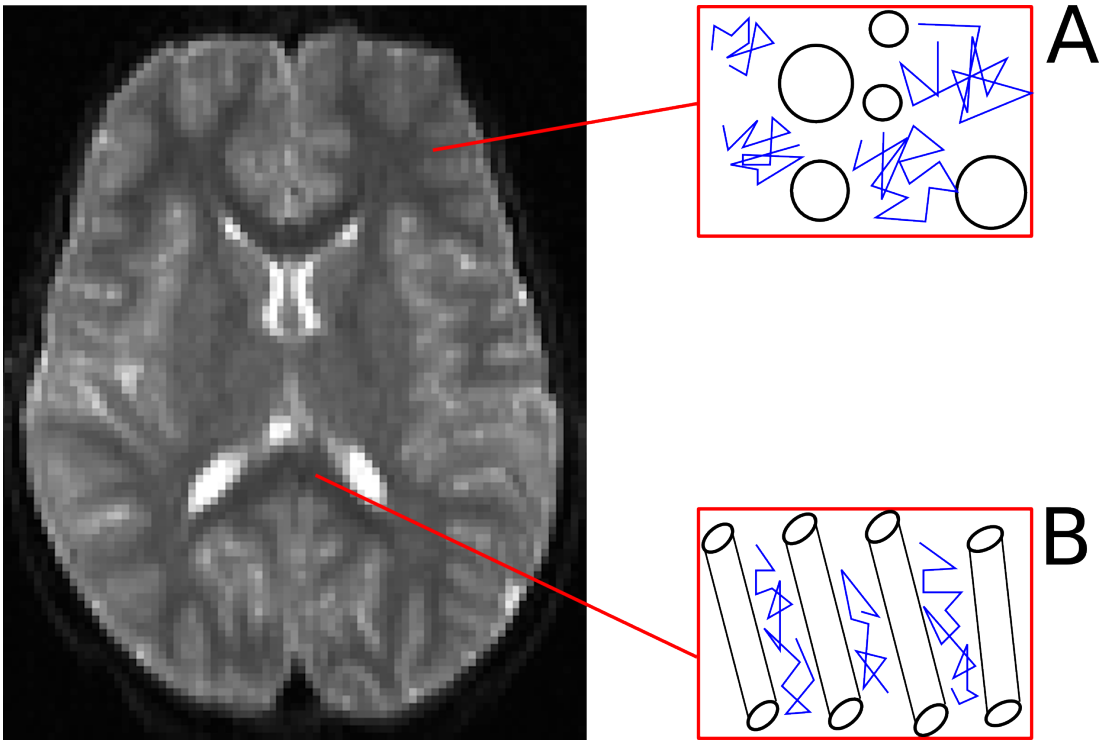

Figure 2-5. Diffusion characteristics in nervous tissue. Diffusion is influenced by cellular microstructures, which can restrict the mobility of water molecules. In isotropic diffusion, such as an area of grey matter (A), molecules (blue) can displace in all directions, while in anisotropic diffusion, such as white matter fibre tracts (B), axonal membranes and myelin sheaths present barriers, therefore restricting the diffusion of water molecules in a preferential direction[169].

Pulse sequences are made sensitive to diffusion by adding diffusion gradients in certain directions on either side of the 180° pulse in a T2-weighted spin-echo sequence. The b-value is the parameter that measures diffusion sensitivity by altering the strength and direction of the gradient. A b-value has units of seconds per square millimetre; a b-value of 0 will result in a typical T2-weighted image, while a typical diffusion-weighted b-value is 1000 s/mm^2. Random motion of the water molecules in the direction of the gradient will result in signal loss on the image because of phase changes of the spins moving in the gradient direction, which results in rapid dephasing and loss of signal. Contrast in DWI is dependent on T2, the ADC and the b-value, and differences in the ADC signal are based on differential diffusion of tissues within the parenchyma.

ADC is generally measured along three axes, and the mean ADC is used for clinical purposes such as acute stroke, where diffusion abnormality due to ischaemia appears a few hours after onset[170]. Clinically, ADC in acute stroke is thought to reflect shifts in fluid between intracellular and extracellular spaces[171].

2.2.2 Diffusion Tensor Imaging

Diffusion tenor imaging (DTI) was developed to characterise diffusion anisotropy, which cannot be determined with the measure of diffusion in three directions. Anisotropy can be quantified by measuring the diffusion tensor, which requires measurements in at least six directions[172]. In the case of anisotropic diffusion, the tensor can be visualised as an ellipsoid (Figure 2-6), with three orthogonal directions (eigenvectors; λ1, λ2, λ3) and diffusion coefficient values for each direction (eigenvalues: v1, v2, v3). The tensor reverts to a sphere when diffusion is isotropic.

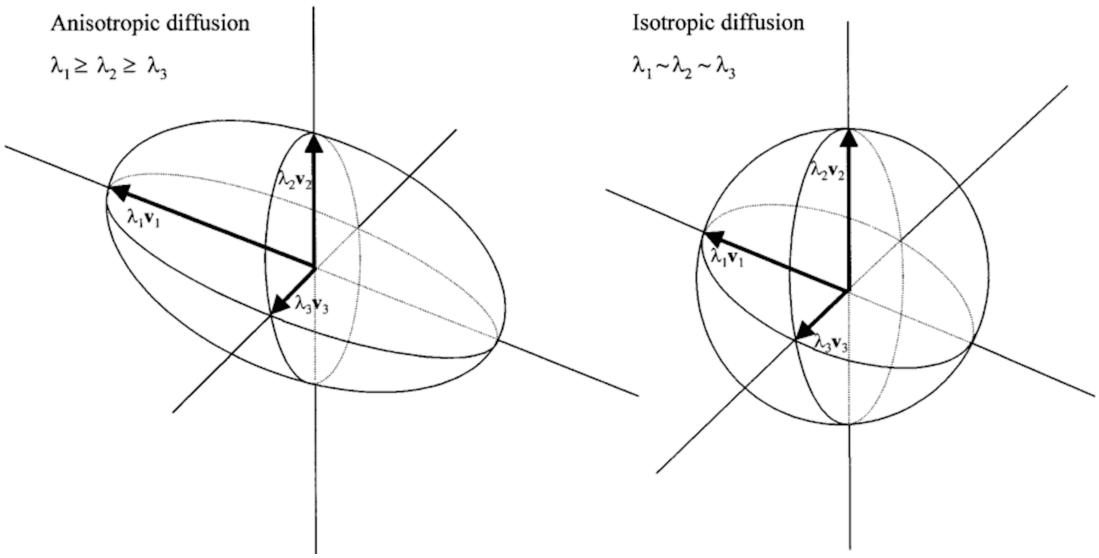

Figure 2-6. Isotropic and anisotropic diffusion tensors, adapted from Wiegell et al.[173]). Isotropic diffusion (right) is characterised by three eigenvalues approximately equal (λ1 ~ λ2 ~ λ3) whereas anisotropic diffusion (left) is characterised by the magnitude of the principle diffusion orientation larger than the two perpendicular directions (λ1 ≥ λ2 ≥ λ3).

From the diffusion tensor model, several quantitative metrics can be calculated. The average water molecular displacement (i.e. mean diffusivity; MD) can be measured as the mean of the three eigenvalues. This is equivalent to the ADC determined from three directions. The degree of anisotropy, or fractional anisotropy (FA), can be derived from the standard deviations of the three eigenvalues.

FA and MD both indicate differences in underlying tissue microstructure. FA values range from 0 (complete isotropy) to 1 (complete anisotropy). High FA values result when the principal eigenvalue (λ1) is greater than the other two (λ2, λ3), reflecting coherence, organisation and/or density of the local tract. MD, which measures the overall magnitude of water diffusion, increases when there is a loss of structure, such as axonal damage or demyelination (*i.e.* degeneration of microstructural cell barriers)[174]. Other metrics of diffusivity, such as axial diffusivity (AD), the magnitude of diffusion along the principal eigenvector of the diffusion tensor (λ1), and radial diffusivity (RD), the average magnitude of diffusion along the two perpendicular eigenvectors (λ2, λ3), provide additional information about the nature of water diffusion changes that have been related to myelination and axonal damage[175].

There are two common ways of analysing DTI data: using a voxel-based approach across the whole brain, or a region-of-interest approach using DTI tractography. Tractography relies on colour-coded maps[176], given by the principle eigenvector, to visualise the orientation of the tensor within each voxel and to reconstruct the major white matter

pathways of the brain by following the continuity and direction of maximum diffusion along white matter fibres from voxel to voxel[177] (Figure 2-7). This non-invasive MRI technique is able to virtually dissect white matter pathways of the living human brain[178], and the method can be applied in neurological and psychiatric disorders, as well as healthy development and aging[174].

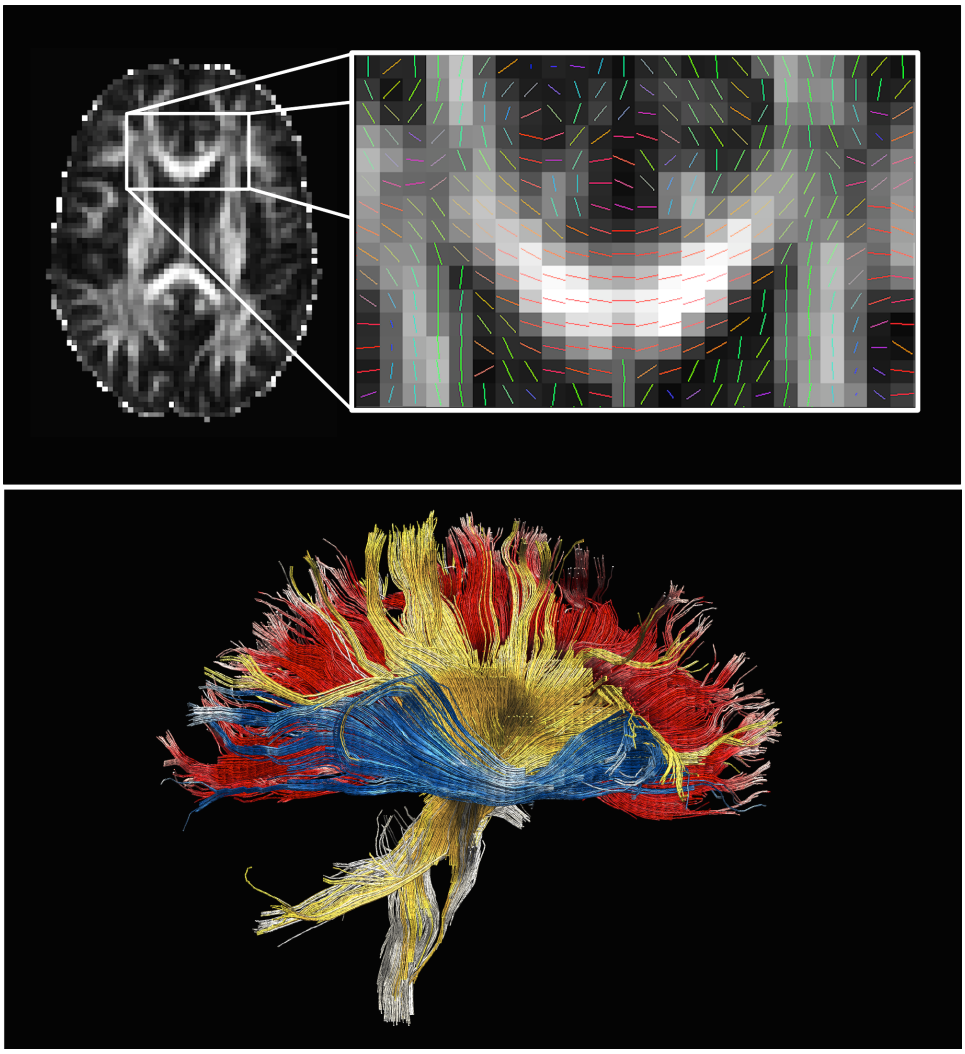

Figure 2-7. DIffusion tensor imaging and tractography. Top panel shows a FA map, and the enlarged area shows the colour-coded principle eigenvectors (*i.e.* red= left/right orientation, green= anterior/posterior orientation, blue= inferior/superior orientation). An algorithm can be used to trace paths following the orientations at each voxel, called streamlines, and virtually 'dissect' white matter pathways. Bottom panel is a tractography image showing the corpus callosum (red), internal capsule/corona radiata (yellow) and inferior fronto-occipital fasciculus (blue). This image won first prize at the 2011-2012 UCL Graduate School's 'Research Images as Art/Art Images as Research' competition.

2.3 Neuroimaging Findings

MRI studies have showed that the majority of overt stroke and SCI occur from a distribution from the internal carotid artery[109], and pathologies are frequently seen in tissue within the anterior cerebral and middle cerebral arterial distribution[179,180]. MRA studies confirm this pattern, as publications have reported stenosis (narrowing) or occlusion of these vessels with relative sparing of the posterior circulation, other than tortuosity[1,181] (Figure 2-8). Stroke and SCI from vertebrobasilar artery circulation occlusion are less common, but have been reported[180,181]. Cerebral infarction is rarely fatal, however approximately 11% of patients with genotype HbSS will experience a clinically apparent stroke by age 20, and up to 24% by age 45[79]. SCI can develop very early in life, with rates between 11-15% in children less than 2 years[107,182,183]. By 6 years of age, at least 25% of children with show evidence of SCI[183], and up to 37% by 14 years of age[184].

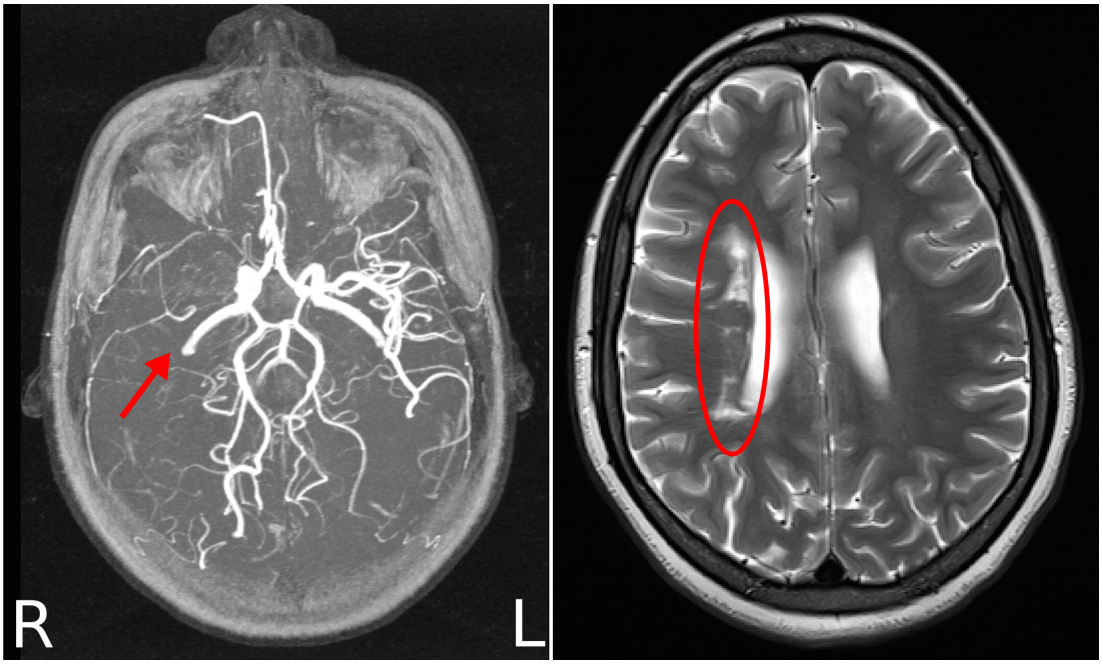

Figure 2-8. Example of a 19-year-old female with HbSS who experienced a clinical stroke. Left panel shows occlusion of the right middle cerebral artery on MRA, and the right panel shows corresponding hyperintense signal on T2-weighted MRI, indicating area of infarction.

2.3.1 Radiological Findings

Although stroke is identified by abrupt onset of neurological deficit, the term 'covert stroke'[185], or SCI was first described in the Cooperative Study in Sickle Cell Disease (CSSCD)[82] to radiologically define an abnormal MRI result in the absence of overt neurological symptoms. An accepted definition of SCI, described for the SIT trial[111,186], is "a MRI lesion measuring at least 3mm in greatest linear dimension, visible in two planes of T2-weighted images (axial and coronal)". SCI can be concurrent with neurological symptoms lasting under 24 hours, but must occur in the absence of a focal neurological deficit compatible with the anatomic location of the MRI lesion[187].

Many studies describe a localisation of SCI to deep white matter, particularly in the arterial borderzones[104,180,181,183,188], where flow is more vulnerable (Figure 2-9). Moser and colleagues[82] found that localised infarcts are usually confined to borderzone white matter while extensive lesions involve both cortex and deep white matter. Infarcts in the subcortical grey matter structures (i.e. head of caudate, cerebellum) are less common[180,181].

Brain injury in children with SCD also extends to concurrent vasculopathy[189] and moyamoya syndrome seen on MRA[82,190,191], as well as generalised[82,104] and focal cortical atrophy[192–195].

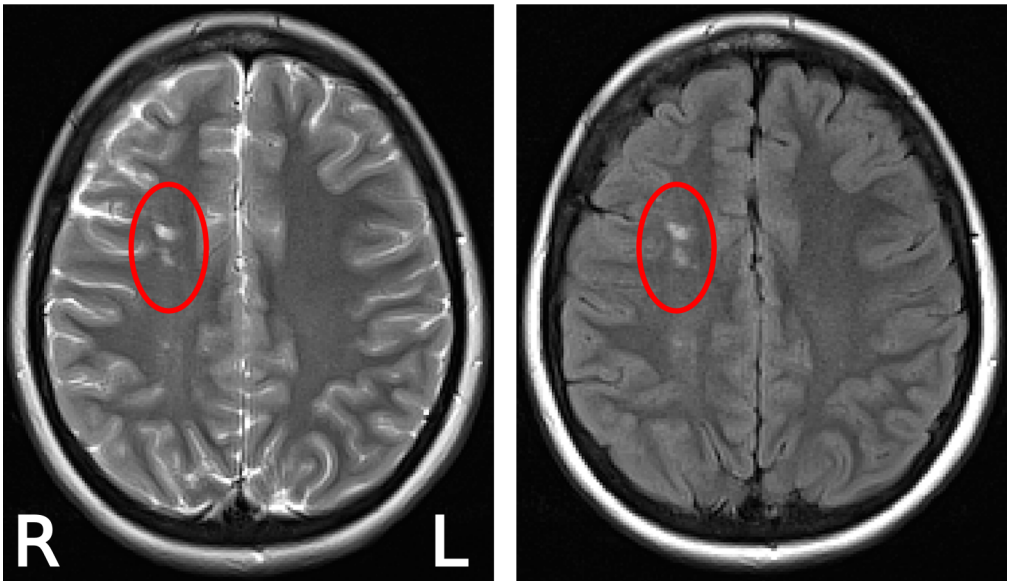

Figure 2-9. An example of right frontal silent cerebral infarcts in a 14-year-old male with HbSS. Both T2-weighted image (left) and fluid-attenuated inversion recovery (FLAIR, right) image show hyperintense signal corresponding to the lesion site.

2.3.2 Acute Silent Cerebral Ischaemic Events

It has been argued that categorically dividing ischaemic events between clinical stroke and SCI may be an oversimplification of the spectrum of brain injury in SCD[196]. Recent research has shown that acute silent cerebral ischaemic events (ASCIE)[112,196], following acute severe anaemia[42,110,197,198], can be detectable using DWI. In acute ischaemia, an area of oedema in the brain has a rapid decline in proton density and appears hyperintense on DWI and decreased on an ADC map, persisting for 10-14 days post-event[170], which can differentiate acute stroke from more remote events[42]. These lesions, which may be transient, are likely under the detection of T2-weighted MRI until SCI develop.

These findings are line with the hypothesis put forward by Steen and colleagues[106]: the SCD brain is a model of diffuse brain injury, microstructural changes in cerebral tissue results from chronic recurrent ischaemic insult, and these changes may not pass the sensitivity threshold that can be visualised on MRI at current clinical field strengths in widespread use.

2.3.3 Quantitative Neuroimaging Findings

In the two decades since MRI was first used to describe the spectrum of neuroimaging abnormalities in SCD, technology has been improving: clinical MRI hardware and software are more advanced, and sophisticated sequences for quantitative processing techniques are being applied to SCD to describe subtle abnormality.

A voxel-based morphometry study[199] using T1-weighted imaging found that in a group with a history of SCI, there were significant decreases in white matter density extending bilaterally from anterior frontal lobe along the ventricles to parieto-occipital lobes, as well as along the corpus callosum (Figure 2-10). This study is consistent with the pattern of white matter lesions described earlier, but also suggests that patients without visible infarcts on T2-weighted MRI may have compromised white matter.

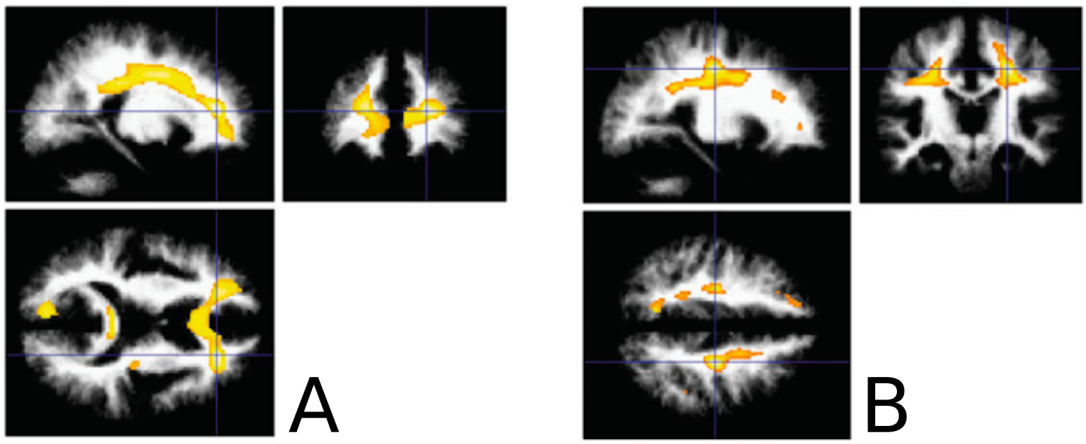

Figure 2-10. Decreased white matter density in the arterial borderzone distribution: results from a voxel-based morphometry study[199]. (A) Areas of significantly decreased white matter density in the SCD patients with evidence of SCI compared to controls. (B) In patients with no evidence of SCI, there were similar bilateral white matter density decreases compared to controls, but the spatial extent of white matter changes were less compared to the group with lesions.

Grey matter volume has also been investigated. One report showed significant reduction in total subcortical grey matter volume (*i.e.* basal ganglia volume) as compared to cortical grey matter volume[200]. In children without evidence of SCI, decreased grey matter volume in bilateral frontal, temporal and parietal lobes was found to correlate with low IQ[201], and one study reported significant thinning of cortex in older children as compared to younger patients in the posterior medial surfaces of both hemispheres[202].

A DWI study showed significant increases in mean regional ADC of patients relative to controls in six regions (left and right frontal, left and right cerebellum, pons, vermis), and in patients with no evidence of infarct, there was increased ADC in four regions (excluding pons and vermis)[203]. Helton and colleagues[204] combined perfusion and diffusion data and found that abnormal appearing white matter, due to leukoencephalopathy and SCI, had not only decreased cerebral blood flow using arterial spin labelling perfusion MRI but also showed decreased FA by DTI.

There are two recent DTI studies of note. One study looked at two groups of children with SCA, some of whom had mild gliosis although none had SCI. Increases in diffusivity and reduced FA in the body of the corpus callosum were found only in patients with mild gliosis, while reduced FA in the centrum semiovale was found in the no-SCI group[205]. Another study compared sixteen SCA patients in a combined quantitative DTI and deterministic tractography analysis. This study used various regions-of-interest across the brain, finding reduced FA in the corpus callosum, centrum semiovale, periventricular areas and subcortical white matter ROIs. Deterministic tractography of the corpus callosum was also

used, showing reduced fibre count (*i.e.* streamlines) and reduced FA in the anterior body of the corpus callosum[206].

2.4 Neurocognitive Findings

Brown and colleagues[113] suggest some factors that accumulate over time, and could explain the compromised intellectual functioning in children with SCD. Recurrent micro-infarctions of the central nervous system, possibly undetected by screening measures, may affect general functioning[207]. Additionally, conditions secondary to anaemia, such as diminished pulmonary function and chronic hypoxic damage can cause brain damage[208]. While the exact mechanisms underpinning cognitive dysfunction in SCD are unknown, there is a substantial literature characterising the effect of SCD on cognition.

2.4.1 General Intelligence

Intelligence quotient (IQ) is the most commonly reported and widely studied standardised measure of cognitive ability in SCD. The first published study was in 1963 in the USA, finding no differences between children with SCD and a group of siblings[209]. Further attention to the subject was most likely deferred due to the on-going civil rights movement of the 1960s, where prejudiced beliefs that black people were inferior to whites were common.

Early studies in the 1980s and 1990s included patient groups without information from MRI, but generally excluded those with history of stroke or abnormal neurological exam. Results from studies at that time were mixed; some reported no differences in full-scale IQ (FSIQ) between patients and controls[210–212], others found patients had lowered intelligence scores than matched controls[102,213–215].

With the routine use of MRI added in the mid-1990s, patients were classed into groups based on history of stroke and presence or absence of SCI. Reports from the CSSCD[104,216] were the first to show a general trend of a spectrum of decreasing intelligence corresponding to lesion burden. Since then, several studies have confirmed that children with history of overt stroke perform significantly worse than children with no stroke[104,217–222]. Further, evidence has also suggested children with silent cerebral infarcts perform worse than those with normal MRI[199,203,216,218,220,223], and that large lesion size is associated with lower FSIQ[224,225]. More studies are needed to elucidate the differences between children with SCD and normal MRI compared to controls; this topic will be discussed in Chapter 4.

2.4.2 Executive Functioning

Historically, SCD has been associated with deficits in executive functioning, an umbrella term for frontal lobe functions such as inhibition, planning, organisation, processing, decision-making, mental flexibility and working memory. Berkelhammer and colleagues constructed a systematic review of the neurocognitive literature in 2007[115], and found 11 out of 13 studies found executive function and attention were impaired in children with SCD, and a strong relationship between degree of cerebral damage and location of injury with executive function performance.

It has been reported that children with SCD show deficits in sustained attention[219,226,227] and cognitive flexibility[217,228] as well as working memory[188,217,221,226,229–231]. Studies have related some executive function deficits to presence of frontal lobe lesions[226,227,232], and a publication that used cognitive screening found the Test of Variables of Attention task was sensitive and specific to identify 86% of children with SCI[233]. There are fewer studies comparing those with no evidence of SCI and sibling controls; the results are mixed. Patients with normal MRI were found to have deficits in visuomotor functions compared to siblings[226,227], while other studies found no differences between those two groups in sustained visual attention[203], working memory[221] or set-shifting[217]. A study of neurologically intact adults with SCD showed deficits in processing speed, working memory and other executive functions compared to controls[234].

2.4.3 Neurocognitive biomarkers

Some indices of disease severity play a role as biomarkers of cognitive functioning. The most commonly reported marker is anaemia, usually measured by haematocrit or haemoglobin levels. Low daytime oxygen saturation may reflect state of chronic hypoxia, and haemoglobin levels are likely to act as a surrogate marker for reduced oxygen delivery to the brain[234]. In neurologically intact children (*i.e.* without cerebrovascular abnormalities), anaemia severity has shown moderate to large correlations with intelligence[113,194,218,235], and may even be related to verbal short-term memory[231] and severity of cognitive impairments in children with SCI[194,218]. Anaemia may also interact with social/environmental factors such as socioeconomic status[236]. Low nocturnal peripheral oxygen saturation was associated with reduced performance on the Tower of London test, which measures strategic planning and rule-learning[162].

Associations have been found between elevated TCD velocities and performance on sustained attention[237] and executive functioning[228,238], as measured by the Behavioural Rating Inventory of Executive Function by a parent.

2.5 Conclusion

This chapter has overviewed neurological and neurocognitive complications associated with SCD. Research has shown ischaemic events significantly impact brain development and function. However in children with no imaging evidence of ischaemic stroke or SCI, it is still unclear what chronic disease-specific effects, such as anaemia and hypoxia, have on the brain. The scope of this thesis is to use quantitative MRI analysis and neuropsychological testing to investigate any neurological differences between patients and their siblings that may underpin the effect of chronic illness.

Chapter 3. Methods

This thesis includes three different cohorts of children and adults with SCD. Participants recruited during the studentship (2012-2013 London Cohort) will be described in this section, while participants from retrospective studies at UCL Institute of Child Health and participants included from the multicentre SIT trial will be described in their corresponding chapters.

Details of participant recruitment, MRI protocol and radiology assessment, cognitive assessment and additional information will be discussed here.

3.1 2012-2013 London Cohort Participant Recruitment

The 2012-2013 London Cohort of SCD patients and their sibling controls were recruited from different ethical approval applications and different NHS sites across London. **Figure 3-1** outlines the participant recruitment.

Inclusion criteria for recruitment were children older than 8 years and adults with sickle cell disease (encompassing genotypes HbSS and HbSC). All participants were screened for any contraindications for MRI by prior telephone conversation with parents. Informed consent was given for all participants prior to MRI and cognitive assessment.

3.1.1 MSc Project: Executive Function – Impact of Pain

The first participants in this cohort were previously recruited in 2011 as part of an MSc project investigating the effect of pain on executive functioning in children with SCD. Included in the ethics were neuropsychological assessment of intelligence and executive functions, questionnaires regarding the child's current pain and MRI investigation. Ethical approval was granted by Southampton Research Ethics Committee (11/H0502/5) and fully informed consent was taken from all patients and their parent/guardian.

Demographics are reported in **Table 3-1**. Participants were recruited from four London sites:

- North Middlesex University Hospital NHS Trust (10 patients, 4 controls),
- Whittington Hospital NHS Trust (16 patients, 4 controls),
- Guy's and St Thomas' NHS Foundation Trust (1 patient, 2 controls), and
- St Mary's Hospital Imperial College NHS Trust (1 patient, 2 controls).

2011 MSc Project	n	Age	Gender	Genotype
Patients	28	9-16 years	17M, 11F	28 HbSS
Controls	12	9-18 years	7M, 5F	6 HbAS, 5 HbAA 1 unknown

Table 3-1. Details of demographics for the participants recruited from the 2011 MSc Project.

3.1.2 Longitudinal Project

In 2012, ethical approval was granted by Portsmouth Research Ethics Committee (13/SC/0042) to recruit and scan patients and sibling controls from three cohorts of children and adults with SCD (2000-2001 Baby cohort[239,240], Non-randomised SIT trial patients[160,186], and 2000-2002 East London cohort[199,241], originally recruited from 1991-1994) as part of a longitudinal follow-up investigation. Each cohort varied in age and details of original study protocol.

❖ **2000-2001 Baby Cohort**

An original infant cohort of 14 patients and 14 controls from the Royal London Hospital, East London between 2000 and 2001 were selected for follow-up. Studies investigating neurodevelopmental delay and precursors of executive function from this cohort have been published[239,240].

From the original patient cohort, 10 patients were recruited to the 2012-2013 London Cohort (1 parent refused participation, 3 patients moved away from London). Two of the 14 original controls were recruited, together with 2 contemporaneous sibling controls. Demographics are reported in **Table 3-2**.

2000-2001 Baby Cohort (Royal London)	n	Age	Gender	Genotype
Patients	10	12-13 years	7M, 3F	10 HbSS
Controls	4	8-19 years	1M, 3F	2 HbAS, 2 HbAA

Table 3-2. Details of demographics for the participants of the London 2012-2013 cohort, originally from the 2000-2002 Baby Cohort, recruited from the Royal London hospital.

❖ Non-randomised SIT Trial Patients

Patients screened, but not randomised, from London centres of the SIT trial were recruited. SIT trial screening MRI investigation was performed at Great Ormond Street Hospital between 2005 and 2010. Reasons for non-randomisation to the trial were absence of baseline SCI or refused participation.

Only patients from Royal London hospital were recruited, as part of the R&D approval. Nine patients were recruited out of a possible 20: 1 patient refused participation, 1 patient died, 6 patients could not be contacted, and 3 patients were already recruited from the 2000-2001 Baby Cohort. One sibling patient and 4 contemporaneous sibling controls were recruited from the Royal London Hospital. Demographics are reported in **Table 3-3**.

Non-randomised SIT Cohort (Royal London)	n	Age	Gender	Genotype
Patients	10	10-18 years	3M, 7F	9 HbSS, 1 HbSC
Controls	4	8-18 years	2M, 2F	4 HbAA

Table 3-3. Details of demographics for the participants of the London 2012-2013 cohort, originally not randomised to the SIT trial, recruited from the Royal London hospital.

❖ 2000-2002 East London Cohort

Patients from the original East London cohort were first scanned in the 1990s[217], and returned again between 2000-2002 for MRI investigation at Great Ormond Street Hospital. Data from this first follow-up cross-sectional study has been published focusing on aspects such as the role of event-related potentials[241] and the detection of brain abnormality using MRI-based voxel-based morphometry[199].

For the third time point of this cohort, only patients from Royal London hospital were recruited, as part of the R&D approval. Out of 19 patients identified still at Royal London hospital, 13 patients were recruited. One patient refused participation and five patients could not be contacted. From 12 original sibling controls, one sibling returned, and 2 familial controls (*i.e.* cousins) were also recruited. Demographics are reported in **Table 3-4**.

2000-2002 East London Cohort (Royal London)	n	Age	Gender	Genotype
Patients	13	18-35 years	8M, 5F	11 HbSS, 2 HbSC
Controls	3	20-29 years	3M	2 HbAS, 1 unknown

Table 3-4. Details of demographics for the participants of the London 2012-2013 cohort, originally from the 2000-2002 East London cohort, recruited from the Royal London hospital.

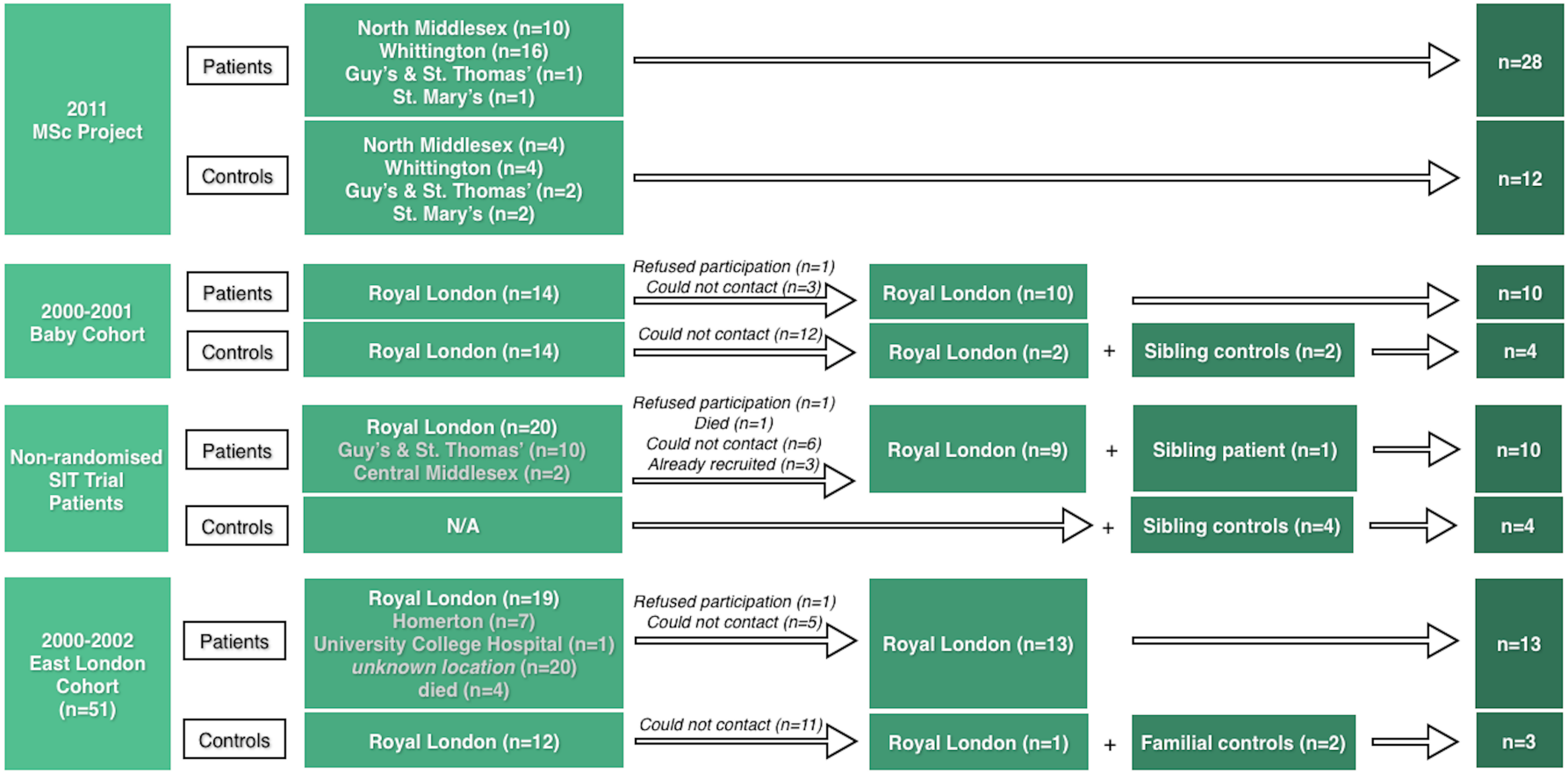

Figure 3-1. Recruitment flow chart diagram for 2012-2013 London Cohort.

3.1.3 Final 2012-2013 London Cohort Sample

The final sample consists of 61 patients and 23 controls; demographics are report in **Table 3-5** and histogram of age distribution is shown in **Figure 3-2.**

	n	Age	Gender	Genotype
Patients	61	8-35 years	35M, 26F	58 HbSS 3HbSC
Controls	23	8-29 years	13M, 10F	11 HbAA 10 HbAS 2 unknown

Table 3-5. Demographics for final 2012-2013 London Cohort sample, consisting of the participants from the 2011 MSc Project and the Longitudinal Project.

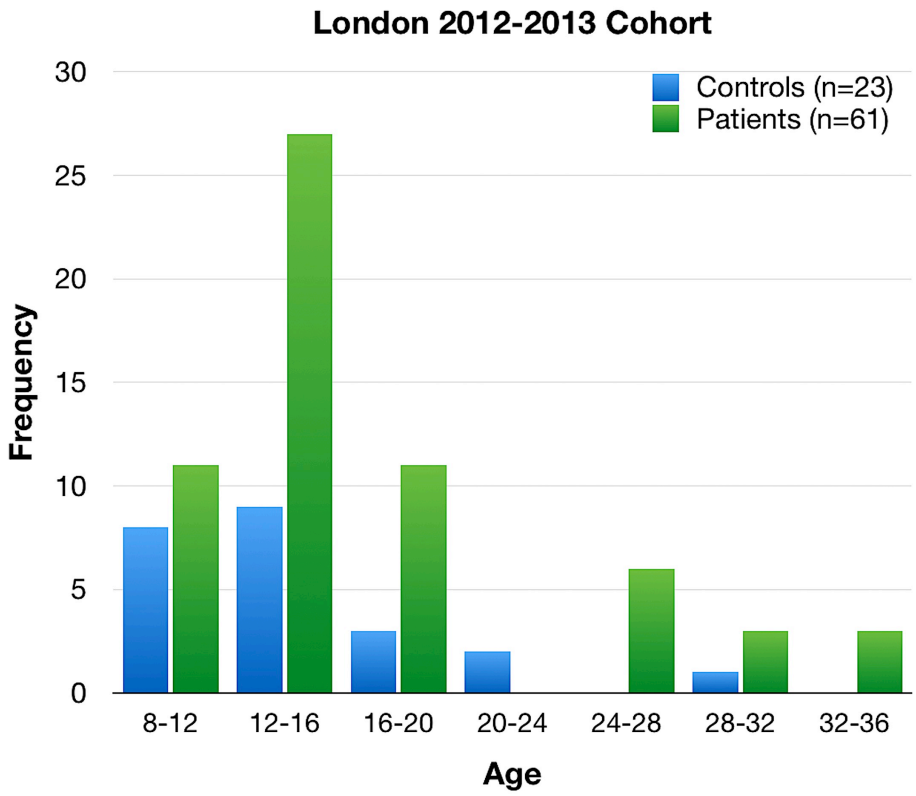

Figure 3-2. Age distribution histogram for final 2012-2013 London Cohort sample, consisting of the participants from the 2011 MSc Project and the Longitudinal Project.

3.1.4 MRI Protocol & Radiology

All participants were scanned at Great Ormond Street Hospital on a 1.5T Siemens Magnetom Avanto system (Siemens, Erlangen, Germany) with 40mT/m gradients and a 32-channel receive headcoil. The following sequences were acquired:

- T1-weighted Fast Low Angle Shot (FLASH) 3D volume (TR= 11ms, TE= 4.94ms, flip angle= 15, voxel size= 1mm^3)
- T2-weighted turbo spin echo sequence (TR= 4920ms, TE= 101ms, voxel size= 0.7 x 0.6 x 4.0mm, slice gap=1.6mm)
- Diffusion-weighted echo planar imaging sequence (TR= 7300, TE= 81ms, voxel size= 2.5mm^3, 60 gradient directions, b=1000s/mm^2, 3 interleaved b=0 images).

All images were visually inspected for artefacts (*e.g.* movement, dental braces), and certain sequences were excluded if necessary. Two independent, experienced neuroradiologists (S.B.[‡], T.C.[§]) read all participants' T2-weighted MRI for lesion diagnosis. In the circumstance of conflicting reports, a third neuroradiologist (D.S.[**]), read the images blind to initial reports. Participants were excluded from analysis if no T2-weighted image was available (n=2).

3.1.5 Lesion size analysis

For the participants in whom abnormal T2s were documented, lesion masks were manually drawn and deemed accurate by agreement of two neuroradiologists. Lesion size was calculated using FMRIB Software Library (FSL)[242]; the size of the voxel multiplied by the slice gap outputs the volume in mm^3.

3.2 Cognitive Assessment

All participants underwent cognitive assessment by trained researchers at the UCL Institute of Child Health. Participants were given:

- **Wechsler Abbreviated Scale of Intelligence (WASI)**[243], a standardised abbreviated version of the Wechsler Intelligence Scale for Children (WISC-III) and the Wechsler Adult Intelligence Scale-Third Edition (WAIS-III). In this study, the two-subtest

[‡] Simon Barker MB ChB, MRCP, FRCR – consultant radiologist (University Hospital Southampton, UK)
[§] Tim Cox MBBS FRCR – consultant radiologist (Great Ormond Street Hospital, London, UK)
[**] Dawn Saunders MD FRCR – consultant paediatric neuroradiologist (Great Ormond Street Hospital, London, UK)

(vocabulary, matrix reasoning) WASI is used, providing full-scale intelligence quotient (FSIQ). Scores are scaled for developmental stage, with a mean of 100 and standard deviation of 15. The WASI is appropriate for children older than 6.

Delis-Kaplan Executive Function System (D-KEFS)[244] is a 90-minute battery for people older than 8 years, which provides reliable and valid measure of executive functions[245,246]. Four standalone tests were used:

- **D-KEFS Tower test** measures strategic spatial planning, rule learning, impulse inhibition and establishing and maintaining cognitive set. The test requires participants to build a series of 9 progressively difficult towers, with a three-pegged base and 5 sizes of coloured discs. For each tower, the participant is given a prearranged set of disks and a picture of what the finished tower should look like, and instructed to build the tower shown in the picture using as few moves as possible. The rules are that only one hand may move the discs and a larger disc cannot be placed on a smaller disc. Total achievement score is based on number of moves and number of completed towers within the time limit, and scaled scores are reported (mean 10, standard deviation 3).

- **D-KEFS Trail-making test – visual scanning condition** measures visuomotor processing speed and attention. In this task, the subject is presented with an A3 landscape page with various circles of different numbers and letters, and asked to make a single mark through all the circles with the number "3", as fast as possible without making mistakes (Appendix A). Completion time is recorded and scaled scores are reported (mean 10, standard deviation 3).

- **D-KEFS Trailmaking test – number-letter switching condition** requires cognitive flexibility, attentional-set shifting and motor speed. In this task, the subject is presented with an A3 landscape page with various circles of different numbers and letters, and asked to draw lines to connect circles with letters and numbers, switching between letter and number (*i.e.* "1-A-2-B-3-C" etc.; Appendix A). Completion time is recorded and scaled scores are reported (mean 10, standard deviation 3).

- **D-KEFS Verbal Fluency test – letter fluency condition** measures systematic retrieval of lexical items and processing speed. In this task, the subject is given 60 seconds to say as many words as he/she can that start with a particular letter (*e.g.* "T"), without giving the names of people's names (*e.g.* "Tom", place names (*e.g.* "Tottenham") or numbers (*e.g.* "Twelve). Total score is calculated as the sum of

correct responses over three sets of this task, and scaled scores are reported (mean 10, standard deviation 3).

- **D-KEFS Colour-Word Interference – inhibition/switching condition**, a version of the commonly known Stroop test, measures naming speed, reading speed, verbal inhibition and cognitive flexibility. The subject is given a page with names of colours written in the same ink colour to the words that are printed, and words written in dissonant ink colours to the words that are printed. In this condition, the subject is asked to switch back and forth between naming the dissonant ink colours and reading the words (Appendix A). Completion time is recorded and scaled scores are reported (mean 10, standard deviation 3).

- **The Behaviour Rating Inventory of Executive Functions (BRIEF)** is a parent questionnaire for children younger than 18, consisting of 86 items in eight non-overlapping behavioural regulation and metacognition clinical scales (Appendix A). The Global Executive Composite score takes into account all the clinical scales and represents the child's overall executive function. BRIEF scaled scores are reported (mean of 50 and standard deviation of 10), where higher scores represent more dysfunction.

3.3 Additional information

On the day of the scan, additional information was asked of participants' guardians (or the adult participant himself or herself), regarding handedness, if the participant was on regular blood transfusion treatment or hydroxycarbamide treatment, if the participant was taking pain medication regularly and how often the participant experienced severe pain episodes, including hospitalisations for pain crises.

3.3.1 Oximetry

On the day of the MRI, peripheral oxygen saturation data was collected over a 5-minute period from a pulse oximeter (Masimo Pronto-7 Pulse CO-Oximeter). This involved making sure the participant was seated at rest and was feeling generally well. Data were excluded if the participant had false acrylic nails (n=1) or if the pulse oximeter did not produce data (n=1).

3.3.2 Haematology

Clinical data from relevant medical records were collected at the discretion of each patient's consultant haematologist. Dates of hospitalisations, treatment history and full blood counts and pulse oximetry readings from clinical notes from up to three years prior to MRI were collected.

3.4 Considerations for Statistical Power

All participants recruited as part of the London 2012-2013 originally had taken part in previous studies at the Institute of Child Health/Great Ormond Street Hospital. It is possible the sample is limited by a sampling convenience bias and results from this thesis may not be representative or generalizable to a greater population of SCD patients.

Statistical power refers to the ability of a sample size to detect a meaningful effect size between groups. If there is inadequate power, one may not be able to detect a difference when it actually exists.

There was no information about past neuroimaging results during the recruitment process; due to the nature of clinically silent cerebral infarcts, it was impossible to gauge how many participants would be allocated to MRI-defined groups. Although there were no prospective sample size or power calculations estimated before recruitment started for this thesis, I intended to achieve adequate statistical power by recruiting as many participants possible to increase sample size in all groups.

Statistical power for the observed effect sizes were calculated where appropriate, and sample size considerations are discussed in context.

3.5 Conclusion

This chapter overviewed the methods of participant recruitment, MRI protocol, radiology assessment and neuropsychological assessment. These methods underlie the following four chapters, which will discuss specific analysis and results.

Chapter 4. Intelligence Quotient in Asymptomatic Children with Sickle Cell Disease

Intelligence quotient is the most commonly reported and widely studied standardised measure of cognitive ability in SCD. Beginning from the late 1980s/early 1990s, many studies have reported patients having lowered global intelligence scores than matched controls, even when excluding those with history of stroke or abnormal neurological examination[102,213–215,247,248].

As mentioned in chapter 2, up to 35% of children with SCD will experience at least one SCI in the first decade of life, in which there is an abnormality seen on T2-weighted MRI in the absence of overt stroke (neurological symptoms lasting more than 24 hours). By definition, SCI are clinically silent and therefore age at which SCI occurred and time lapse between SCI and cognitive testing are unknown. Presence of SCI has been associated with general cognitive dysfunction[104], as well as specific deficits in executive functions, including sustained attention, cognitive flexibility and working memory[217,219,227,232,233].

The first study that used MRI to classify patients into groups based on whether SCI are present or absent was published in 1996[104]. Collaborators in the United States CSSCD linked presence of abnormality on MRI and measurable global cognitive dysfunction. Since then, several studies looking at intelligence have confirmed that children with SCI (SCI+) perform worse than those without evidence of SCI (SCI-)[199,203,216,218,220,223], including one CSSCD study that reported presence of SCI was associated with decreases in IQ over a period of 8-16 cross-sectional years[220]. Some have reported that larger lesion size in SCI+ patients is associated with lower FSIQ[221,249], suggesting there may be a threshold of injury severity associated with lowered IQ[224].

There are fewer publications that had included a control population to investigate differences in IQ between individuals with SCD who have normal MRI and those without SCD. These studies are necessary to elucidate differences in neurocognitive outcome that may be due to subtle aspects of the disease, such as chronic anaemia and hypoxia[250], and attempt to separate them from sociological and environmental effects. Within those studies that have used a control group, some have used pseudo-controls (*i.e.* normative databases[106,216]) that may not be appropriately matched for non-neurological factors known to influence intelligence, such as socioeconomic status[251], parental education[252] and school absences[220].

4.1 Hypotheses

The purpose of this chapter is to review the literature on intelligence in relation to SCI and other factors in children with SCD. To be eligible for review, the study must have included a paediatric SCD population, used MRI to define presence of absence of SCI and/or stroke and used a Wechsler intelligence scale measure that reported FSIQ.

Beyond the review, this chapter also includes previously unreported data from the 2012-2013 London cohort, including a sibling control group, which will be used to test hypotheses based on the review of the existing literature. The following hypotheses are tested:

- There is a stepwise progression of decreasing IQ with lesion status: (*i.e.* SCI+ patients will have lower FSIQ than SCI- patients, and SCI- patients will have lower mean FSIQ than the sibling control group), and
- Lesion size in SCI+ patients will correlate with FSIQ.

4.2 Methods

Sixteen publications are included in this review (Table 4-1). This review is supplemented by 48 SCD patients and 19 sibling controls (aged 8-18) from the 2012-2013 London cohort. In the patient group, three MRI-defined subgroups were identified from T2-weighted MRI:

- Those with previous history of stroke (n=4; all male; mean age: 15.44 years ± 3.02),
- Those with evidence of SCI (n=13; 8 male; mean age: 14.14 years ± 2.48), and
- Those with no evidence of SCI (n=31, 16 male; mean age: 13.29 years ± 2.70).

4.2.1 Statistical Analysis

To test differences between groups, an analysis of variance was performed. A post-hoc least significant difference (LSD) that uses *t*-tests for pairwise comparisons between group means was used. Bivariate Pearson's *r* correlations were performed between lesion size and FSIQ.

4.3 Results

4.3.1 FSIQ Scores Across All Studies

All sixteen studies included SCI- and SCI+ groups, six studies included a group with history of stroke, and six included a control group (Table 4-1 and Figure 4-1).

All studies that reported FSIQ in stroke patients found scores were considerably lower than other groups of SCD patients; four of six studies reported significantly lower scores[104,219–221]. Mean FSIQ in those with stroke ranged from 65.9[221] to 76.9[220], almost two standard deviations lower than the healthy population mean derived from Wechsler manuals.

For the patients with evidence of SCI, mean FSIQ scores ranged from 70.6[216] to 93.12[252]. Four studies showed SCI+ patients had a significantly lower FSIQ scores than SCI- patients (effect sizes ranged -0.56 - -0.79)[199,216,220,252], and one study with a nonsignificant difference between SCI+ and SCI- also showed a moderate effect size of -0.61[217]. However, four other studies found no statistical difference between SCI+ and SCI- patients with small effect sizes of -0.23[218], -0.45[253], 0.29[188] and -0.08[231].

Six studies included in this literature review included a control group (Table 1, Figure 4-2). Two studies that used a normative database of matched controls found SCI- patients to have significantly lower mean FSIQ, with moderate to large effect sizes (-0.63[216] and -0.99[106]). The remaining four studies recruited matched controls contemporaneously with patients. Two studies used a sibling group[217,218], one study used a control group in which half of the total participants were siblings[199], and one study used age-, gender- and socioeconomic status-matched controls[221].

Of the two studies that used a sibling control group, one found a nonsignificant 6-point lower mean FSIQ in patients than controls with an effect size of -0.5[217] and the other found SCI- patients had a 4-point reduction in FSIQ; although but statistical difference was not tested[218]. The effect size was calculated as -0.23.

Of the other two studies, one with 39% (12/31) sibling controls found a significant 9-point difference in FSIQ with an effect size of -0.73[199]. Finally, in the study using a matched, non-sibling control group, there was a nonsignificant 3-point reduction in the SCI- group compared to controls (effect size of 0.26)[221].

None of these studies analysed the relationship between lesion volume in SCI+ patients and FSIQ.

Author(s)	Patient Group	Patient Subgroups	Control Group	Battery	Control FSIQ: mean (sd)	SCI- FSIQ: mean (sd)	SCI+ FSIQ: mean (sd)	Stroke FSIQ: mean (sd)	Notable Findings
Armstrong *et al.* (1996)	HBSS/HbSC (n=194)	n=9 stroke n=24 SCI+ n=161 SCI-	none	WISC-R	N/A	90 (1.7)	82.8 (2.9)	70.8 (5)	Stroke < SCI+ (FSIQ, PIQ) Stroke < SCI- (FSIQ, PIQ, VIQ)
Steen *et al.* (1998)	SCD (n=22)	n=10 SCI+ n=12 SCI-	n=30 from "historical data of healthy siblings"	WISC-R WISC-III	88 (16.1)	78.9 (8.9)	70.6 (12.1)	N/A	SCI+ < SCI- and controls (FSIQ) SCI- < controls (FSIQ) controls < population mean
Watkins *et al.* (1998)	SCD (n=39)	n=5 stroke n=4 SCI+ n=30 SCI-	n=15 sibling controls	WISC-III WPPSI-R	92.07 (12.2)	86.03 (12)	79 (5.7)	67.6 (16.6)	Stroke < SCI- and controls (VIQ, PIQ, FSIQ) SCI+ < SCI- < controls (nonsignificant)
Bernaudin *et al.* (2000)	SCD (n=173)	n=12 stroke n=20 SCI+ n=101 SCI-	n=76 sibling controls	WISC-III WPPSI-R	90.3 (14.3)	86.6 (17.1)	82.6 (15.7)	73.5 (14.4)	SCI+ < SCI- (VIQ) *no statistical comparison between SCI- and controls.
Brown *et al*. (2000)	HbSS/HbSC (n=63)	n=22 stroke n=11 SCI+ n=30 SCI-	none	WISC-III	N/A	81.67 (16.68)	81.91 (14.43)	75.05 (15.53)	Stroke < SCI+ and SCI-
Wang *et al.* (2001)	HbSS (n=185)	n=20 stroke n=43 SCI+ n=122 SCI-	none	WISC-R WISC-III	N/A	84.8 (13.5)	77.2 (13.7)	76.9 (17.2)	Stroke < SCI+ and SCI- (FSIQ, VIQ, PIQ) SCI+ < SCI- (FSIQ, VIQ)

Author(s)	Patient Group	Patient Subgroups	Control Group	Battery	Control FSIQ: mean (sd)	SCI- FSIQ: mean (sd)	SCI+ FSIQ: mean (sd)	Stroke FSIQ: mean (sd)	Notable Findings
Schatz *et al.* (2002)	HbSS (n=27)	n=18 SCI+ n=9 SCI-	none	WASI	N/A	89.9 (7.9)	81.9 (12.4)	N/A	*no statistical comparison between SCI+ and SCI- Larger lesion volume associated with lower FSIQ
Steen *et al.* (2003)	HbSS (n=49)	n=16 SCI+ n=33 SCI-	none	WISC-R WISC-III	N/A	81.1 (11)	78.6 (16.1)	N/A	In patients, FSIQ decreased with age SCI+ < SCI- (VIQ)
Steen *et al.* (2005)	HbSS (n=54)	n=24 SCI+ n=30 SCI-	standardised matched sample from the WISC-III	WISC-III	91.37 (12.19)	79.4 (11.9)	excluded from analysis	N/A	SCI- < controls (FSIQ)
Baldeweg *et al.* (2006)	HbSS/HbSC (n=36)	n=16 SCI+ n=20 SCI-	n=31 (12 siblings)	WISC-III WAIS	101 (11)	92 (14)	82 (13)	N/A	SCI+ < SCI- (FSIQ, VIQ, PIQ) SCI- < controls (FSIQ, VIQ)
Hogan *et al.* (2006)	SCD (n=30)	n=17 SCI+ n=13 SCI-	none	WISC-III WAIS-R	N/A	87.4 (8.1)	82.5 (12.5)	N/A	No difference between SCI+ and SCI- (FSIQ)
Kral *et al.* (2006)	HbSS (n=27)	n=5 SCI+ n=22 SCI-	none	WASI	N/A	87.59 (11.42)	90.60 (3.05)	N/A	No different between SCI+ and SCI- (FSIQ) Negative association between chronologic age and FSIQ
Schatz & Buzan (2006)	HbSS (n=28)	n=8 stroke n=8 SCI+ n=12 SCI-	n=16 matched controls	WISC-III	97.9 (11.8)	94.5 (14.2)	92.9 (12.8)	65.9 (14.8)	Stroke < SCI- and controls (FSIQ)

Author(s)	Patient Group	Patient Subgroups	Control Group	Battery	Control FSIQ: mean (sd)	SCI- FSIQ: mean (sd)	SCI+ FSIQ: mean (sd)	Stroke FSIQ: mean (sd)	Notable Findings
Hijmans *et al.* (2011)	HbSS/HbS β-thalassaemia (n=34)	n=12 SCI+ n=9 SCI-	none	WISC-III WAIS-III	N/A	80 (9)	79 (14.4)	N/A	No difference between SCI+ and SCI- (FSIQ)
Hollocks *et al.* (2012)	HbSS (n=10)	n=1 SCI+ n=9 SCI-	none	WASI	N/A	87 (16.12)	*Excluded from analysis*	N/A	SCI- FSIQ in the low average range
King *et al.* (2014)	HbSS/HbS β-thalassaemia (n=150)	n=107 SCI+ n=43 SCI-	none	WASI WPPSI-III	N/A	100.53 (13.08)	93.12 (12.5)	N/A	SCI+ < SCI- (FSIQ) Negative association between chronologic age and FSIQ
2012-2013 London cohort (previously unreported)	HbSS/HbSC (n=64)	n=31 SCI- n=13 SCI+ n-4 stroke	n=19 sibling controls	WASI WASI-II	107.79 (11.78)	99.81 (13.48)	93.46 (10.70)	96.75 (8.62)	SCI+ and SCI- < Controls No significant difference between SCI+ and SCI- No correlation between lesion size and FSIQ or age

WISC, Wechsler Intelligence Scale for Children; WISC-R, Wechsler Intelligence Scale for Children-Revised; WPPSI-R, Wechsler Preschool and Primary Scales of Intelligence - Revised; WASI, Wechsler Abbreviated Scale of Intelligence; WAIS, Wechsler Adult Intelligence Scale

Table 4-1. Review of FSIQ literature in paediatric SCD using MRI-defined groups.

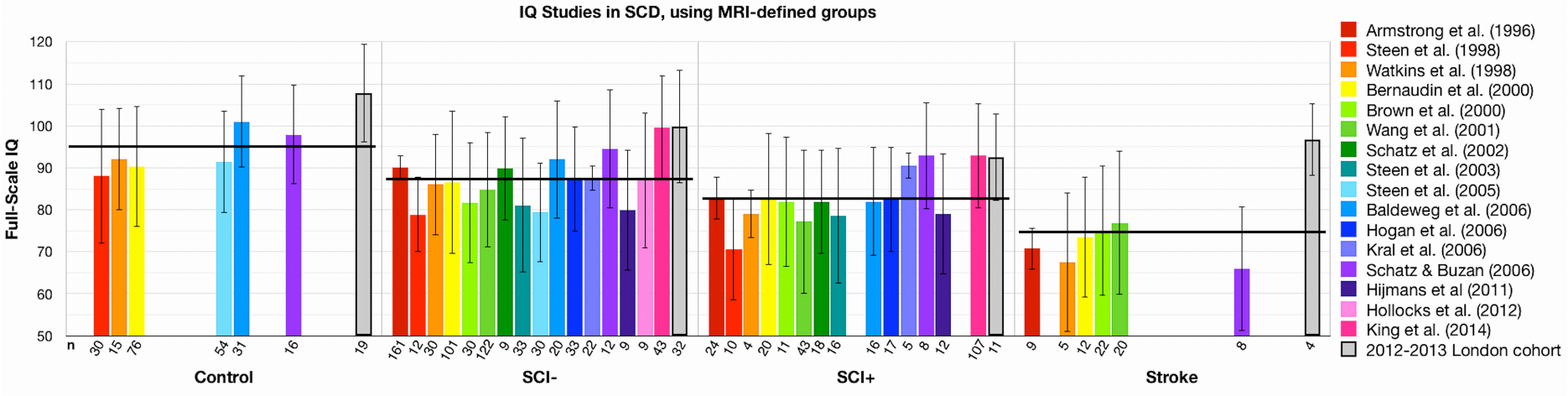

Figure 4-1. Review of FSIQ literature in paediatric SCD using MRI-defined groups. Horizontal black lines represent mean FSIQ of the entire group, including previously unreported data from the 2012-2013 London cohort. Italicised numbers on x-axis indicate number of subjects in each group.

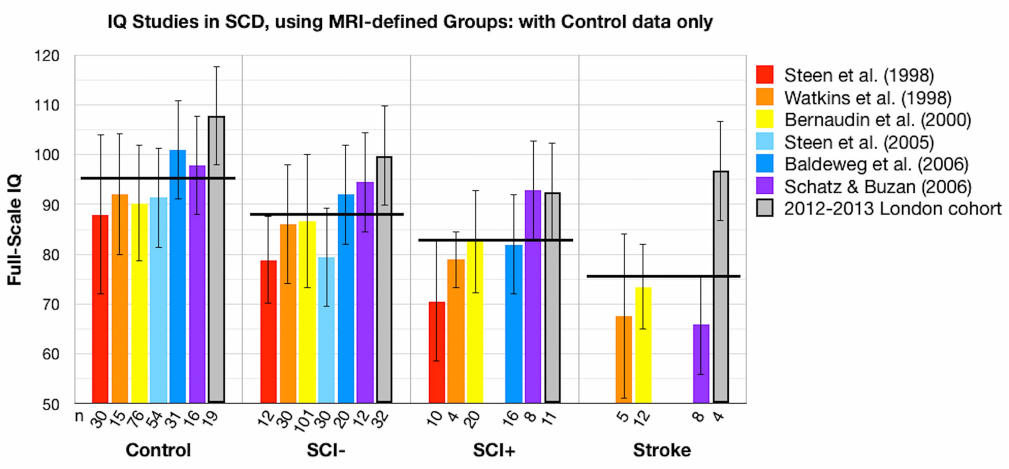

Figure 4-2. Review of FSIQ literature in paediatric SCD using MRI-defined groups, in which only studies that used non-SCD control groups were included. Horizontal black lines represent mean FSIQ of the entire group, including previously unreported data from the 2012-2013 London cohort. Italicised numbers on x-axis indicate number of subjects in each group.

4.3.2 Previously Unreported Data

FSIQ results from the 2012-2013 London Cohort sample are reported in Table 4-2. Mean FSIQ for the control group was 107.79 ± 11.78, for the SCI- patient group was 99.81 ± 13.48, for the SCI+ patient group was 93.46 ± 10.70, and for the stroke patient group was 96.75 ± 8.62. Figures 4-1 and 4-2 show a graphical representation of the current study group means in relation to the previously reported data from sixteen studies under review. While the SCI- and SCI+ groups' data fall within the range of previously reported FSIQ of similar groups, the sibling control group mean is higher than previous studies, and 7 points higher than the population mean. The SCI- and SCI+ group means are within normal intelligence ranges. Similarly, the stroke group mean FSIQ is nearly 20 points higher than the highest previously reported data, although there are only 4 patients comprising the group.

The stroke group was excluded from further analysis due to low subject numbers. An analysis of variance showed significant differences between the three groups (controls, SCI-, SCI+: ANOVA F=5.335, p=0.007), with the controls group having significantly higher FSIQ than the SCI- group (7.98 mean point difference; *t*=2.129, p=0.032, effect size= 0.62) and the SCI+ group (14.33 mean point difference; *t*=3.505, p=0.002, effect size=1.26). There was no significant difference between the SCI- and SCI+ groups (*t*=1.506, p=0.140, effect size=0.50). (Table 4-2)

	Control	**SCI-**	**SCI+**		p
n	19	31	13		
Genotype	11 HbAA 8 HbAS	31 HbSS	12 HbSS 1 HbSC		
Age	12.72 ± 3.12	13.29 ± 2.70	14.14 ± 2.48	ANOVA F=0.947	p=0.394
Gender	9M, 10F	16M, 15F	8M, 5F	χ^2=0.636	p=0.728
FSIQ	107.79 ± 11.78	99.81 ± 13.48	93.46 ± 10.70	ANOVA F=5.335	p=0.007[b,c]
[a]SCI+ < SCI-, [b]SCI+ < Controls, [c]SCI- < Controls					

Table 4-2. Demographics and FSIQ scores of the 2012-2013 London cohort.

Although the difference in means was significant (p=0.032) between control and SCI- groups, the statistical power for the moderate effect size (*d*=0.62) was 55%. In order to achieve 80% power, 42 participants would have been required in each group.

There was no significant difference in means between the SCI- and SCI+ groups. The statistical power for the moderate effect size (d=0.50) was 32%; 64 participants would have been required to achieve 80% power.

4.3.3 Lesion size and FSIQ

In the SCI+ subjects, lesion size and FSIQ data are shown in Table 4-3. The locations of the lesions varied: 69% (9/13) had lesions in the frontal lobe, 54% (7/13) in the parietal lobe, and 46% (6/13) had lesions in more than one lobe. Two patients had lesions in subcortical regions (head of caudate, cerebellum). One extreme outlier (Subject 13) was excluded from lesion size analysis due to diffuse lesions. In the remaining 12 SCI+ patients, there was no significant correlation between lesion size and FSIQ (r=0.068, p=0.833) or age (r=-0.188, p=0.558).

	Gender	**Age (years)**	**Lesion Location**	**Lesion Size (mm^3)**	**FSIQ**
1	M	16.49	L Frontal	41.36	104
2	M	12.94	R Frontal	58.82	89
3	M	10.64	R Corpus Callosum	64.33	104
4	M	18.58	Bilateral Cerebellar, L Parietal	91.69	92
5	M	12.86	L Head of Caudate	108.45	95
6	F	17.90	R Frontal	128.67	94
7	M	12.56	L Parietal and Frontal	147.71	72
8	F	16.77	R Parietal and Frontal	189.33	97
9	F	14.02	R Parietal and Frontal	205.87	88
10	F	12.47	R Parietal	275.72	107
11	M	12.01	Bilateral Frontal, L Parietal	443.82	76
12	F	13.93	Bilateral Frontal	755.46	105
13	M	12.69	Bilateral Frontal and Parietal, Left Occipital	11449.58	92

Table 4-3. Lesion size and location of SCI+ patients.

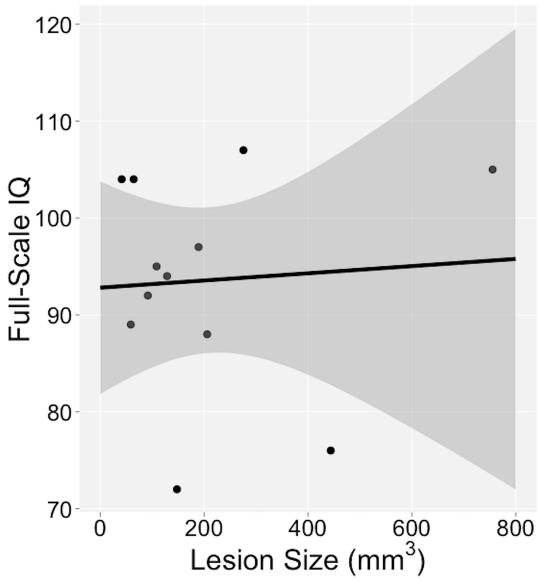

Figure 4-3. Lesion size and FSIQ plot. There was no significant correlation between size of lesion (mm^2) and full-scale IQ in 12 SCI+ patients.

4.4 Discussion

The results from the previously unreported data are in line with aforementioned research: both SCD patients with or without SCI have significantly lower FSIQ than sibling controls. Further, this study found no significant difference in FSIQ between patients with or without SCI, although there was a moderate effect size suggesting that patients with SCI performed worse than those without. These results suggest that presence of lesions, or lesion size alone, may not account for differences in general cognitive ability, and other mediating factors potentially relating to the disease process could play a role.

4.4.1 Neuroimaging Correlates of IQ

There has been some groundwork in finding neuroimaging correlates of intelligence in the paediatric SCD literature. One study split patients into a high- and low-IQ group, using the Kaufman's Brief Intelligence Test; the authors found children in the low-IQ group had smaller grey matter volume in bilateral frontal, temporal and parietal lobes compared to the high-IQ group[201]. Schatz and Buzan[221] found that the size of the corpus callosum on the midsagittal section was reduced in patients with SCI compared to those without, but the size of the corpus callosum provided no explanatory power for general cognitive function. However, these studies did not take into account any factors known to influence both brain

morphometry and IQ. In contrast to a report of poor correlation between TCD velocity and FSIQ[238], a strong, inverse correlation has been found between performance IQ and FSIQ and bilateral cerebral blood flow (CBF) by perfusion MRI[254], with the strongest association between anterior and right-sided CBF and performance IQ. The authors suggest measures of performance IQ may be sensitive to global oxygen delivery.

4.4.2 Effect of chronic disease on IQ

Previous studies have shown SCD-related markers of disease severity to correlate with intelligence. There have been links with anaemia severity[194,218,223,236]; more specifically, haematocrit[194,218] and the interaction between age and haematocrit[188], that have also been shown in non-SCD populations[255–257]. This correlation between anaemia and IQ could be due to a direct impact on the brain (*i.e.* anaemia-induced hypoxia/ischaemia) or due to indirect influences on processes such as the body's response to anaemic hypoxia exposure[258], which leads to increased cerebral blood flow[259–261] and cerebral blood flow velocity[180,253], reduction in cerebrovascular reserve[91] and subsequent large and small vessel injury/ischaemia[92]. Chronically altered cerebral circulation may lead to a cycle of long-term hypoxia[194] and cognitive dysfunction[262]. Other SCD-related biomarkers previously linked to cognitive outcome include growth delays[263], possibly linked to poor nutrition[215], that may have an effect on the development and maturation of the brain[200,221].

4.4.3 Effects of Silent Infarction on IQ

Children with evidence of SCI on MRI have long been reported to have cognitive dysfunction[216,220,264], and the discrepancy in FSIQ between SCI+ and SCI- patients is approximately 4-7 points[104,218,220]. Drawing a parallel with the hypothesised pathophysiology in elderly adults in the general population, SCI in children with SCD are considered to be secondary to small vessel disease, in which white matter in the frontal lobe borderzones between the anterior and middle cerebral arteries is most affected[78]. However, in general, it is difficult to control for the effects of unilateral/bilateral infarction, number of infarcts and when they occurred. In a study looking specifically at the influence of lesion burden on intelligence[224], small infarct volume appeared to have minimal impact on global cognitive ability but larger volume was associated with lowered FSIQ scores in eight patients with SCI. This study suggests there may be a threshold of lesion size before IQ is affected. Our results with a slightly larger sample size of twelve indicate no significant relationship between quantitative lesion size and FSIQ. While all of the patients had relatively small lesions, one patient had very large, diffuse lesions, yet with an IQ still in the normal range. As Schatz and colleagues[224] suggest, only a longitudinal study in a large group of paediatric

SCD patients with SCI could demonstrate if SCI is associated with progressive decline in IQ.

The data from SCI+ patients in this sample are typical of previous reported studies: small sample size and unknown information such as age when SCI occurred and time lapse between study MRI and age when SCI occurred. It is likely that patients experience repeated infarction[78,265], and large lesion size due to one event or repeated events may result in different cognitive profiles.

Other populations also experience SCI in childhood due to chronic conditions. People with obstructive sleep apnoea or people living in high-altitude locations may have white matter abnormality[266] and cognitive dysfunction[267–269]. Obstructive sleep apnoea can also be comorbid with SCD[270,271], which may exacerbate hypoxia.

One study described worsening cognitive performance with presence of periventricular hyperintensities in patients with obstructive sleep apnoea[272], but to date, no studies have explicitly investigated the relationship between size of lesion and cognition in those conditions.

4.4.4 Effect of Age on IQ

There was one finding in this study that was not related to the original study hypotheses yet worthy of consideration. In a meta-analysis, Schatz and colleagues[114] suggested there is evidence of cognitive effects worsening with age. Included in the review, they found some studies reporting older children performing worse than younger children[113,210,220], but others not finding that pattern[194,211,213,214,247]. More recent reports did find a significant negative association with FSIQ and age in combined SCI- and SCI+ patients[188,221,252]. The results from the current study show a negative, but nonsignificant, correlation between age and FSIQ in patients (excluded n=4 stroke; r= -0.209, p= 0.173). When divided into MRI-defined groups, there was a positive, trend-level correlation between age and FSIQ in the SCI+ group (r= 0.141, p=0.065), but a negative, but nonsignificant correlation in the SCI- group (r= -0.277, p= 0.131). It is difficult to interpret positive and negative associations between age and FSIQ. A positive association could reflect longer time of recovery post-injury and perhaps an effect of treatment with hydroxycarbamide or regular blood transfusion for patients with SCI, while a negative association could reflect a longer time exposed to chronic hypoxia and subacute brain damage associated with acute hypoxic events such as pain crises or acute chest syndrome[113].

4.4.5 Statistical considerations

For the significant difference in IQ between Control and SCI- groups, statistical power was calculated as 55%. This implies that in replicated studies of the same sample size of different participants, a significant result will only be found 55% of the time. For the non-significant difference in IQ between SCI- and SCI+ groups, it is likely the study was underpowered (32% power calculated) and significant differences may be found by increasing sample size, in line with recent literature[252].

The exploratory correlation between lesion size and IQ was non-significant and had very low statistical power. It is possible the population correlation is actually close to zero or the sample size is far too small and the test required a far larger number of participants.

4.4.6 Limitations

This addition to the study is limited by not including details of socioeconomic status and parental education in the analysis, both widely accepted to influence a child's IQ performance[113,114,220,252]. This analysis used a sibling control group to control for those factors. However, that information is important to know to understand how the social context of the child interacts with the disease process[114] to adequately understand the cause of cognitive deficits in children without abnormal MRI findings.

Full-scale IQ was the only measure of cognitive ability discussed in this chapter because historically it has been the most widely studied. In this review, including previously unreported data, FSIQ was obtained from the versions of the WASI in four studies and the versions of the WISC in seven studies. While the WASI gives a brief measure of FSIQ from two or four subtests, the WISC FSIQ is made up of ten verbal and performance subtests. Although WASI FSIQ and WISC FSIQ are correlated[243], it is possible that FSIQ is too broad a measure to disentangle specific, subtler cognitive functions. While the Wechsler scales are a reliable measure of general cognitive ability, some argue that they fail to relate to real-world performance[273]. Academic achievement may be a more appropriate outcome measure; children with SCD suffer a chronic illness and exhibit poor school attendance, recurrent hospitalizations and economic hardship[80,220,236,251,274,275], in which functional impairment can endure into adulthood[276].

4.5 Conclusion

This chapter reviewed the FSIQ literature in paediatric SCD studies that have used MRI-defined groups to determine differences between patients with or without SCI. Although the

differences in intelligence between those with and without SCI have been more widely studied, the results from this chapter added to a gap in the literature regarding the differences between those children with no evidence of SCI and an appropriately matched sibling control group: SCD patients with and without SCI perform worse than sibling controls, although no statistical differences in FSIQ were found between SCI+ and SCI- patients.

Chapter 5. Subcortical and Cerebellar Volumetric Differences in Sickle Cell Disease

Previous studies have shown structural neuroanatomical differences between patients with evidence of silent cerebral infarcts (SCI+), patients without lesions (SCI-) and healthy controls. A voxel-based morphometry study showed that in SCI+ patients, there is evidence of bilateral white and grey matter density decreases in areas corresponding to the arterial borderzone distribution[199]. Similar white and grey matter density decreases were found in SCI- patients compared to controls, but those results were not as widespread and also nonsignificant. In a cohort of two groups of SCI- paediatric patients, one study reported significant cortical thinning in older children as compared to younger patients in the posterior medial surfaces of both hemispheres[202]. Decreased grey matter volume in bilateral frontal, temporal and parietal lobes was also found to correlate with low IQ in SCI- children[201].

Two studies have focused on subcortical grey matter. One found reduced volume of the caudate head[195], while the other found reduced volume of central grey matter (*i.e.* total basal ganglia volume)[200], but none have reported on specific subcortical volumes.

There is reason to hypothesize volumetric deficits in subcortical grey matter. SCD has been described as a model of diffuse brain injury, damaged by chronic anaemia and hypoxia[194]. Inadequate oxygenation of brain tissue is compensated for my increasing cerebral blood flow[204,259,260,277] and dilation of the cerebral vasculature. When metabolic demands increase, there may not be enough reserve to ensure sufficient oxygenation, rendering the child at high risk for cerebral ischaemia. Subcortical structures, such as the hippocampus, are particularly vulnerable to hypoxia[278,279].

5.1 Hypotheses

This chapter focuses on grey matter volumetric differences in specific, parcellated subcortical structures. An original report describing a cross-sectional analysis of the East London cohort scanned between 2001-2002, which has been published in the British Journal of Haematology in 2013[280], is located in Appendix B.

This chapter extends that previously reported data by including a follow-up analysis of a larger cohort of children and adults with SCD. By combining recent and retrospective data acquired over a ten-year period, this chapter intends to: confirm volumetric deficits in a step-wise progression according to radiological status (*i.e.* SCI+ patients have most volume

loss, followed by SCI- patients and controls), establish the natural history of subcortical volumetric development as a function of age, and determine any relationship with measures of general intelligence.

5.2 Details of Sample

Data from patients and controls aged 6-30 years were collected from:

- East London 2000-2002 retrospective cohort, described previously[199,241,280] in Chapter 3: (33 patients, 21 controls)
- London centre of the Silent Infarct Transfusion (SIT) trial screening MRI[160], scanned between 2005-2007, described previously in Chapter 3: (26 patients)
- Prospective 2012-2013 London Cohort, described previously in Chapter 3: (45 patients, 21 controls)
- Healthy controls from on-going studies at Great Ormond Street Hospital/Institute of Child Health, scanned contemporaneously with the 2012-2013 London cohort: (28 controls)

5.2.1 Duplicate data

Some patients who were part of the original 2000-2002 East London cohort returned as part of the 2012-2013 London Cohort, scanned approximately 10 years after the original study. Similarly, some patients who were screened, but not randomised to the SIT trial returned as part of the 2012-2013 London cohort, scanned approximately 5-7 years after the original trial screening MRI. In total, 14 adolescents and adults returned; only the most recent datasets were included.

5.2.2 Final Sample

The final dataset included HbSS and HbSC genotypes, and was comprised of 69 controls, 56 SCI- patients 28 SCI+ patients.

Figure 5-1 shows a graphical representation of subject inclusion and exclusion. Individual subjects were excluded if there was history of overt stroke at time of scan, presence of ischaemic lesions in subcortical grey matter areas on T2-weighted MRI and poor quality data/failed subcortical segmentation. Figure 5-2 shows graphically the distribution of subjects' age and gender overlaid on age boxplots.

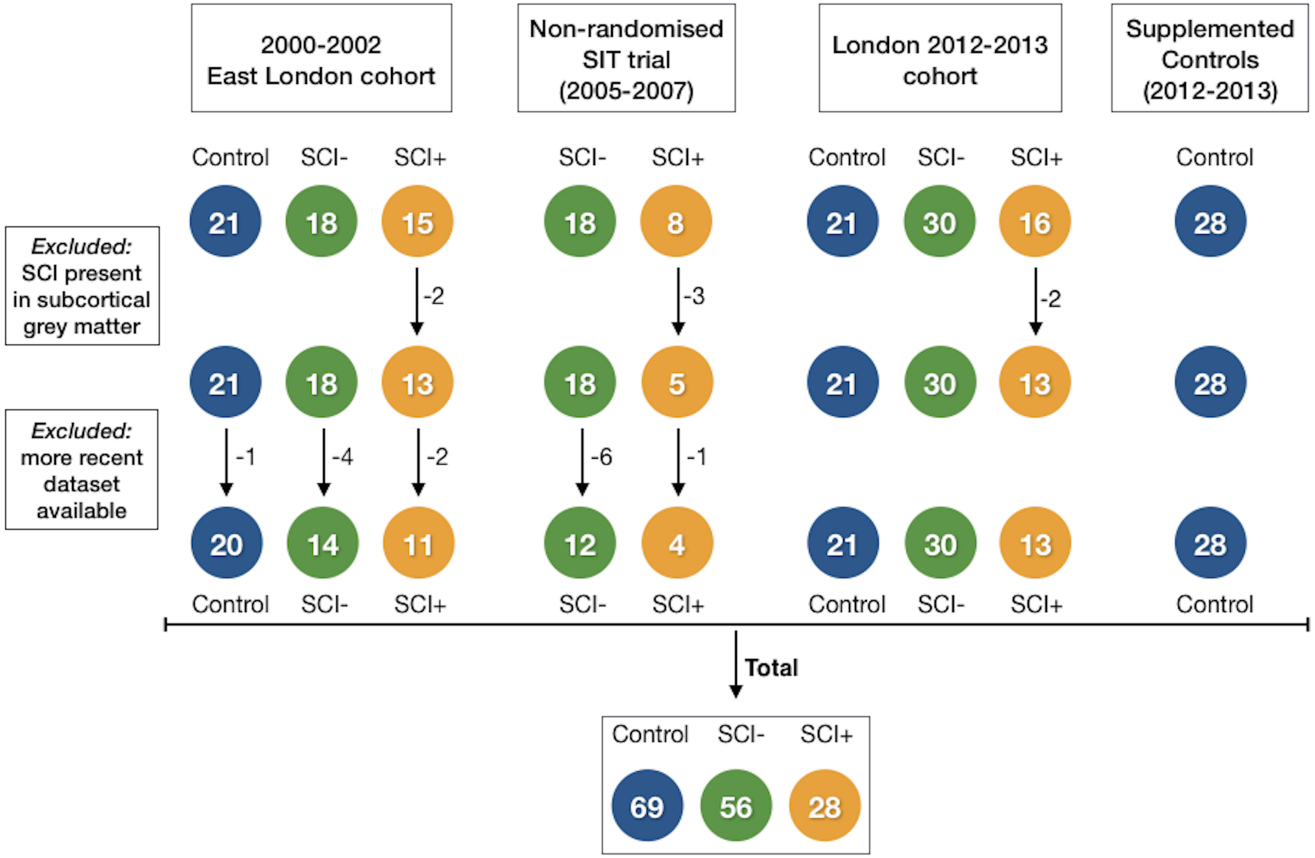

Figure 5-1. Subject inclusion and exclusion flowchart for volumetric analysis.

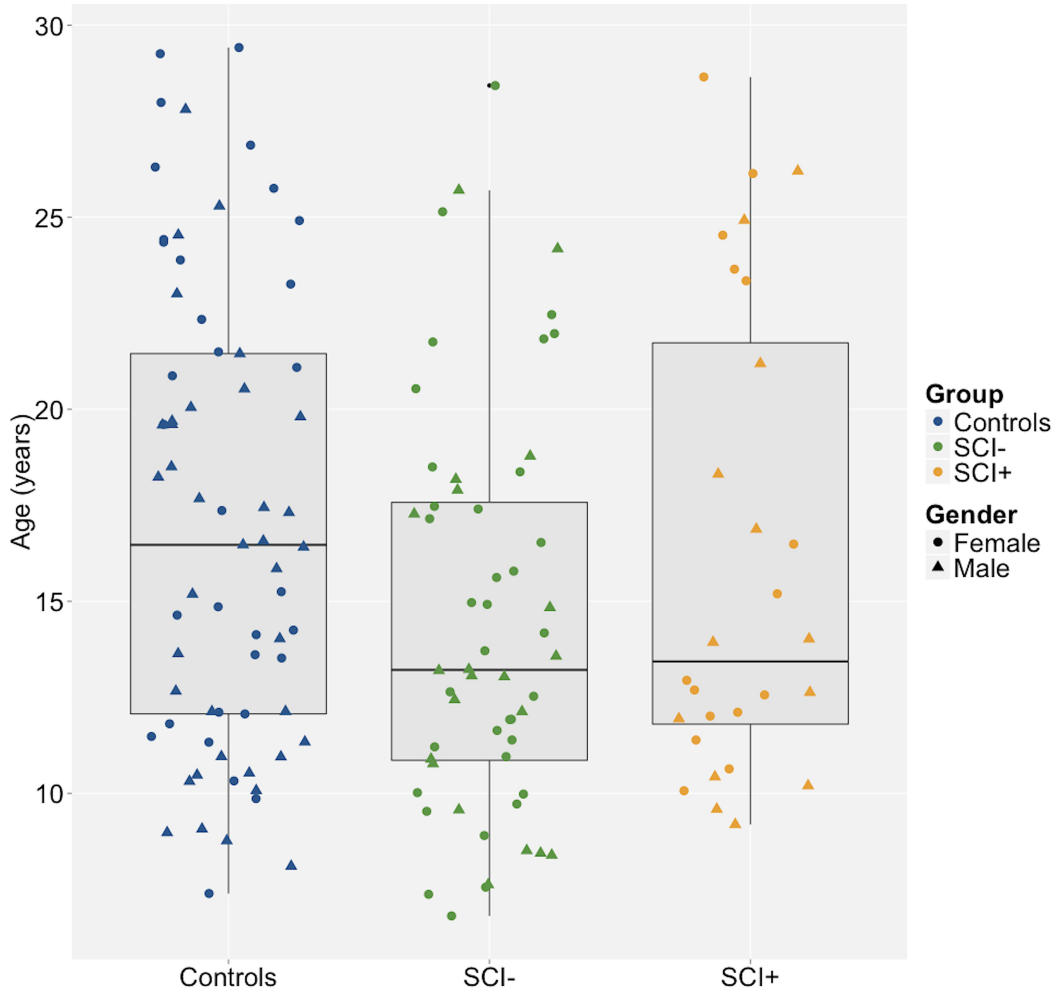

Figure 5-2. Distribution of age and gender by group of the final sample for volumetric analysis.

5.2.3 Cognitive Assessment

A measure of full-scale IQ was collected to analyse relationships between intelligence and volumes of subcortical structures. Only data from the 2-subtest WASI-I or WASI-II was included, available from the 2012-2013 London Cohort (30 SCI- patients, 13 SCI+ patients, 21 controls) and an additional 16 control subjects supplemented to the study. Cognitive data from the retrospective East London cohort was excluded because only the WISC-III was available and the time lapse between recent and remote cognitive testing was too long to ensure reliable results.

5.3 MRI Investigation

MRI was performed over a 10-year period at Great Ormond Street Hospital, in which three 1.5T MRI scanners were used.

5.3.1 2000-2002 East London Cohort MRI acquisition

As described previously for the 2000-2002 East London cohort[199,253,280], 25 patients and 20 controls were scanned on the 1.5T Siemens Vision system (Siemens, Erlangen, Germany). Sequences included:

- Axial T2-weighted turbo spin-echo sequence
    - TR: 3458ms, TE: 96ms, voxel size: 7.5 x 0.43 x 0.43mm)
- T1-weighted three-dimensional Fast Low Angle Shot (FLASH) sequence
    - TR: 16.8 milliseconds, TE: 5.7 milliseconds, flip angle: 21 degrees, voxel size: 1.0 x 0.8 x 0.8mm.

Concurrently with scanning, a consultant paediatric neuroradiologist evaluated all images and determined whether SCI were present. All MRIs of SCA without lesions were reviewed a second time, jointly with a second consultant paediatric neuroradiologist to confirm the initial evaluation.

5.3.2 Non-randomised SIT trial (2005-2007) MRI acquisition

Ten patients from the non-randomised SIT cohort were scanned between 2005-2007 on the 1.5T Siemens Symphony scanner (Siemens, Erlangen, Germany). Sequences included:

- Axial T2-weighted turbo spin-echo sequence
    - TR: 5000ms, TE: 100ms, voxel size: 5.0 x 0.9 x 0.9mm
- T1-weighted Fast Gradient Echo sequence
    - TR: 1900ms, inversion time: 1100ms, TE: 4.15ms, flip angle: 15 degrees, voxel size: 1.25 x 1.0 x 1.0mm.

5.3.3 Additional controls MRI acquisition

MRI acquisition for the forty-nine patients and 21 controls from the 2012-203 London Cohort has been previously described in Chapter 3. An additional 28 controls from on-going studies at the Institute of Child Health/Great Ormond Street Hospital were scanned using the same sequences.

As mentioned in Chapter 3 of this thesis, two independent neuroradiologists read non-randomised SIT screening MRI and all subjects' MRI from the 2012-2013 London cohort to determine whether SCI were present, and a third neuroradiologist over-read for discrepancies. Of the twenty-nine SCI+ patients, eleven had left-hemisphere, ten had right-hemisphere and eight had bilateral infarcts. Twenty-three (79%) had frontal lobe infarcts.

5.4 Volumetric Analysis

Automatic subcortical volumetric segmentations were analysed using Freesurfer image analysis suite v5.1 for Mac OS X, documented at the website: https://surfer.nmr.mgh.harvard.edu. This software has been described in technical detail previously[281–287]. For each individual dataset, Freesurfer inputs whole-head high-resolution T1-weighted images. The software pipeline includes: motion correction[288], removal of non-brain tissue using a hybrid watershed/surface deformation procedure[287], automated Talairach transformation, segmentation of subcortical white matter and deep grey matter structures[282,284], intensity normalisation[289], and steps that continue processing to include grey and white matter surface reconstruction. Specifically for the automatic subcortical segmentation processing stage, Freesurfer performs six steps: linear registration to the Gaussian Classifier Atlas, canonical normalisation and registration, registration and subcortical labelling of individual structures[282].

To minimize methodological errors, each dataset was visually inspected for data quality. Subcortical volumes that were assessed included left and right cerebellar cortex, left and right thalamus, left and right caudate, left and right putamen, left and right pallidum, left and right hippocampus, left and right amygdala, left and right accumbens, and total subcortical grey matter volume (Figure 5-3). Intracranial volume was also collected from Freesurfer output for statistical analysis.

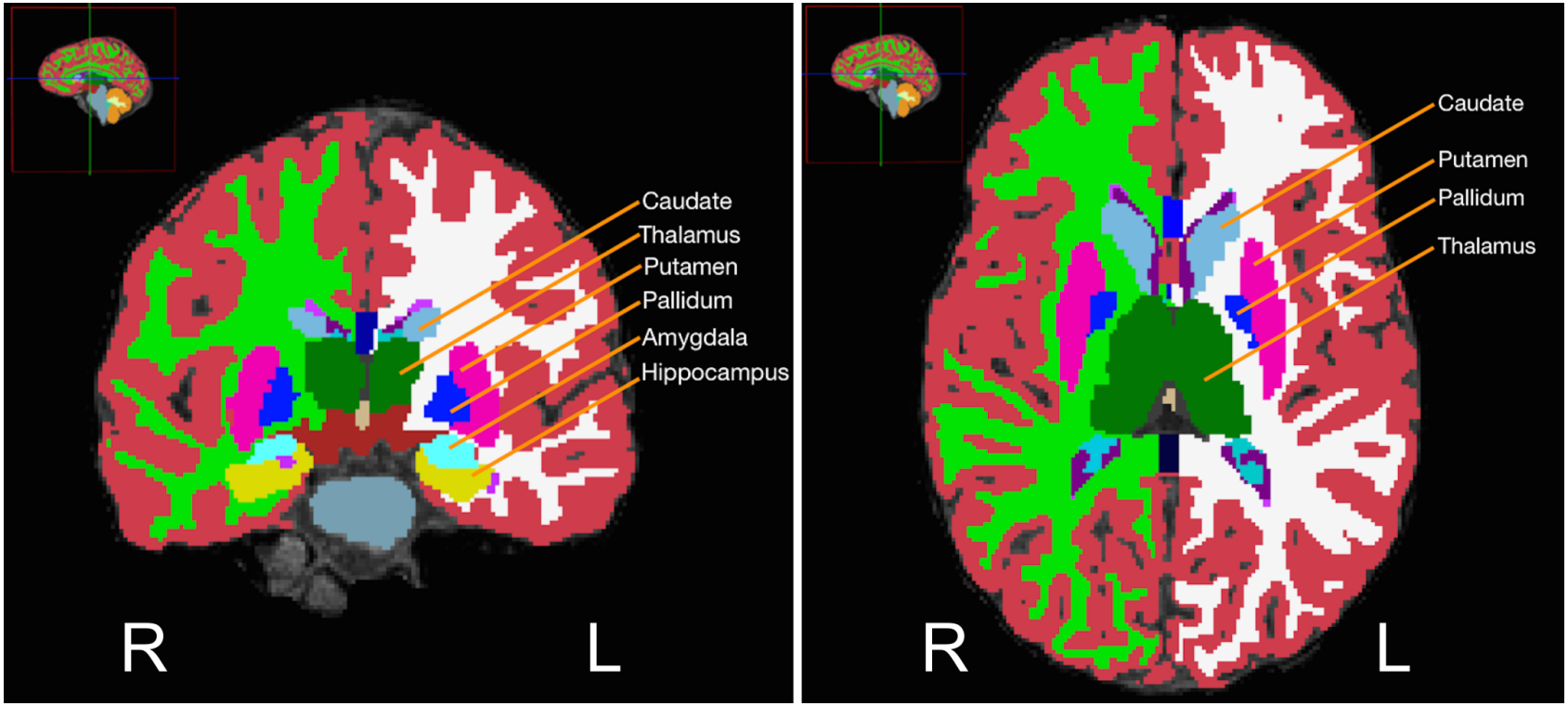

Figure 5-3. Freesurfer subcortical segmentation output. Coronal (left) and axial (right) images showing most of the structures analysed, except for nucleus accumbens and cerebellar cortex. Total subcortical grey matter volume is a summation of the eight structures.

5.5 Statistical Analysis

All statistical analyses was performed in R. Subcortical structures from Freesurfer output were tested for significant deviations from a normal distribution using Shapiro-Wilk tests. An analysis of covariance (ANCOVA) was performed to control for age, gender and intracranial volume against subcortical volume variables in the three groups, and *p*-values corrected across variables to control the false discovery rate (with $p<0.05$ considered significant). The Tukey-Kramer method was used to perform post-hoc tests to determine which groups' means were significantly different from one another.

For each group, two Pearson's correlations were carried out between residual data of each subcortical volume (corrected for intracranial volume and gender) with age and FSIQ.

5.6 Results

Demographics are reported in Table 5-1. There was a significant difference in age between the three groups (ANOVA; F=3.238, p=0.042); mean age of controls was significantly higher than the SCI- group (*t*=2.580, p=0.011). There were no differences in gender ratio between the groups. There was a significant difference in FSIQ score between the three groups; the control group had significantly higher IQ scores than both patient groups, but there was no difference between SCI- and SCI+ groups.

	Control (n=69)	**SCI-** (n=56)	**SCI+** (n=28)	
Age in years mean (sd)	17.12 (5.95) range: 7.39-29.42	14.51 (5.17) range: 6.81-28.43	16.14 (6.09) range: 9.19-28.65	ANOVA F=3.238, p=0.042 post-hoc: controls > SCI- (*t*=2.58, p=0.011)
Gender	32M, 27F	35M, 21F	15M, 13F	χ^2= 3.231, p=0.199
Genotype	59 HbAA 10 HbAS	51 HbSS 5 HbSC	27 HbSS 1 HbSC	
FSIQ* mean (sd)	111.54 (14.43)	98.57 (13.18)	92.69 (10.74)	ANOVA F=12.837, p<0.0005 post-hoc: controls > SCI- (p=0.0005) controls > SCI+ (p=0.0005) SCI- > SCI+ (p=0.192)
	*FSIQ was available for 37 controls (21 familial controls), 30 SCI- patients, and 13 SCI+ patients.			

Table 5-1. Demographics of final sample for volumetric analysis.

5.6.1 Group Differences

ANCOVA results are summarised in Table 5-2. Figure 5-4 shows a graphical representation of the group means in those measures that were significantly different between groups, after correction for multiple comparisons. After correcting for the effects of age, gender and intracranial volume, volumes for total subcortical grey matter volume, bilateral cerebellar cortices, bilateral amygdalae and right putamen were significantly different between the three groups.

For total subcortical grey matter volume, controls had significantly greater mean volume than both the SCI- and SCI+ groups. Similarly, for the bilateral cerebellar cortices and left amygdala, controls had significantly greater mean volumes than both the SCI- and SCI+ groups. For the right amygdala, the control group had significantly greater mean volume than the SCI- group. In the right putamen, controls and the SCI- group had significantly greater mean volumes than the SCI+ group, although there was no statistical difference between controls and SCI-. For all these significant results, moderate to large effect sizes were found (Table 5-2). Statistical power for the effect sizes ranged from 69-97%. The left hippocampus showed trend-level differences between Control and SCI+ groups (effect size= 0.54 with 70% statistical power). In order to achieve 80% power for the same effect size, 31 SCI+ patients would have been needed.

These results are in line with previously reported data from the 2000-2002 East London cohort, which reported a general trend of decreasing means corresponding to radiological status (*i.e.* presence or absence of SCI)[280]. Controls generally had the largest mean volumes, followed by the SCI- group, then the SCI+ group. These results indicate patients with SCD, in which SCI is present or absent, are at risk for subcortical grey matter volumetric deficits.

(mm^3)	Control (n=69)	SCI- (n=56)	SCI+ (n=28)	ANOVA F	ANOVA p	Post-hoc
Intracranial Volume	1532863.03	14886260.86	1503160.55			
Left Cerebellar Cortex	57533.46	54924.89	53884.29	**6.381**	**0.002****	a**, d= 0.65 b*, d= 0.50
Left Thalamus	7544.74	7419.30	7521.39	0.149	0.866	
Left Caudate	3831.94	3771.48	3748.14	0.084	0.917	
Left Putamen	5420.70	5447.21	5260.25	0.609	0.546	
Left Pallidum	1713.58	1664.70	1665.36	1.698	0.187	
Left Hippocampus	3999.52	3883.80	3751.93	3.016	0.052	a†, d= 0.54
Left Amygdala	1479.04	1371.89	1355.89	**6.424**	**0.002 ****	a*, d= 0.55 b**, d= 0.52
Left Accumbens	535.33	561.82	556.61	0.346	0.708	
Right Cerebellar Cortex	60028.39	55993.29	55302.32	**10.785**	**4.28×10^{-5} *****	a***, d= 0.76 b***, d= 0.68
Right Thalamus	7535.17	7439.11	7314.82	0.736	0.481	
Right Caudate	3734.45	3674.75	3576.79	0.509	0.602	
Right Putamen	5340.78	5305.68	4899.25	**5.994**	**0.003 ****	a**, d= 0.69 c*, d= 0.70

(mm^3)	Control (n=69)	SCI- (n=56)	SCI+ (n=28)	ANOVA F	ANOVA p	Post-hoc
Right Pallidum	1586.94	1580.64	1481.07	2.323	0.101	
Right Hippocampus	4031.13	3898.38	3850.68	1.473	0.233	
Right Amygdala	1572.41	1429.18	1462.00	**7.115**	**0.001 ****	b**, d= 0.64
Right Accumbens	516.29	535.64	533.36	0.205	0.815	
Subcortical Grey Matter Volume	196415.20	187084.64	185281.25	**8.473**	**3.30×10^{-4} ****	a**, d= 0.67 b**, d= 0.61
	[a]Post-hoc: Controls > SCI+, [b]Post-hoc: Controls > SCI-, [c]Post-hoc: SCI- > SCI+ *after correction for multiple comparisons* *p<0.05, **p<0.01, ***p<0.001, [†]indicates trend (p<0.1), d: Cohen's *d* for effect size					

Table 5-2. Means and standard deviations of subcortical volumes.

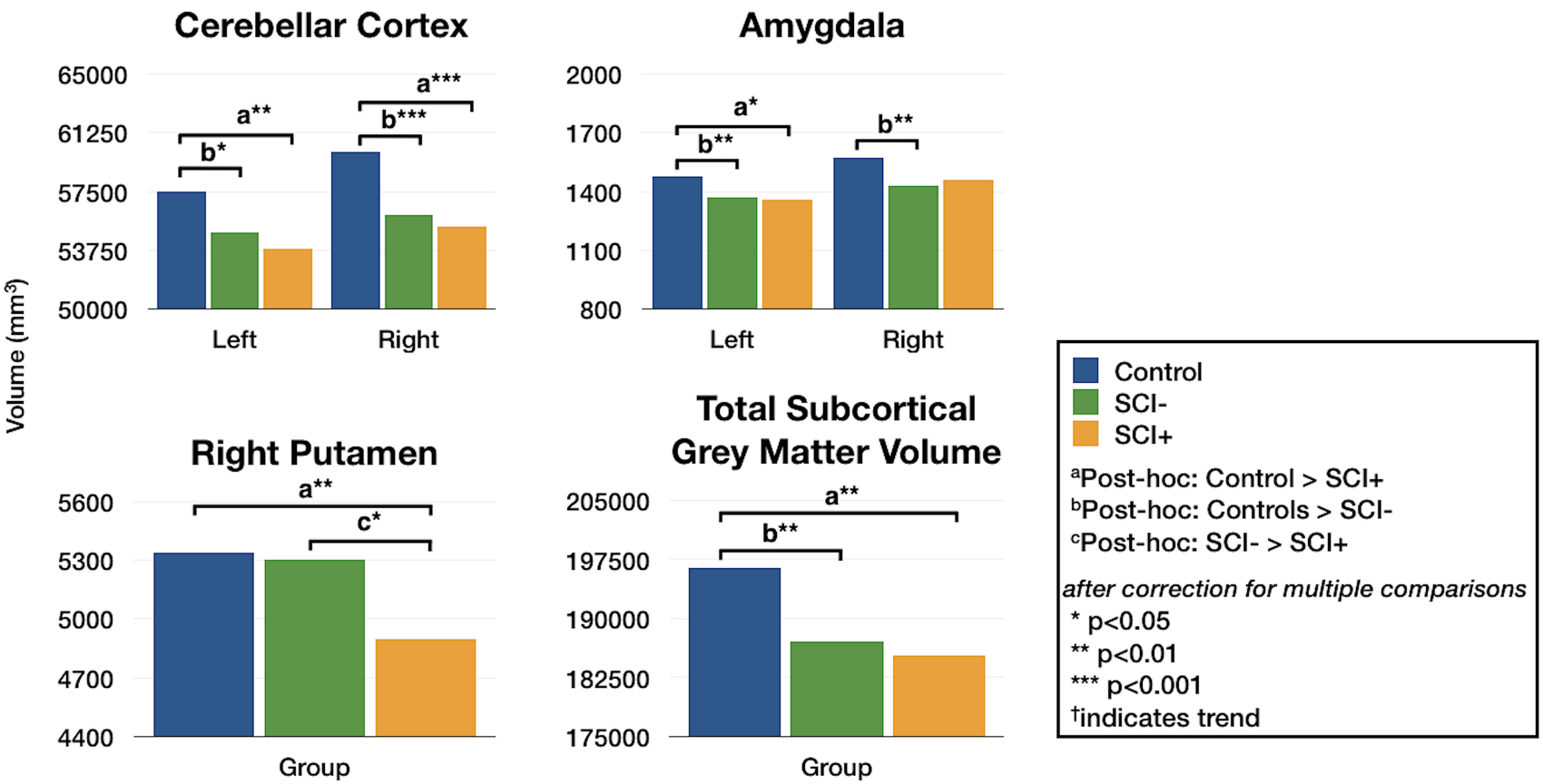

Figure 5-4. ANCOVA results of significant subcortical volumes.

5.6.2 Correlation with Age

Pearson's *r* correlations were performed between age and each group's subcortical volumes, using residual data corrected for intracranial volume and gender. Table 5-3 shows correlation results for each group, and significance after correction for multiple comparisons.

In the control group, generally all correlations were negative, indicating decrease in volume with increasing age. The majority of correlations in the SCI- group were also negative, except for positive correlations for left thalamus and right hippocampus. More positive correlations were found in the SCI+ group, in the bilateral cerebellar cortices, bilateral amygdalae, left accumbens, and total subcortical grey matter volume.

Both putamena showed significant negative correlations with age, in both the controls (left putamen: r= -0.430; right putamen: r= -0.462) and SCI- group (left putamen: r= -0.414; right putamen: r= -0.487) with over 90% power. Both pallida showed a significant negative correlation in the SCI- group (left pallidum: r= -0.476; right pallidum: r= -0.513) with over 97% power. The right pallidum significantly correlated with age in controls (r= -0.317, with 76% power) while the left pallidum showed a trend-level correlation (r= -0.273, with 62% power). To achieve 80% power in the right and left pallidum, the sample size would need to include 76 and 103 control subjects, respectively. In the SCI- group, both accumbens nuclei showed a significant negative correlation (left accumbens: r= -0.430, with 92% power; right accumbens: r= -0.363, with 79% power). In the control group, only trend-level negative correlations were found; for the left accumbens the correlation was r= -0.298 with 70% power and the right accumbens was r= -0.281 with 44% power. To achieve 80% power for the correlation of left and right accumbens with age, the sample size would need to include 86 and 97 control subjects, respectively. The left cerebellar cortex volume significantly negatively correlated with age in the SCI group (r= -0.312, with 65% power), but no significant correlations were found in the control or SCI+ groups. To achieve 80% power, 79 SCI- patients would have been required for this correlation.

Figure 5-5 shows the residual data scatter plots for volumes that showed significant correlations with age (bilateral putamena, bilateral pallida, bilateral accumbens nuclei, left cerebellar cortex), separated by Control, SCI- and SCI+ groups.

	Control (n=69)				**SCI-** (n=56)				**SCI+** (n=28)	
	Pearson's *r*	p	Power	*n* for 80% power	Pearson's *r*	p	Power	*n* for 80% power	Pearson's *r*	p
Left Cerebellar Cortex	-0.153	0.211			**-0.312**	**0.019***	65%	79	0.249	0.200
Left Thalamus	-0.222	0.066			0.105	0.443			-0.080	0.685
Left Caudate	-0.184	0.206			-0.159	0.243			-0.388	0.041
Left Putamen	**-0.430**	**0.00023****	96%	-	**-0.414**	**0.0015****	90%	-	-0.405	0.032
Left Pallidum	**-0.273**	**0.023†**	62%	103	**-0.476**	**0.00021****	97%	-	-0.369	0.053
Left Hippocampus	-0.177	0.146			-0.005	0.968			-0.033	0.867
Left Amygdala	-0.205	0.092			-0.158	0.246			0.174	0.375
Left Accumbens	**-0.298**	**0.013†**	70%	86	**-0.430**	**0.00093****	92%	-	0.289	0.136
Right Cerebellar Cortex	-0.158	0.196			-0.190	0.162			0.270	0.165
Right Thalamus	-0.141	0.248			-0.116	0.394			-0.012	0.952
Right Caudate	-0.216	0.075			-0.263	0.051			-0.426	0.024
Right Putamen	**-0.462**	**0.000064****	98%	-	**-0.487**	**0.00014****	97%	-	-0.248	0.204
Right Pallidum	**-0.317**	**0.008***	76%	76	**-0.513**	**0.000051*****	99%	-	-0.316	0.102
Right Hippocampus	-0.076	0.534			0.075	0.583			-0.087	0.659
Right Amygdala	-0.074	0.547			-0.049	0.718			0.376	0.049
Right Accumbens	**-0.281**	**0.019†**	44%	97	**-0.363**	**0.0059***	79%	57	-0.444	0.018
Subcortical Grey Matter Volume	-0.179	0.140			-0.222	0.099			0.185	0.346
	*p<0.05, **p<0.01, ***p<0.001 (after correction for multiple comparisons) †indicates trend (p<0.1)									

Table 5-3. Cross-sectional correlations of subcortical volumes with age.

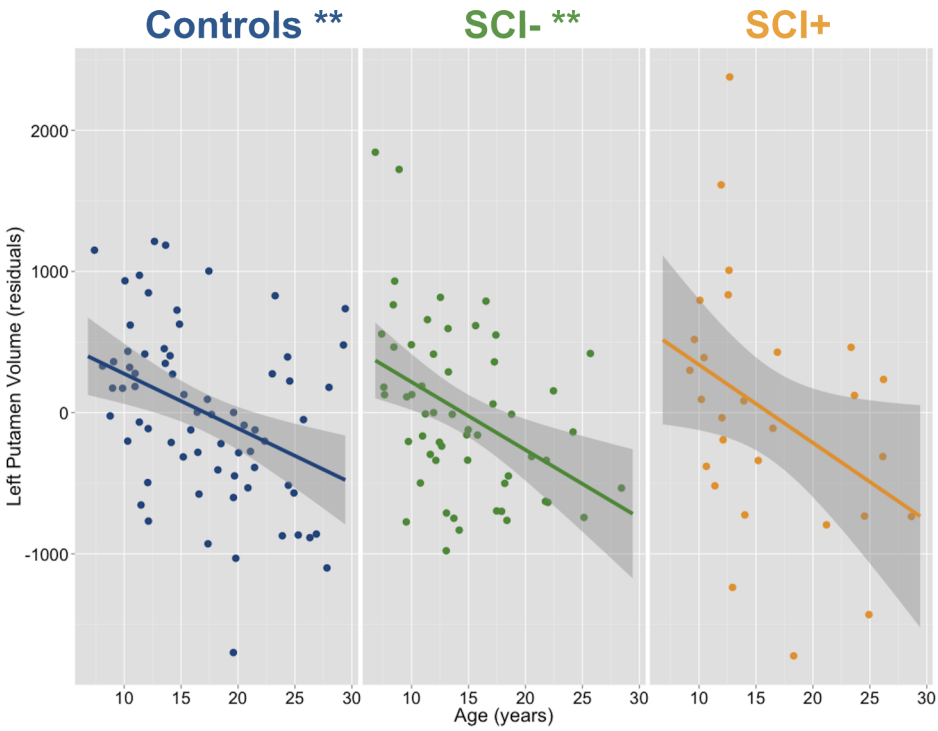
Controls **
SCI- **
SCI+
Left Putamen Volume (residuals)
2000
1000
0
-1000
10
15
20
25
30
Age (years)

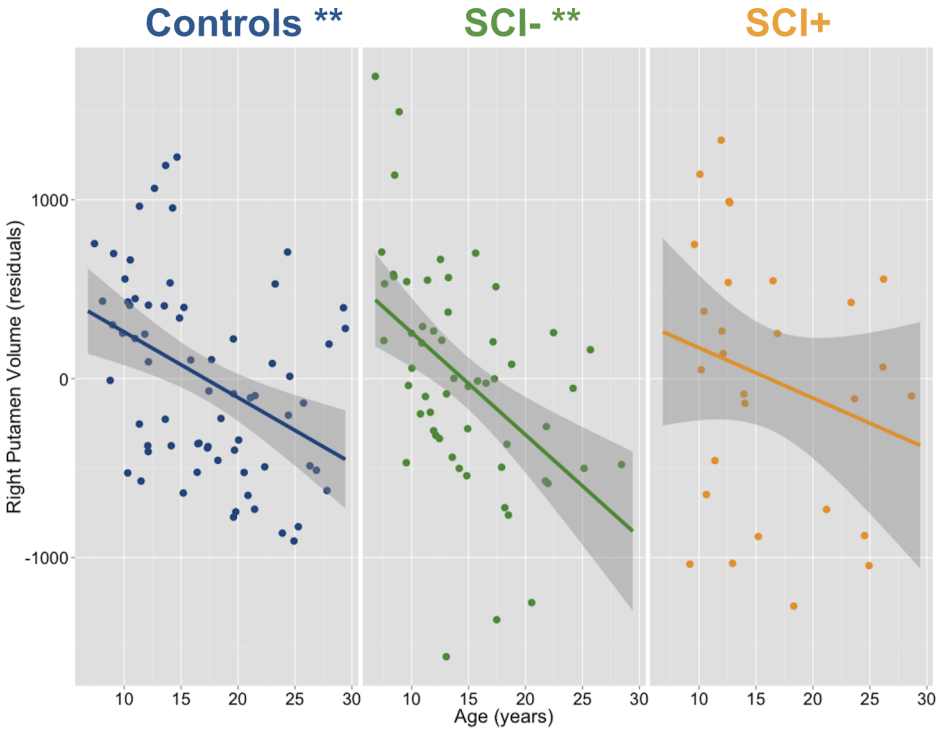
Controls **
SCI- **
SCI+
Right Putamen Volume (residuals)
1000
0
-1000
10
15
20
25
30
Age (years)

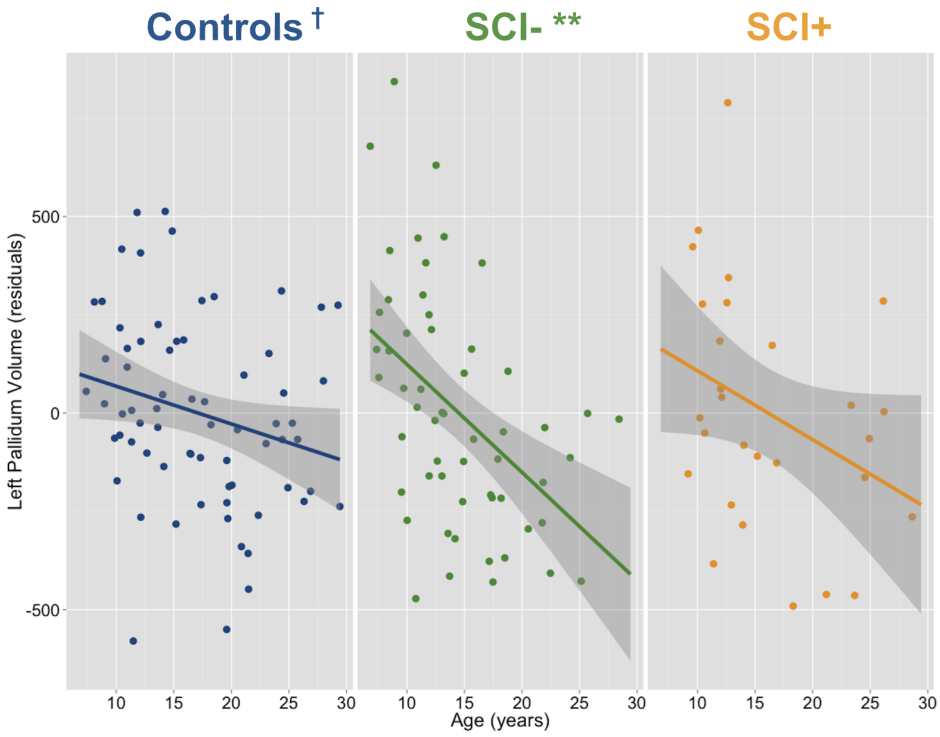
Controls †
SCI- **
SCI+
Left Pallidum Volume (residuals)
500
0
-500
10
15
20
25
30
Age (years)

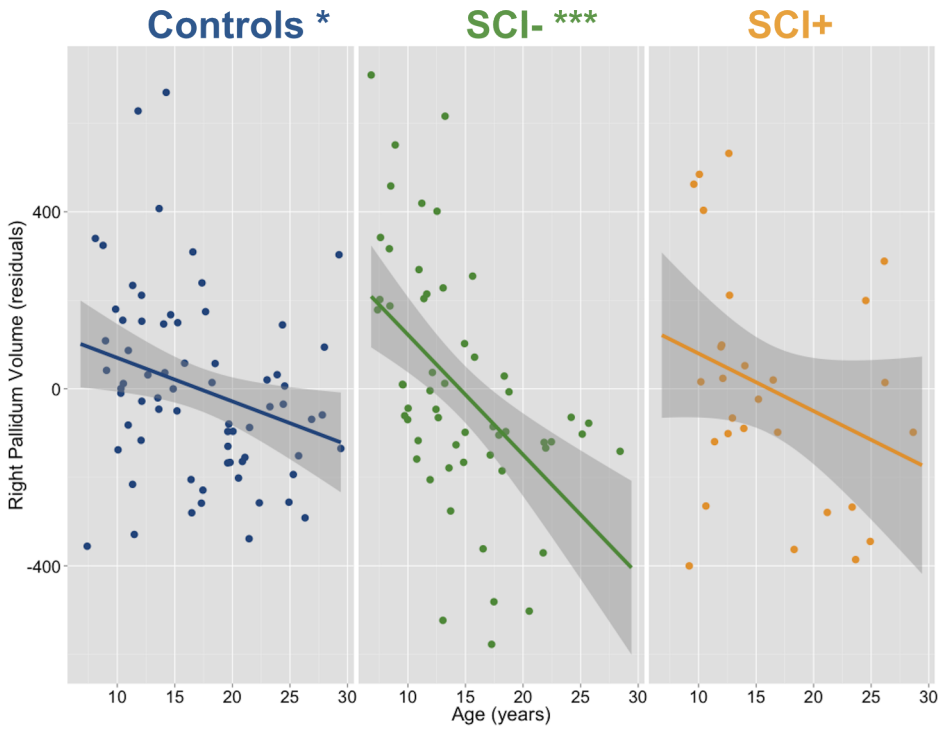
Controls *
SCI- ***
SCI+
Right Pallidum Volume (residuals)
400
0
-400
10
15
20
25
30
Age (years)

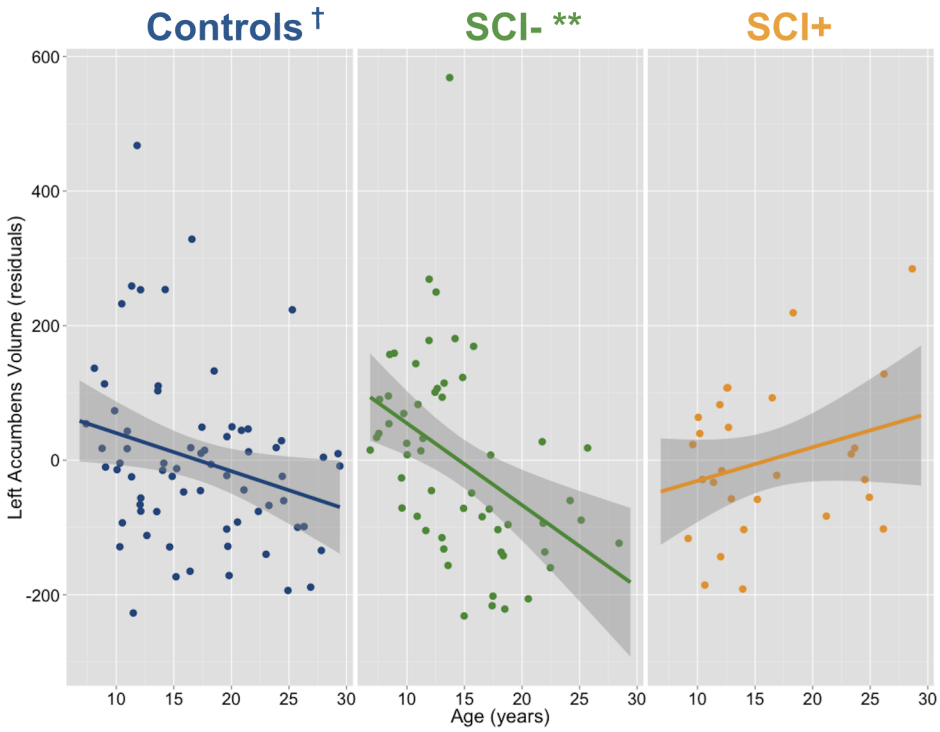
Controls †
SCI- **
SCI+
Left Accumbens Volume (residuals)
600
400
200
0
-200
10
15
20
25
30
Age (years)

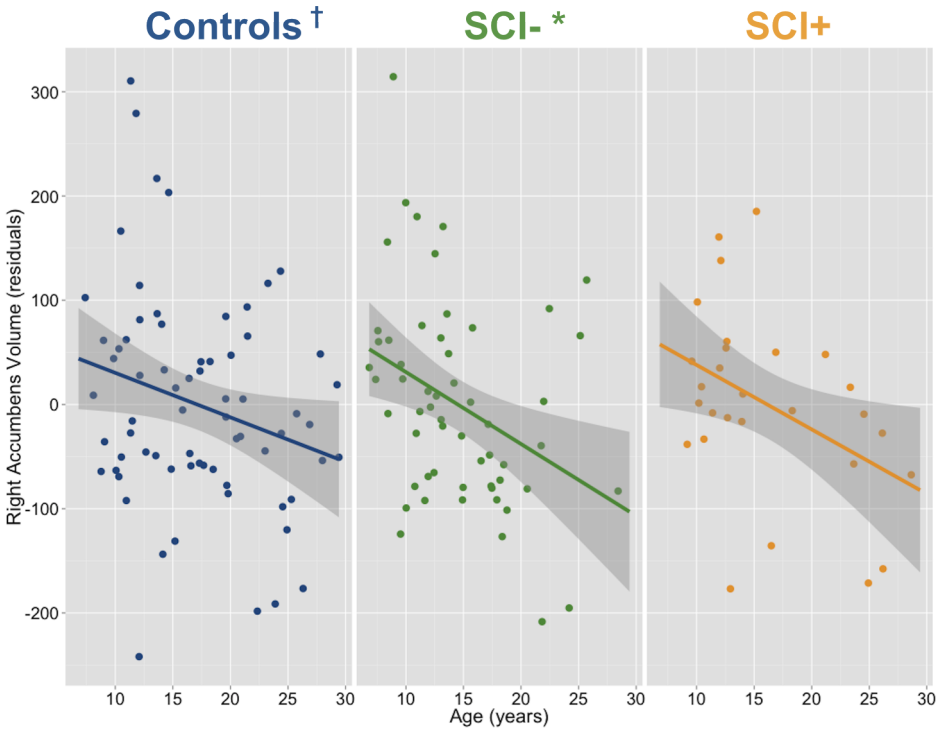
Controls †
SCI- *
SCI+
Right Accumbens Volume (residuals)
300
200
100
0
-100
-200
10
15
20
25
30
Age (years)

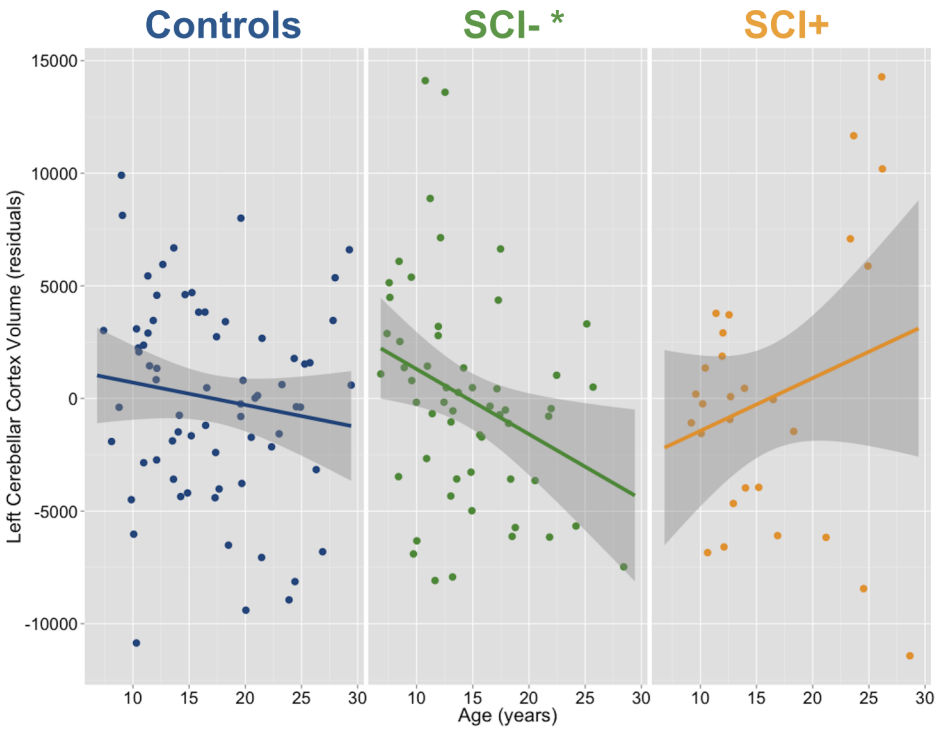

Figure 5-5. Cross-sectional correlations with age. There are seven plots to this figure: residual data (corrected for intracranial volume and gender) of the left- and right-hemisphere putamen, pallidum, acumbens and left cerebellar cortex correlation plots with age. Significance is indicated by star notation at the top of each graph (***p<0.001, **p<0.01, *p<0.05, †p<0.1).

5.6.3 Correlation with IQ

FSIQ from WASI tests were available for 37 control subjects, 30 SCI- patients and 13 SCI+ patients. Pearson's *r* correlations were performed between age and each group's subcortical volumes, using residual data corrected for intracranial volume age, gender and the interaction between age and gender. There were no significant correlations between any volume and FSIQ in any subject group.

5.7 Discussion

This chapter specifically investigated volumes of subcortical structures in patients with SCD, with and without SCI, compared to controls. One previous report found volumetric decreases in central grey matter[200]; however this current study found more specific

significant differences of volumes of the bilateral cerebellar cortices, bilateral amygdalae, and right-hemisphere putamen, as well as total subcortical grey matter volume.

This study follows a voxel-based morphometry analysis[199], which found significant decreases in white matter density bilaterally. These authors also reported a trend regarding cortical grey matter density; in the lesion group, grey matter density was decreased along the medial wall of the frontal and the parietal lobes surrounding the cingulate sulcus, and in the patients without lesions, grey matter density reductions were seen in the same, but smaller, regions. Our findings are in line with these reports, as the trend for decreasing subcortical volumes followed similar ordering of groups by radiological status (*i.e.* SCI+ < SCI- < Controls).

5.7.1 Comparison with Previously Reported Data

A subset of these data has been published previously in the British Journal of Haematology[280]. This study expanded on that short report with a larger cohort and a wider age range. The original study, with 13 SCI- patients, 13 SCI+ patients and 20 controls, indicated significant group differences in the bilateral cerebellar cortices, bilateral hippocampi, bilateral amygdalae, bilateral pallida, right-hemisphere caudate, right-hemisphere putamen and total subcortical grey matter volume. After adding more subjects, original group differences remained significant for the bilateral cerebellar cortices, bilateral amygdalae, right putamen, and total subcortical grey matter volume; however, results were no longer significant in the bilateral hippocampi, bilateral pallida, and right caudate. In the original study, group differences in the bilateral hippocampi, left pallidum and right caudate were significant just under $p<0.05$, with the control group having significantly larger mean volume than the SCI+ group. In the right pallidum, controls had significantly larger mean volume than both SCI- and SCI+ groups ($p<0.01$). In the current, expanded cohort, these results are no longer significant, possibly due to larger sample size and more statistical power that nulled.

Figure 5-6 shows bar graphs from the original study, compared with the analysis from the expanded cohort for the volumes of the structures that remain significant with the expanded analysis. In the right cerebellar cortex and bilateral amygdalae, the difference between controls and SCI- group was found to be more highly significant, and statistical significance remained between controls and SCI+ groups. In the right putamen, there was a new finding in the current expanded study: SCI- patients had significantly larger volume than SCI+ patients ($p<0.05$), which is the only statistical difference in any volume between those two groups. Results for total subcortical grey matter volume remained significant in the current study.

There were more statistical differences between Controls and patient groups than between the SCI- and SCI+ groups. This provides further evidence to support the hypothesis that lesion size alone may not be predictive of brain injury[221], as volumetric deficits are seen in patients without visible lesions compared to controls. This is in line with previous studies showing cortical grey matter loss[202] in patients with no visible abnormality on T2-weighted MRI. It is possible that deficits in brain volume are a result of SCD-specific chronic physiological processes, such as perfusion abnormalities as well as chronic, intermittent anaemia and hypoxia.

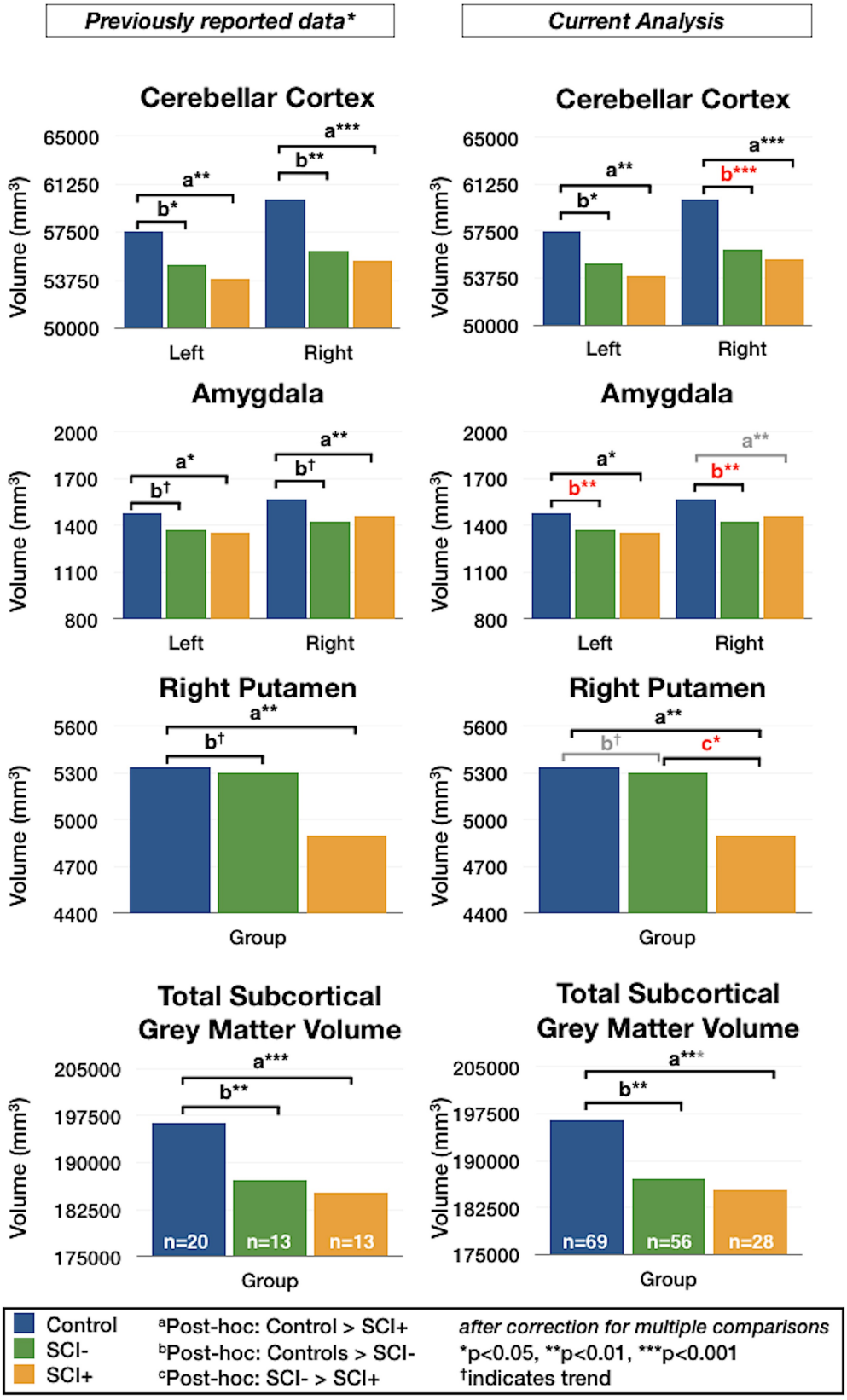

Figure 5-6. Comparison of results with previously reported data[280], in which sample sizes were smaller (*i.e.* previously reported data: Controls: n=20, SCI-: n=23, SCI+: n=13; current analysis: Controls: n=69, SCI-: n=56, SCI+: n=28). Red post-hoc lettering indicates results that became significant in current analysis, and grey post-hoc lettering indicates results that are no longer significant in current analysis.

5.7.2 Correlation with Age

The current study showed significant negative correlations with age in both the control group and the SCI- group in the bilateral putamena, pallida and accumbens nuclei. While correlations with age between controls and the SCI- group were similar in the bilateral putamena, in the bilateral pallida and bilateral accumbens nuclei, the SCI- group showed stronger and more statistically significant correlations with age than controls.

Cross-sectional data from healthy subjects aged 4-18 years, without use of any covariates, show a curvilinear (inverted-U curve) shape for subcortical grey matter volume and several subcortical structures (thalamus, caudate nucleus, putamen and globus pallidus) and cerebellum[290]. This study sampled 325 individuals and there was wide inter-subject variability and large confidence intervals; however, total subcortical grey matter volume displayed an increase in volume until approximately age 11.5 years, then an age-related decrease. A significant age-related increase in volume was found for the thalamus, while significant age-related decreases were found for the caudate and globus palldius[290]. The current findings of the volume of the pallidum are in line with that study.

A longitudinal two-timepoint study of subcortical brain maturation in healthy children aged 11-17 years showed age-related increases in the hippocampus, pallidum and left accumbens, and age-related decreases in the putamen, caudate, thalamus and right accumbens[291]. There were no significant positive correlations with age in this current study, although the current findings for the accumbens are in line with those results.

For the bilateral accumbens nuclei, bilateral pallida and left cerebellar cortex, significant negative correlations with age were stronger in the SCI- group than controls, although formal statistical testing was not done to determine differences in age by group interactions. These volumes may suggest specific biomarkers for subcortical volumetric deficit as a function of age. However, these data cannot discern between whether children with SCD have smaller brain volume at a younger age initially, whether this is an indication of atrophy with increasing age or what factors specific to SCD may cause this process. Further research could investigate functions associated to the nucleus accumbens in adolescents and adults with SCD. In multiple sclerosis, similar volumetric reductions of the nucleus accumbens have been found, potentially due to loss of myelin and/or axons[292,293], and smaller nucleus accumbens volume correlated with steeper cognitive decline in older people[294].

There were no significant correlations with age in the SCI+ group. This is in line with findings of differing patterns of subcortical volumetric growth as reported previously[200], with brain volume increasing in SCD at an age when brain volume in controls had already stabilised. That study did not discern patients with or without visible SCI on T2-weighted

MRI, so specific group trajectories are unknown. However, the authors suggest the possibility that developmental processes occur at a slower rate in children with SCD compared to healthy controls, similar to evidence in SCD for a somatic growth delay[263,295]. The notion that SCD is a type of neurodevelopmental disorder has also been described in the cognitive literature[296].

5.7.3 Silent Cerebral Infarction and Brain Development

SCI are clinically silent and it is unknown when neurological abnormalities occur. The lack of epidemiological studies to determine the natural history of SCI remains a limitation[105]. It has been reported that SCI occurs in one-quarter of children under 6 years[183] and one-third of children under 14 years[297]. There are few studies in very young children, as children generally do not tolerate MRI investigation younger than age 6; however studies have reported SCI in 4 of 39 children (10%) between 7-48 months of age[107], and 3 of 23 infants (13%) with a mean age of 13 months[182]. It is unknown whether the first incidence of SCI can occur in adolescence, or whether there is an "incidence plateau"[105] during adolescence into adulthood.

This study excluded multiple within-subject scans; taking into account only the most recent MRI from 14 subjects that had repeat 3D T1-weighteed MRI. However, a slightly larger group of patients from the 2000-2002 East London cohort and the 2005-2007 SIT trial cohort with T2-weighted MRI returned for follow-up scans as part of the 2012-2013 London cohort. An experienced neuroradiologist read each subjects' baseline and follow-up T2-weighted image to determine any progression of neurological abnormality (*i.e.* new or enlarged lesions).

In the 2000-2002 East London cross-sectional study, 10 subjects with T2-weighted MRI (3 SCI-, 7 SCI+, age range: 7-23 years) had a follow-up MRI scan 10-12 years later. All 3 SCI- patients and 4 SCI+ patients at baseline had no reported change at follow-up MRI. However, 3 male SCI+ patients had evidence of new SCI during the interim. Patient 1 was 17 years old at baseline MRI with evidence of a right frontal white matter lesion – at age 28 at follow-up MRI there was evidence of a new right-hemisphere peritrigonal lesion. Patient 2 was 21 years old at baseline MRI with evidence of a left parietal white matter lesion – at age 33 at follow-up MRI there was evidence of two new frontal lobe white matter lesions. Patient 3 was 7 years old at baseline MRI with left peritrigonal lesions – at age 18 at follow-up MRI there was evidence of two bilateral cerebellar white matter lesions.

In the group not randomised to the SIT trial, 7 patients (6 SCI-, 1 SCI+, age range 7-10 years) had a follow-up scan 4-7 years later. All 7 subjects showed no further abnormality on the follow-up scan.

Interestingly, two of the three SCI+ patients that did show progression of abnormal MRI had developed new SCI after age 18; however all three patients that showed progression of abnormality had existing SCI at baseline, giving no information on whether there is an "incidence plateau" of first SCI in childhood[105].

5.7.4 Limitations

This study investigated group differences in subcortical volumes cross-sectionally, in which the large scatter of data and large standard error sizes may reshape interpretation of results. Ideally, matched control and patients samples of longitudinal within-subject data from a young age would provide information about the long-term rate of growth and/or atrophy over childhood, adolescence and into adulthood in people with SCD.

In this study, the group sizes were different and there were fewer subjects encompassing the middle and oldest of the age range within the SCI- and SCI+ groups, leading to a significantly older control and SCI+ group than the SCI- group. The sparsity of data that cover the entire age range limits the ability to ascertain nonlinear relationships; therefore linear functions were used, similar to earlier reports[290,298,299].

This study also includes data collected over a twelve-year period on three different 1.5T MRI scanners at Great Ormond Street Hospital. Although the majority of patients and controls were scanned on the newest system, image resolution of the T1-weighted volume scan varied within one millimetre in voxel dimensions, potentially skewing volumetric results. For each individual subject before any volumetric segmentation or labelling, Freesurfer automatically corrects for non-uniformity in signal intensity and computes an affine transformation to standard atlas space. These steps acted to standardize all subjects' scans within the sample and reduce variability in volumetric calculation[300].

5.8 Conclusion

This study shows that previously described cortical atrophy and white matter abnormalities in SCD are accompanied by volumetric loss of tissue in subcortical grey matter structures. Although the SCI- group showed significant negative correlations with age comparable to the control group, there were no significant correlations in the SCI+ group. These findings are consistent with the hypothesis of a global diffuse pattern of brain injury, with complex patterns of brain development. Future research should explore longitudinal within-subject studies and relationships with cognition and 'soft' neurological signs[101] over time.

Chapter 6. Evidence for brain atrophy in paediatric SCD: Findings from the Silent Infarct Transfusion (SIT) Trial

Silent cerebral infarction (SCI) is caused by several possible circular processes: small vessels can be occluded by irreversibly sickled cells, leading to microcirculatory ischaemia in the arterial borderzones where flow may be relatively low compared with metabolic demand, and abnormally high arterial blood velocities can cause injury to the endothelial cells lining the vascular wall, leading to distal stenosis and occlusion[89,90]. Presence of SCI is a risk factor for additional neurologic injury, including clinical stroke and progression of SCI[108,301].

The profile of lesions occurring in the non-motor areas of the brain, particularly the frontal lobes[104,224], has also been associated with marked deficits in cognitive performance. Several studies have reported lower IQ scores in patients with SCI compared to those with normal MRI[216,218,220,223]. Other domains such as executive functioning[115], sustained attention[219,226,227], cognitive flexibility, working memory[230] and processing speed[217,219,233,253], have also been reported to be affected.

Studies have shown brain morphological changes in children with SCD. A voxel-based morphometry study showed children with SCI had significant decreases in white matter density extending along the ventricles in an arterial borderzone distribution[199], compared to those with normal MRI. Cortical thinning has been reported in older children with SCD and normal MRI compared to controls[202]. Specific volumes of subcortical structures are also decreased in children with SCI, with the largest significant decreases in those with SCI, followed by those with normal MRI and controls[280].

Little is known about long-term brain morphometric changes in children with SCD and SCI. The Silent Infarct Transfusion (SIT) trial (principal investigator Dr Michael DeBaun, Washington University School of Medicine) provides the unique opportunity to study intra-subject changes over approximately three years during childhood and adolescence. The SIT trial focuses on blood transfusions as therapeutic intervention, based on compelling evidence from the previous STOP I (Stroke Prevention in Sickle Cell Anemia) trial, that showed a clear benefit of transfusion in preventing stroke[123]. Evidence from the STOP I trial also showed none of the 18 patients with baseline silent infarcts who were receiving transfusions developed new MRI lesions over a 36-month follow-up period, whereas of 29 untreated children with baseline silent infarction, 52% developed new MRI lesions or suffered overt strokes[109]. The primary hypothesis of the SIT trial was that transfusion therapy would result in at least 86% reduction in new overt and silent strokes. Also,

secondary hypotheses put forward were that transfusion therapy will limit further decline in general intellectual abilities when compared to the observation arm and that the overall benefit of transfusion therapy will outweigh the risks associated with the treatment.

The present study examines brain volume change over 3 years in children that participated in the SIT trial to determine the impact of blood transfusion therapy on brain volume. The study employed structural image evaluation of T1-weighted anatomical MRI data using normalisation of atrophy (SIENA)[302], a semi-automated quantification of two-timepoint whole-brain percent brain volume change. SIENA is a reliable measure of estimating longitudinal changes in global brain volume[302] and has been utilised in disorders such as multiple sclerosis[303] and small vessel disease[304,305], as well as traumatic brain injury[306,307] and normal aging populations[308,309]. To date, there are no studies investigating longitudinal brain volume change in children with SCD. In line with the hypotheses of the SIT trial, the primary hypothesis of this exploratory study is that transfusion therapy will have a protective effect on any brain volume loss that may occur due to progression of cerebrovascular disease.

6.1 Methods

1.1.1 Design of the SIT Trial

In this multicentre study, 29 clinical centres participated; 1211 children between the ages of 5 and 15 were screened and 196 patients randomised to either blood transfusion or observation. Details of the inclusion and randomisation criteria have previously been published[160,186]. Design of the SIT trial is shown in Figure 6-1.

Participants who were randomised to observation received standard care, while those randomly assigned to transfusion received a transfusion approximately monthly to maintain haemoglobin concentration greater than 9 g/dL and haemoglobin S concentration less than 30%[160].

The definition of SCI, as determined by the SIT trial investigators, is an increase in signal intensity seen on T2-weighted MR images, with no history of neurological deficit lasting more than 24 hours. For the SIT trial, the MRI lesion must measure at least 3mm in greatest linear dimension, visible in at least 2 planes of fluid-attenuated inversion recovery (FLAIR) T2-weighted images (axial and coronal)[111,186]. Two neuroradiologists had to agree that lesions were present and could not be explained by abnormality on neurological exam.

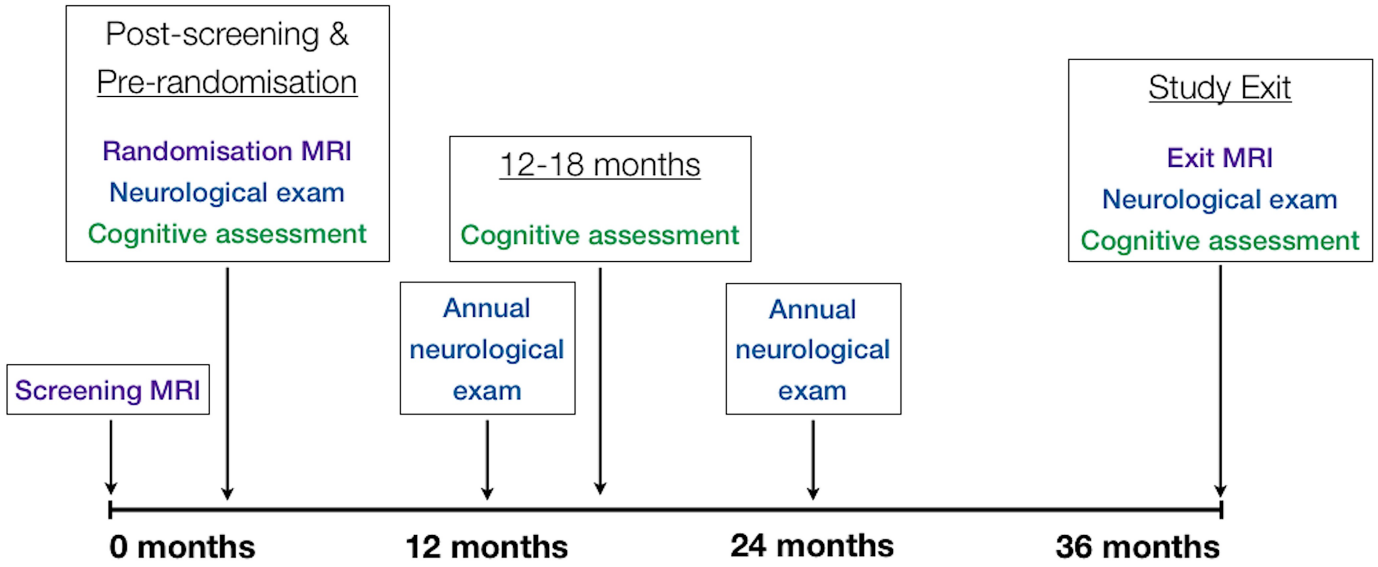

Figure 6-1. Design of the SIT trial.

6.1.1 Participants

Inclusion criteria for the present study included: randomisation to the SIT trial (*i.e.* patients with evidence of SCI at baseline), and MRI investigation at pre-randomisation *and* trial exit. MRI at both time points had to be on a 1.5T scanner, and must have included a 3D T1-weighted sequence for volumetric analysis.

6.1.2 Scanner Variability

Study participants from 5 US and 2 UK sites were included in this study. At 6 sites, 23 patients were scanned on the same system on both pre-randomisation and exit MRI. At 4 sites, 9 patients' exit MRI investigation was performed on a different scanner from pre-randomisation MRI. Refer to Figure 6-2 for details of MRI sequences.

Analysis included a binary factor to explain variability in whether the same or a different scanner was used. Patients were coded as having the same scanner system if the scanner underwent a software upgrade in the interim (n=6 patients at 3 sites).

6.1.3 SIENA %BVC analysis

SIENA[302] (FSL[242]; http://www.fmrib.ox.ac.uk/) was used to estimate percentage brain volume change (%BVC). SIENA goes through four steps to calculate %BVC between two time points:

1. Whole head data is used to extract brain and skull images. Automatic brain extraction masks were manually checked to ensure adequate brain extraction and exclusion of non-brain tissue[310].
2. The two brain-masked images are aligned to each other and sampled to a halfway space.
3. Tissue type segmentation is carried out to find brain/non-brain edge points, and
4. Perpendicular edge displacement between the two time-points is estimated. The mean edge displacement is calculated as the global estimate of %BVC. A negative %BVC indicates 'atrophy', while a positive %BVC indicates 'growth' (Figure 6-3).

SIENA %BVC was calculated for each patient for the time lapse between the pre-randomisation and exit MRI scans, then calculated as a %BVC/year index to control for varying time lapses between scans.

Site	*n*	Pre-randomization MRI 3D T1 sequence	Different scanner at exit MRI	Exit MRI 3D T1 sequence	Notes
1	1	1.5T Siemens Avanto TR: 1660, TE: 2.91, α: 15° voxel size: 1.25 x 1 x 1mm	No		
2	1	1.5T Siemens Sonata TR: 1900, TE: 3.93, α: 15° voxel size: 0.5 x 0.5 x 1.25mm	No		
3	2	1.5T GE Genesis Signa TR: 12.4, TE: 2.48, α: 30° voxel size: 0.6 x 0.98 x 0.98mm	Yes	1.5T GE Signa Excite TR: 11.87, TE: 5.16, α: 20° voxel size: 1.2 x 0.98 x 0.98mm	
	5	1.5T GE Signa Excite TR: 11.84, TE: 5.14, α: 20° voxel size: 1.2 x 1.02 x 1.02mm	No*	1.5T GE Signa HDxt	*3/5 patient's exit MRI had upgraded scanner software
4	6	1.5T Philips Gyroscan Intera TR: 8.45, TE: 3.99, α: 8° voxel size: 1.25 x 1 x 1mm	No*	1.5T Philips Intera	*2/6 patient's exit MRI had upgraded scanner software
	1	1.5T Philips Intera TR: 8.45, TE: 3.99, α: 8° voxel size: 1.25 x 1 x 1mm	Yes	1.5T Philips Achieva TR: 8.45, TE: 3.99, α: 8° voxel size: 1.25 x 1 x 1mm	
5	2	1.5T Siemens Symphony TR: 1900, TE: 4.15, α: 15° voxel size: 1.25 x 1 x 1mm	Yes	1.5T Siemens Avanto TR: 1900, TE: 4.15, α: 15° voxel size: 1.25 x 1 x 1mm	
6	3	1.5T GE Signa Excite TR: 7.91, TE: 4.20, α: 15° voxel size: 1.3 x 1 x 1mm	No*	1.5T GE Signa HDxt	*1/3 patient's exit MRI had upgraded scanner software
7	4	1.5T Siemens Symphony TR: 1900, TE: 4.15, α: 15° voxel size: 1.25 x 1 x 1mm	Yes	1.5T Siemens Avanto TR: 1900, TE: 4.15, α: 15° voxel size: 1.25 x 1 x 1mm	
	7	1.5T Siemens Avanto TR: 1900, TE: 4.15, α: 15° voxel size: 1.25 x 1 x 1mm	No		

Figure 6-2. Details of MRI sequences across 7 sites of the SIT trial.

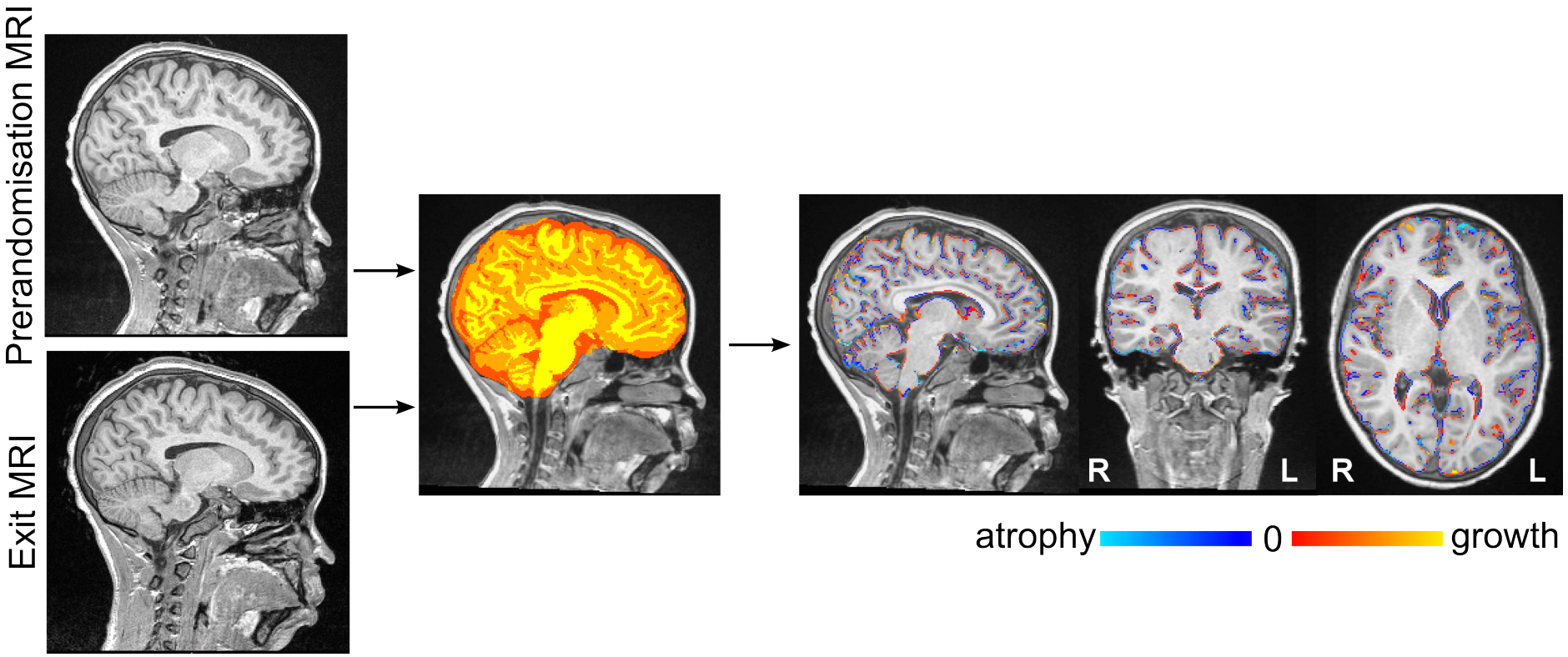

Figure 6-3. SIENA analysis pipeline.

6.1.4 Cognitive Data

Neuropsychological data were acquired at baseline (around the time of pre-randomisation MRI) and study exit. A measure of Full-Scale IQ (FSIQ) was collected from the 4-subtest Wechsler Abbreviated Scale of Intelligence (WASI). Change in FSIQ per year was calculated by the difference in FSIQ scores divided by the time lapse between cognitive testing.

6.1.5 Statistical Analysis

Statistical analyses were computed with R (http://www.r-project.org/). The intent for statistical analysis was to investigate differences between treatment groups while controlling for factors known to influence brain structure and volume.

A model was fitted to the data to examine the influence of treatment group, while controlling for any effect of age, gender, scanner variability, and also the interactions between treatment group, age, gender and scanner variability. A Pearson's product moment correlation (*r*) was carried out to correlate age-, gender-, and scanner-corrected residual data of %BVC/year and FSIQ.

6.2 Results

Forty-one participants met the inclusion criteria. Due to poor quality data, 9 patients were excluded from analysis, leaving 32 patients (16 on observation, 16 on transfusion). Demographics and results for the SIENA cohort are displayed in Table 6-1. There was a significant difference in gender distribution between the two groups (χ^2= 4.571, p=0.037), but no significant difference in age. There were no significant differences in baseline or exit FSIQ, although effect sizes were 0.53 and 0.65, respectively. The mean time lapse between pre-randomisation MRI and exit MRI in both groups was 3.2 years, range 2.8-3.5 years.

6.2.1 Effect of Treatment

After applying the model that took into account age, gender and variability in scanner, there was no difference in %BVC/year between the two groups (observation: mean= -0.62%, sd=0.44%; transfusion: mean= -0.96%, sd=1.00%; ANOVA F=0.0013, p=0.972). The effect size of the difference in means was calculated as -0.44, and the ANOVA F test had 67% statistical power. For the same effect size with 80% statistical power, there would needed to include 22 patients per group.

6.2.2 Effect of Age

There was a significant influence of age at pre-randomisation to the trial on %BVC/year (ANOVA F=8.842, p=0.007). There was also a trend for a group by age interaction (ANOVA F=4.157, p=0.054). In the observation group, correlation with age was non-significant (*r*= 0.193, p=0.473), but in the transfusion group, correlation between %BVC/year with age was significant (*r*= -0.663, p=0.003), indicating older children who underwent transfusions had greater %BVC/year than those on observation (Figure 6-4).

6.2.3 Correlation with FSIQ

Baseline and exit FSIQ assessments were available for 29 patients (15 on observation, 14 on transfusion). There were no significant differences in mean FSIQ/year change (observation: mean=-0.61, sd=2.38; transfusion: mean=-0.12, sd=3.55; t= 0.179, p=0.666). Residual data of SIENA %BVC/year (corrected for age, gender, and variability in scanner) did not correlate significantly with FSIQ/year change (*r*=0.068, p=0.725).

Sample n	32			
Genotype	27 HbSS 2 HbS B^0-thalassaemia *3 unknown*			
By Treatment Group	Observation (n=16)	Transfusion (n=16)		
Gender	6M, 10F	12M, 4F	χ^2= 4.571, p=0.037	
Age at Pre-randomisation MRI (years; mean ± sd)	9.41 ± 2.54	11.06 ± 2.12	*t*= -1.99, p=0.055	
Cognitive Data[a]	Observation (n=16)	Transfusion (n=16)		Effect size (Cohen's *d)*
Baseline FSIQ (mean ± sd)	95.87 ± 7.78	88.71 ± 13.56	*t*=1.725, p=0.096	0.65
Exit FSIQ (mean ± sd)	94.33 ± 10.30	88.07 ± 13.34	*t*= 1.428, p=0.164	0.53
FSIQ/year (mean ± sd)	-0.61 ± 2.38	-0.12 ± 3.55	*t*=0.179, p=0.666	0.16
MRI Analysis	Observation (n=16)	Transfusion (n=16)		
Time lapse (years)	mean= 3.20 ± 0.22 range: 2.84-3.84	mean= 3.11 ± 0.13 range: 2.93-3.47		
SIENA % Brain Volume Change[†]	mean= -0.62 ± 0.44% range: -1.80 - 0.24	mean= -0.96 ± 1.00% range: -2.91 ± 0.319	ANOVA F= 0.0012, p=0.972	0.44
[a]available for 29 of 32 subjects who had baseline and exit FSIQ available. [†]calculated per year (*i.e.* volume change/time lapse).				

Table 6-1. Demographics and results of SIENA analysis.

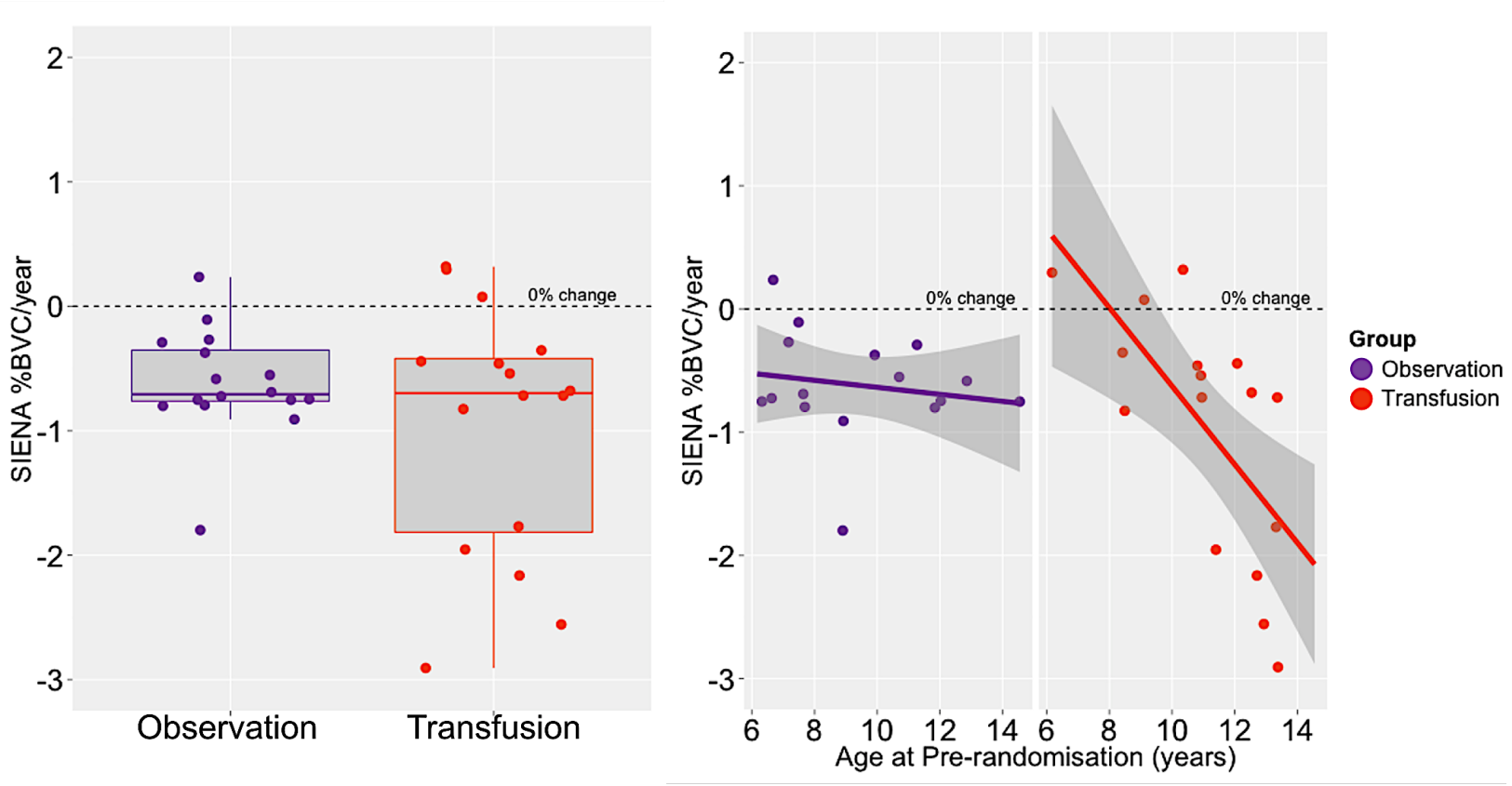

Figure 6-4. SIENA %BVC/year between observation and transfusion groups. Left: Boxplot indicating differences in variation of %BVC/year between groups. Right: Scatter plot with age at pre-randomisation between groups.

6.3 Discussion

This is the first study to date to investigate within-subject longitudinal change in brain volume in children and adolescents with SCD. This study aimed to characterise rates of annual growth or atrophy in a subset of children with SCD with existing SCI who were randomised to the SIT trial. Our primary hypothesis was not supported; over approximately a three-year period, there were no significant differences in brain volumetric change between the observation and transfusion arms of the trial. Further, the results do show a significant group by age interaction, driven by the transfusion group. This suggests that older children who underwent transfusions had greater brain volume loss than those who were on observation. These results suggest that transfusion treatment has a differential effect on %BVC/year with age.

6.3.1 %BVC/year compared with other populations

In a healthy population between the ages of 4 and 18 years, total brain volume was shown to follow an inverted U-shaped curve, increasing until about age twelve, then decreasing by quadratic age of 0.09%[290]. The observed rate of atrophy in the patients in this study was 0.62% for those on no treatment and 0.96% for those on transfusion therapy. There was a significant difference in gender proportion between the two patient groups, but after this factor was taken into account, along with age at pre-randomisation and scanner variability, showed no statistical differences between the two groups.

The rates of atrophy from this study are greater than the reported 0.15% error in reproducibility experiments in healthy adult subjects[302], and greater than previous reports in healthy aging populations. In volunteers aged 50-75 years, %BVC/year was -0.4%[308], and in volunteers aged 38-82 years, it was -0.23% ± 0.36%[309]. Two studies have investigated brain atrophy in adults with cerebral small vessel disease, finding values of %BVC/year of -0.56% ± 0.74%[304] and -0.914% ±0.16%[305]. The values in middle-aged and elderly patients with small vessel disease and cerebral autosomal-dominant arteriopathy with subcortical infarcts and leukoencephalopathy (CADASIL) are in line with our results. Although the SIT trial showed reduction of recurrence of cerebral infarct in the transfusion arm[160], there is no evidence from our study for a protective effect on progressive cerebral atrophy, perhaps because the mechanisms causing recurrent infarction and progressive atrophy are different.

6.3.2 %BVC/year compared with other SCD longitudinal data

Six adolescents with no evidence of baseline SCI and therefore not randomised to the SIT trial returned for follow-up MRI between 3.6 and 7.9 years later. All six had baseline and follow-up MRI on the same scanner system (at Site 7: see Table 6-1 for sequence details). On follow-up MRI, all six were declared to still have no evidence of SCI and none were on regular transfusion treatment. For these six patients (mean age at first scan: 8.53 years, range: 8.08 - 10.23 years, 3 males), mean %BVC/year was -0.58% (range: -1.28 – 0.24%).

Due to small sample sizes, formal statistical testing was not performed, although effect sizes were calculated between groups. The difference between the SIT observation group (n=16, mean %BVC/year: -0.62%) and the no-SCI group was 0.04% (effect size: -0.08). The difference between the SIT transfusion group (n=16, mean %BVC/year = -0.96%) and the no-SCI group was 0.38% (effect size: -0.41; Figure 6-5).

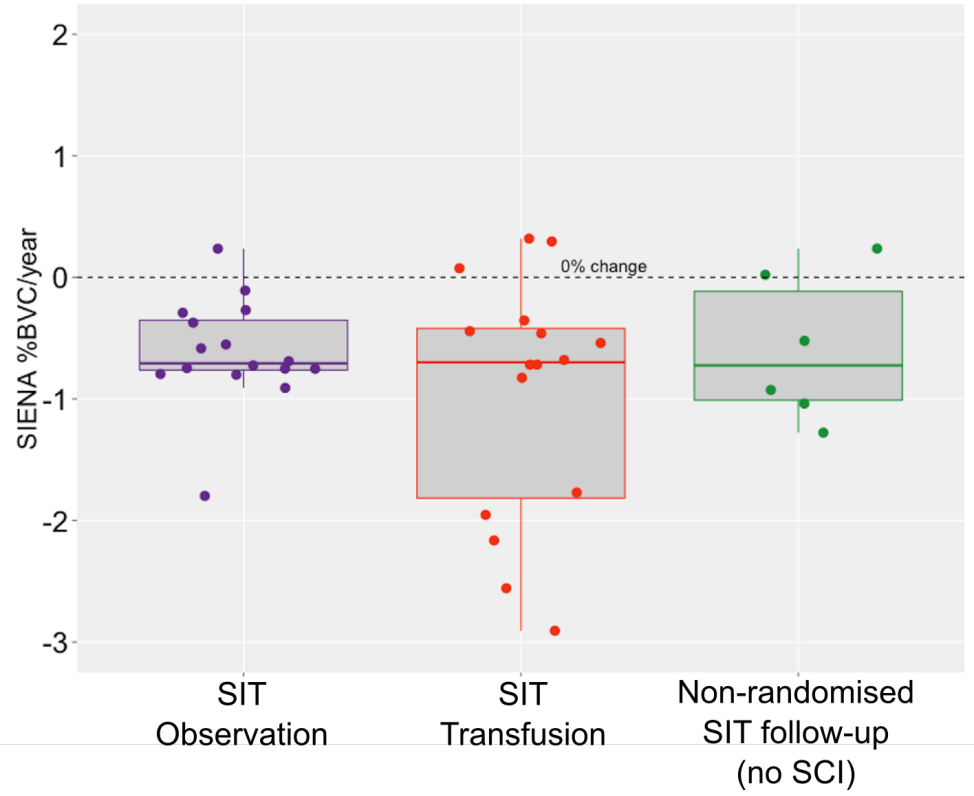

Figure 6-5. Comparison with longitudinal non-radomised SIT patient data.

Additionally, one male sibling control subject originally scanned in 2002 as part of the East London cohort returned in 2013 for a follow-up MRI. Age at first scan was 18.34 years, and the %BVC/year calculated between the two time points was -0.47% (not pictured in Figure

6-5). This rate of change falls within range of similar healthy, but slightly older, populations[308,309].

The inclusion of a 'control' group with no evidence of SCI on MRI allows for some further interpretation of the SIT trial reported atrophy results. Although statistical testing between the two SIT groups and the no SCI group was not performed, there are no obvious differences in the mean %BVC or range of %BVC between the two untreated groups (*i.e.* SIT observation group and the no SCI group), suggesting that rates of atrophy are not solely due to presence of existing cerebrovascular disease. These preliminary findings give some indication that atrophy may be a result of subtler effects of chronic disease on the brain, rather than exclusively presence of SCI.

6.3.3 Limitations

This study is limited by unavailability of clinical data from this trial. During the analysis of this work, main trial findings had yet to be published and medical data was therefore not shared. Clinical information regarding disease severity (*i.e.* markers of anaemia such as haemoglobin, haematocrit and oxygen saturation) may have mediating effects on these reported results.

In a multicentre longitudinal study over years, it is difficult to guarantee that clinical scanner systems will stay the same for all acquired scans for the duration of the study. Change in intensity of tissues from different scanner systems may introduce systematic error for automatic segmentation software. SIENA segments the brain and estimates the outer skull surface for both pre-randomisation and exit time points and uses 12-parameter affine transformation (translation, rotation, scaling and skew) to register the two images[302]. Then, brain edge points in both images are compared, and SIENA estimates motion of each brain edge point from one time point to the next. One study investigating intra-scanner variability error noted SIENA mean edge displacement algorithm is relatively insensitive to changes in intensity of tissues from one scan to the next[311]. A reproducibility study to explain the variance in longitudinal volumetric data in children is therefore warranted.

6.4 Conclusion

This chapter showed evidence of longitudinal brain atrophy in children with SCD who were randomised in the SIT trial. Although the main trial results showed transfusion therapy reduced risk of new or progressive SCI, the results from this study show no protective effect of transfusion therapy on rate of brain atrophy.

Chapter 7. White matter abnormalities relate to oxygen saturation in asymptomatic children with sickle cell anaemia

Up to 35% of patients who have silent cerebral infarcts (SCI)[78,110], with MRI lesions typically present in the deep white matter of the centrum semiovale in arterial borderzone regions, usually between the anterior and middle cerebral arterial territories[312]. SCI are common within the first decade of life, and can have devastating effects on cognitive abilities, including intelligence[104,218] and executive functioning[115,248]. Children with SCA with no evidence of infarction or abnormalities on conventional T2-weighted MRI still show reduction in cognitive function compared to healthy age- and race-matched controls[106,114,220]; therefore one can assume there may be abnormalities in the brain beyond the detection of conventional MRI methods[200] and that the presence of discrete lesions alone may not describe total brain injury.

The mechanisms for white matter injury in SCA are unclear. Cerebral haemodynamics are often abnormal; there is high global cerebral blood flow but regional reductions, increasing the risk of ischaemia in the territories of stenosed large vessels and the borderzones between them[92,93,259]. The risk of tissue injury is also increased by chronic anaemia [79] and low oxygen saturation[313], leading to further sickling of the red blood cells[314], increased white cell, platelet, and endothelial activation and adherence of sickled cells to the vascular endothelium[315]. Low daytime and nocturnal peripheral oxygen saturation has previously been linked to risk of overt stroke[94,313], lower IQ[252] and poorer performance on executive function tasks[162] in SCA. Lower IQ and worse executive function, as well as neuronal injury in the hippocampus, have been reported in children with sleep-disordered breathing/obstructive sleep apnoea in the general population experiencing similar nocturnal oxygen desaturation[316–318]. The disruption to breathing, which results in reduced oxygen saturation, has been shown to interfere with synaptic plasticity and consequently various cognitive functions[319]. However in children with SCA, there are no data on any direct link between brain structure, oxygen saturation and haemoglobin.

Diffusion tensor imaging (DTI) provides information about white matter microstructure. The technique known as tract-based spatial statistics (TBSS)[242] is a whole-brain voxel-wise analysis without the need for prior determination of tracts of interest. It registers white matter, rather than the whole brain, between subjects, resulting in improved registration, reduced partial volume effects and no smoothing limitations. There are few diffusion data in SCA. TBSS was used[205] to compare two groups of children with SCA, some of whom had mild gliosis although none had SCI. Increases in diffusivity and anisotropy reduction in the

body of the corpus callosum (CC) was found only in patients with mild gliosis, while anisotropy reduction in the centrum semiovale was found in the no-SCI group; however, results were not significant at the 95% confidence level.

A recent study compared sixteen SCA patients (age range of 11-45 years) and a matched control group in a combined quantitative DTI and deterministic tractography analysis[206]. This study used various regions-of-interests (ROI) across the brain, finding reduced FA in the CC, centrum semiovale, periventricular areas and subcortical white matter ROIs. Deterministic tractography of the CC was also used, showing reduced fibre count (*i.e.* streamlines) and reduced FA in the anterior body of the CC. However, these results are limited because a significant proportion of the patient group (6 of 16 patients) had SCI present, potentially augmenting the results. In addition, the effect of a wide age range on diffusion data was not controlled for, and there was no correction for multiple comparisons after which the findings might not be statistically significant. These studies did not include relationships between white matter and any physiological measures.

The objective of this study was to investigate differences in white matter structural integrity in children with SCA and controls. This study only compared those with SCA and no evidence of abnormalities on T2-weighted MRI to elucidate differences in only the normal-appearing white matter. We hypothesized firstly that there is structural damage, detectable by using a whole-brain voxel-wise white matter analysis, and secondly that the degree of damage is related to reduced daytime oxygen saturation and steady-state haemoglobin.

7.1 Methods

7.1.1 Participants

Child and adolescent participants were recruited as part of the 2012-2013 London cohort (described in Chapter 3). Inclusion criteria consisted of: participant age between 8 and 18 years, and having both T2-weighted and DTI sequences.

7.1.2 Physiological Measures

From the medical records, peripheral oxygen saturation measurements were collected within 3 years of the date of the MRI scan at regular clinic visits when the patient was generally well, including a measurement taken on the day of MRI over a 5-minute period from a pulse oximeter (Masimo Pronto-7 Pulse CO-Oximeter). Patients had between 3 and 9 measurements (median 4), and the average oxygen saturation was calculated and used in subsequent analyses.

Steady-state haemoglobin was also recorded from the closest available full blood count to MRI date from patient's medical records.

7.1.3 Neuropsychological Variables

A measure of full-scale IQ (FSIQ) was obtained using the WASI. For measures of executive function, five tests were acquired from the D-KEFS test battery: Tower test (Tower) which measures strategic planning and rule learning, Trailmaking Test Visual Scanning condition (Scanning) which measures visuomotor processing speed and attention, Trailmaking Test number-letter switching condition (Switching) which measures cognitive flexibility (*i.e.* multitasking and simultaneous processing), Verbal Fluency letter condition which measures systematic retrieval of lexical items, and Colour-Word Interference which measures verbal inhibition and cognitive flexibility. The BRIEF parent form was obtained for children younger than 16, yielding a global executive composite that represents the child's overall function. Details of neuropsychological tests are reviewed in Chapter 3. Demographics are reported in Table 7-1.

7.1.4 MRI Acquisition

Details of the MRI protocol are reviewed in Chapter 3.

7.1.5 DTI Preprocessing

All scans were visually inspected for abnormalities due to motion, or other artifacts. The DTI data were preprocessed using TractoR version 2.3[320] and FMRIB Software Library (FSL) version 5.0[242]. Within each subject, a reference b=0 volume was brain extracted[321], and diffusion-weighted volumes were registered to this volume to correct for eddy current distortions. A diffusion tensor was derived at each voxel using a standard least-squares process to provide a voxel-wise calculation of FA, MD, AD and RD.

7.1.6 TBSS Whole-Brain Analysis

Voxel-wise statistical analysis of FA data was carried out using tract-based spatial statistics (TBSS). Each subject's FA image was aligned to every other one and the 'most representative' image was identified as the target image, which was then affine-aligned to MNI standard space. All subjects' FA data were transformed to standard space by combining nonlinear registration to the representative target FA image and affine transform to standard space. A mean FA skeleton (threshold at FA=0.2) was created by restricting to

voxels with the highest FA at the centre of the major WM tracts. Each participant's FA data were projected onto the mean skeleton to allow for voxel-wise cross-subject statistics. In a similar manner, MD, AD and RD data were projected onto the skeleton, and these data were used for voxel-wise permutation-based analysis. Age and gender were included as covariates in the TBSS analyses, which included structural comparisons between patient and control groups, and correlations with oxygen saturation and haemoglobin in the patient group only. Results were corrected for multiple comparisons using threshold-free cluster enhancement (TFCE).

7.2 Results

Forty-three patients with homozygous SCA (HbSS) and eighteen controls, including twelve siblings, were initially scanned. Thirty SCA patients had no abnormality on T2-weighted MRI, while twelve SCA patients were excluded due to presence of SCI. Ten subjects (six patients and four controls) were excluded because of poor quality DTI data (*i.e.* dental brace artefact, head motion, systematic vibration artifact[322]). The final dataset used for DTI analysis included twenty-five children and adolescents with SCA without SCI and fourteen age- and race-matched controls. Figure 7-1 shows a graphical representation of excluded subjects and Table 7-1 describes demographics of the final dataset in which DTI data were analysed.

In the patient group, two children were undergoing regular transfusion treatment (abnormal transcranial Doppler ultrasound, top-up for painful crises), two additional children had transfusions within three months prior to scan, three children were on hydroxycarbamide treatment and seventeen children were receiving no treatment.

Figure 7-1. Flowchart detailing the process of subject exclusion from analysis.

	SCA (n=25)	Control (n=14)		Effect size (Cohen's *d*)
HbS genotype	25 HbSS	8 HbAS, 6 HbAA		
Age (mean, sd)	13.07 (2.82)	13.71 (2.93)	t=0.679, †p=0.501	
Gender	13M, 12F	7M, 7F	$\chi 2$=0.014, p=0.905	
FSIQ (mean, sd)	103.12 (11.95)	108.29 (11.69)	t=1.305, †p=0.200	0.436
Tower (mean, sd)[a]	9.25 (2.71)	9.86 (2.11)	t=0.720, †p=0.476	0.240
Scanning (mean, sd)	9.60 (3.63)	10.00 (2.88)	t=0.354, †p=0.725	0.118
Switching (mean, sd)[a]	8.29 (3.37)	7.93 (3.45)	t=-0.318, †p=0.753	0.106
Verbal Fluency (mean, sd)[a]	10.29 (2.71)	10.43 (2.90)	t=0.146, †p=0.884	0.048
Colour-Word Interference (mean, sd)	8.76 (3.22)	8.79 (3.07)	t=0.024, †p=0.981	0.008
BRIEF Global Executive Composite (mean, sd)[b]	52.18 (10.03)	51.17 (10.73)	t=-0.275, †p=0.785	0.092
Oxygen saturation[c]	mean: 96.70% range: 91-100%	mean: 99% range: 99-99%		
Haemoglobin[d]	mean: 8.29 g/dl range: 6.40-12.20	-		

FSIQ= WASI 2-subtest Full-Scale Intelligence Quotient

Tower= Delis-Kaplan Executive Function System (D-KEFS) Tower test

Scanning= D-KEFS Trailmaking Test – Visual Scanning condition

Switching = D-KEFS Trailmaking Test – Switching condition

Verbal Fluency = D-KEFS Verbal Fluency – Letter condition

Colour-Word Interference= D-KEFS Colour Word Interference – Inhibition/Switching condition

BRIEF = Behaviour Rating Inventory of Executive Function (parent form).

†Student's t test.

[a]Scores available for 24 of 25 SCA subjects.

[b]Scores available for 12 controls and 22 patients.

[c]Oxygen saturation available for all SCA subjects and 5 of 14 controls.

[d]Haemoglobin available in all SCA subjects.

Table 7-1. Demographics, physiological and behavioural scores for DTI analysis.

7.2.1 Physiological Measures

Oxygen saturation was available for all patients and five controls, and haemoglobin was available for twenty-two patients; patients had lower haemoglobin oxygen saturation and haemoglobin than published norms of healthy non-SCA children[323] (Table 7-1).

7.2.2 Neuropsychological variables

There were no significant differences between the patient and control groups regarding age, gender, IQ or any executive function measures (Table 7-1). Mean IQ and D-KEFS scores (except Switching) were lower in patients, and BRIEF scores were higher in patients, but these differences were not statistically significant and had small effect sizes (Table 7-1, Figure 7-2).

In the control group, eight had sickle cell trait (HbAS) and six had normal haemoglobin genotype (HbAA). Between HbAS and HbAA, there was no significant difference in:

- mean IQ score (HbAS=109.6, HbAA=106.5, t=-0.480, p=0.640),
- mean Scanning score (HbAS=9.8, HbAA=10.3, t=0.413, p=0.690),
- mean Switching score (HbAS=7.9, HbAA=8.0, t=0.064, p=0.952),
- mean verbal fluency score (HbAS=10.75, HbAA=10.00, t=-0.464, p=0.651), and
- mean colour-word interference score (HbAS=8.38, HbAA=9.33, t=0.563, p=0.584).

Children with HbAS had significantly better Tower scores than HbAA (HbAS=11.1, HbAA=8.2, t=-3.605, p=0.004). Between 7 HbAS and 5 HbAA subjects, there were no differences in BRIEF global executive composite score (HbAS=48.71, HbAA=54.60, t=0.931, p=0.374).

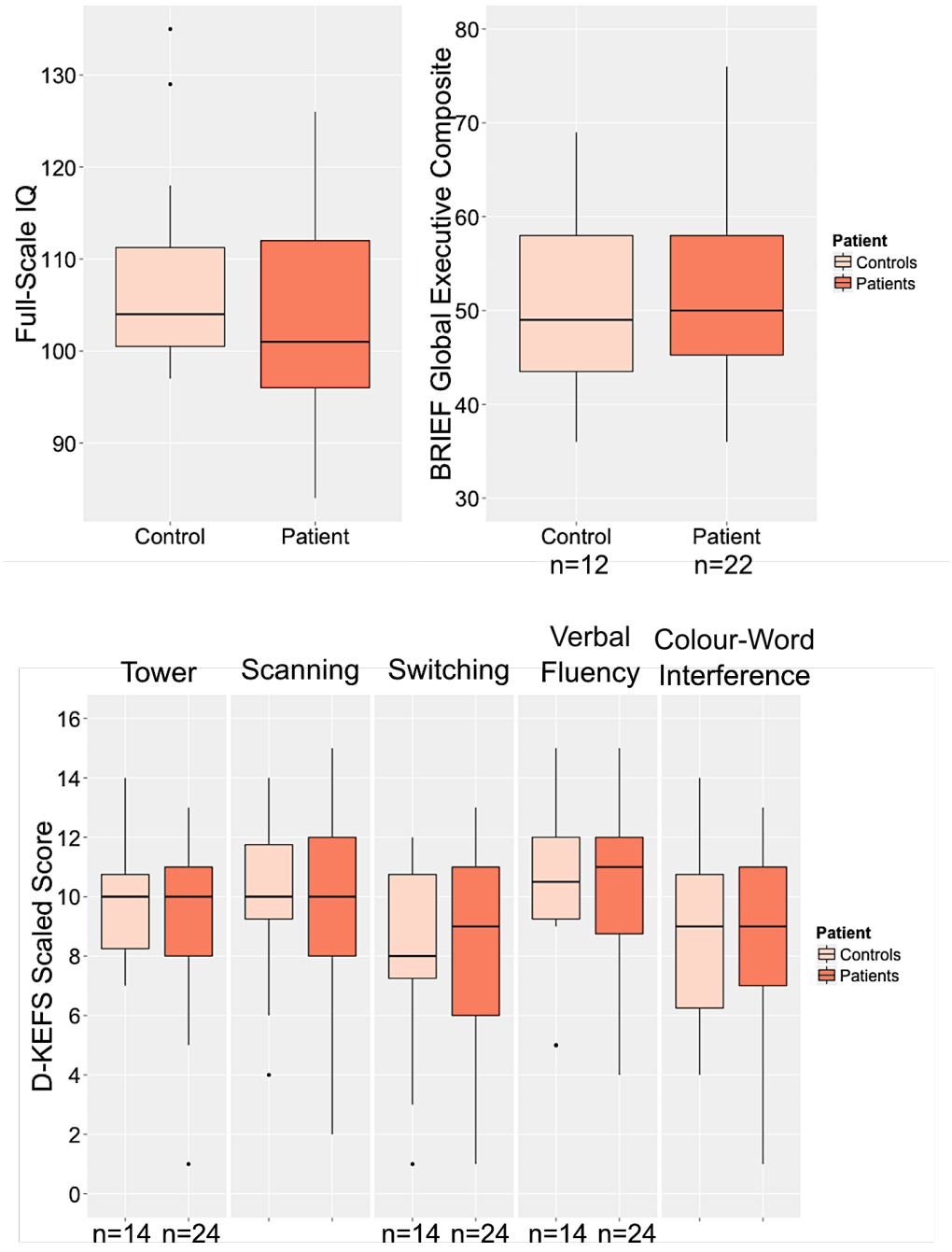

Figure 7-2. Results of neuropsychological testing. Patients scored lower on WASI full-scale IQ (top left) and higher on BRIEF global executive composite (top right), but differences were not statistically significant. On the D-KEFS measures, patients scored lower on all tests except Switching; differences were not statistically significant.

7.2.3 Structural TBSS results between patients and controls

Results of the TBSS analysis comparing patients and controls are shown in Figure 7-3. After controlling for the effects of age and gender, FA was significantly lower in patients than controls ($p<0.05$) in the cerebral peduncles and cerebellum. Widespread increases in MD were found. Across frontal and parietal lobes, genu of the CC, and subcortical structures and cerebellum, patients had significantly higher MD than controls ($p<0.05$). RD was significantly higher in patients than controls in the frontal and parietal lobes, and bilaterally in the internal capsule, anterior thalamic radiations, corticospinal tract and cerebellum ($p<0.05$). No significant structural differences were found between patients and controls for AD.

7.2.4 TBSS correlation with oxygen saturation and haemoglobin

Results of the TBSS analysis testing correlations between DTI parameters and oxygen saturation and haemoglobin are shown in Figure 7-4. In the patient group, a significant negative correlation was found between RD and daytime oxygen saturation in a cluster in the genu of the CC ($p<0.05$; TFCE-corrected). Mean raw values of RD from the ROI that significantly negatively correlated with SpO_2 were extracted and a highly significant correlation was found ($r= -0.650$, $p=0.0004$) with 96% statistical power (Figure 7-4, top right panel).

A trend-level negative correlation was found between RD and haemoglobin in the midbody and posterior parts of the CC ($p<0.1$; TFCE-corrected). Mean raw values of RD from the ROI that significantly negatively correlated with haemoglobin were extracted and a significant correlation was found ($r= -0.456$, $p=0.022$) with 75% statistical power (Figure 7-4, bottom right panel). To achieve 80% statistical power, 36 patients would have been required.

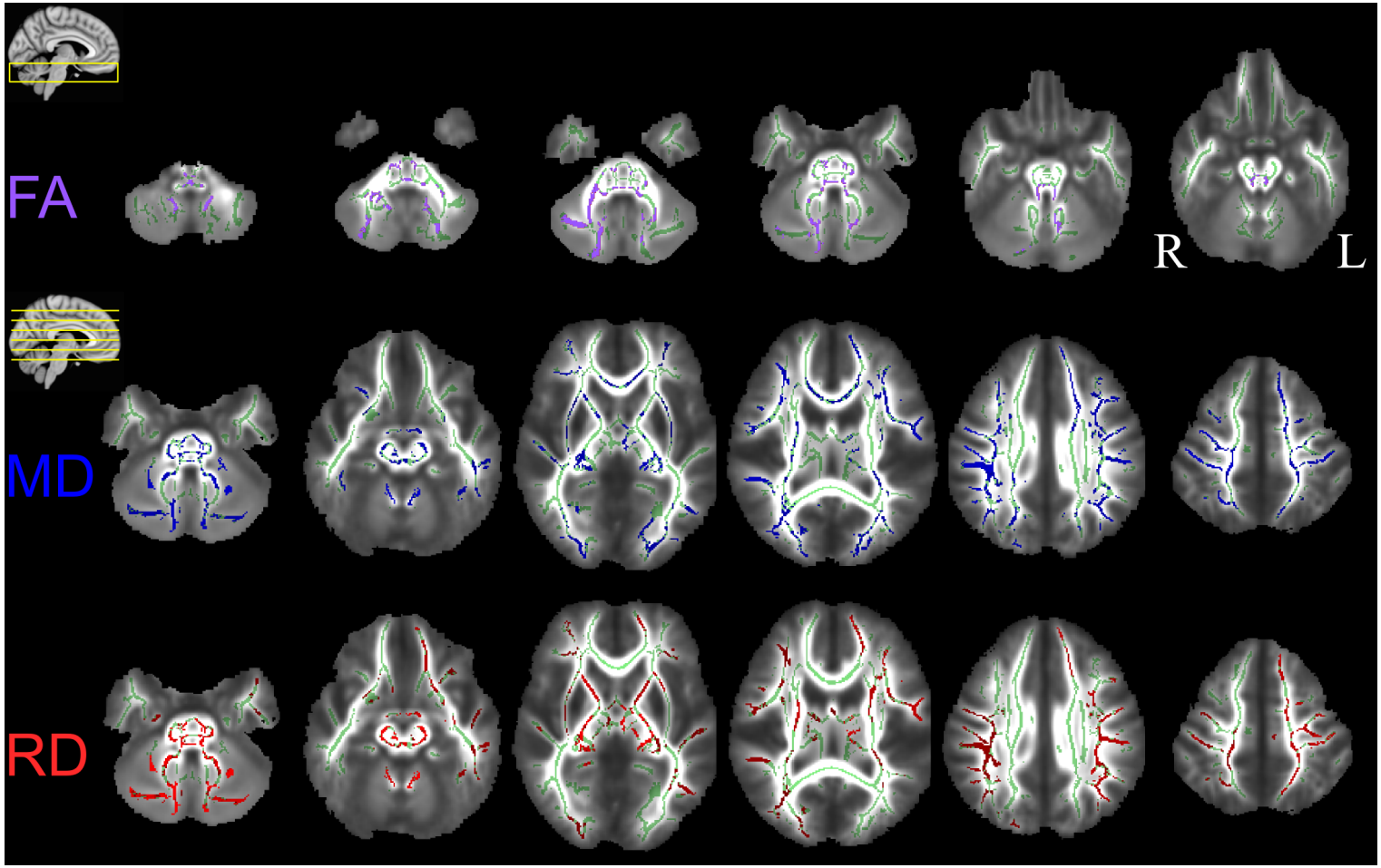

Figure 7-3. Whole-brain TBSS results. Top panel: FA – purple voxels indicate areas in which SCA patients had significantly lower FA than controls. Middle panel: MD – blue voxels indicate areas in which SCA patients had significantly higher MD than controls. Bottom panel: RD – red voxels indicate areas in which SCA patients had significantly higher RD than controls. All results significant at $p<0.05$ (TFCE corrected) and overlaid on the group white matter skeleton (green) and the study-specific mean FA template.

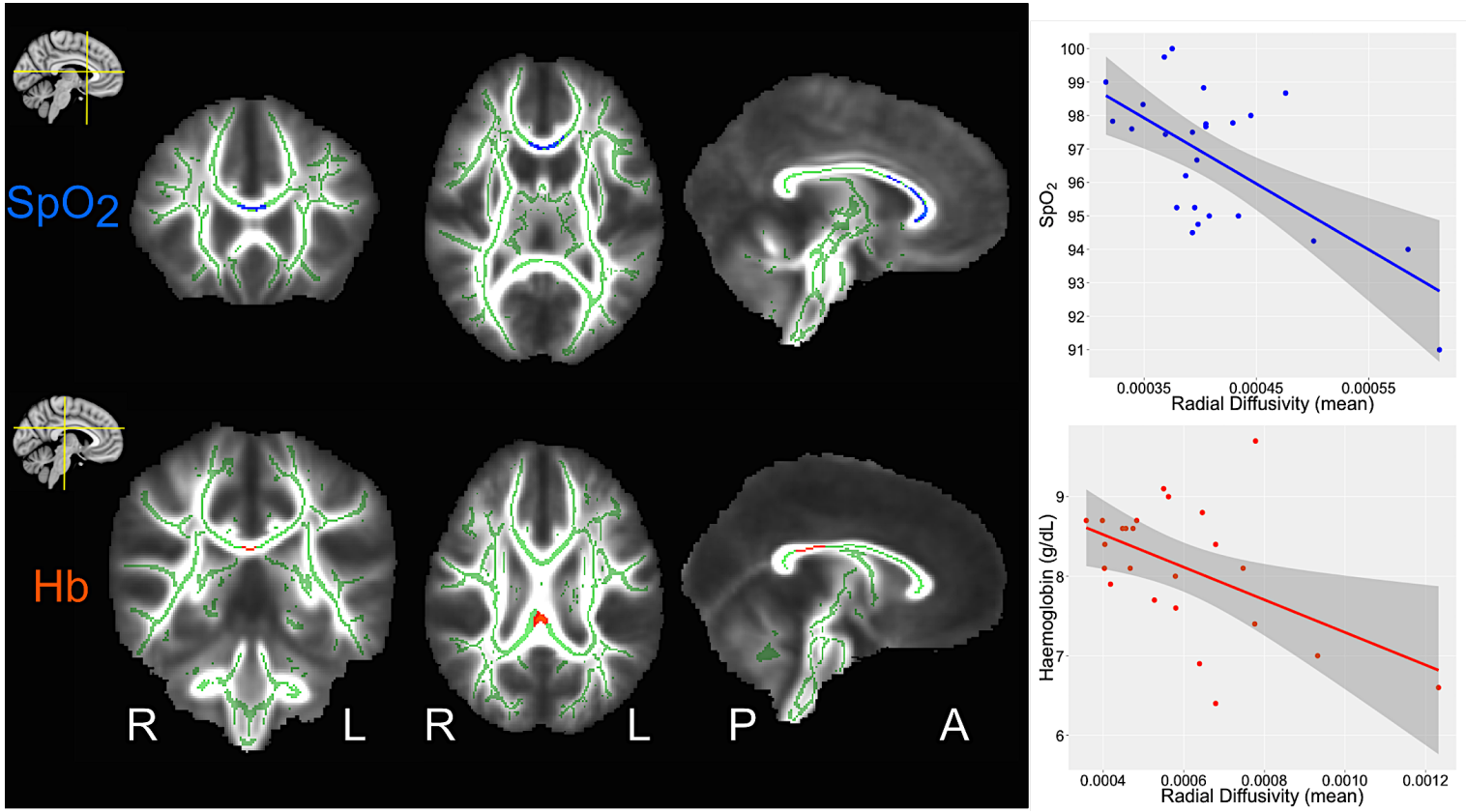

Figure 7-4. TBSS correlations with daytime oxygen saturation and steady-state haemoglobin in patients only. Top panel: Blue voxels indicate areas in which RD significantly negatively correlated with daytime peripheral oxygen saturation ($p<0.05$). Bottom panel: Red voxels indicate areas in which RD negatively correlated with haemoglobin ($p<0.1$). All results TFCE corrected and overlaid on the group white matter skeleton (green) and the study-specific mean FA template. RD data shown in plots are mean values from the region-of-interest shown on the mean FA template.

7.3 Discussion

This is the first diffusion MRI study in children with SCA with no evidence of MRI abnormalities to link brain microstructure with physiological markers of disease severity. Specifically, oxygen saturation was found to correlate significantly with RD in the anterior CC and there was a trend-level correlation between steady state haemoglobin and RD in the midbody of the CC, suggesting a relationship between chronic oxygen desaturation and anaemia and white matter microstructural integrity in this population of asymptomatic children with SCA. This study also confirmed the presence of widespread white matter abnormalities. FA was found to be significantly lower in patients, mainly in cerebellar white matter, and MD and RD significantly higher in patients in widespread regions in the centrum semiovale and subcortical and cerebellar white matter.

The sample of children with SCA with no SCI showed no differences compared to the control group in terms of IQ and six measures of executive function: tests of visual processing speed, planning and cognitive flexibility and verbal fluency, as well as a parent questionnaire. We can conclude that differences in microstructural white matter were not due to underlying differences in cognitive ability in these domains.

This study builds upon and extends a previous TBSS study in which three groups (SCA-mild gliosis, SCA-no lesions and controls) were compared[205] and there were anisotropy reductions and increases in diffusivity in the CC and centrum semiovale, with the greatest effects seen in the mild gliosis group, followed by the no lesion group, compared to controls[205]; however, all results were only approaching statistical significance. Our study found more widespread and statistically significant differences between SCA patients with no SCI compared to controls in FA and diffusivity measures.

There were statistically significant differences in RD, but not AD. AD is thought to reflect structural coherence and alignment of axons in white matter, while RD is thought to reflect axon density and membrane permeability[324]. Reduced myelination can be represented by elevated RD, without a change in AD[175], despite the fact that RD is approximately 30% of the magnitude of AD[325]. This is consistent with results from previous paediatric TBSS studies[326–328].

7.3.1 Link with oxygen saturation and haemoglobin

There is an established link between oxygen desaturation and poor cognitive function[252] as well as risk of stroke[79], but it is still unclear whether this involves a relationship between chronic oxygen desaturation and/or chronic anaemia and white matter damage in children

with no SCI. Acute silent cerebral ischaemic events, that may or may not develop into visible SCI, occur relatively frequently[112], particularly in relation to acute anaemia[42]. Our data confirms that oxygen desaturation also renders the brain at continual risk for hypoxic-ischaemic injury[329]. In diffusion data, high RD could be due to myelin loss and axonal damage, and is likely to be related to the cycle of hypoxia, endothelial inflammation, and tissue injury in children with SCA without SCI.

In the present study, there was a significant negative correlation between oxygen saturation and RD in the anterior CC and a negative trend-level correlation between haemoglobin and RD in the midbody of the CC using the whole-brain TBSS analysis. Correlations of mean raw RD values of the ROI and oxygen saturation and haemoglobin had 96% and 75% statistical power, respectively. Although oxygen saturation and haemoglobin are correlated[330], one study found that only a small proportion of variance in steady-state oxygen desaturation was explained by chronic anaemia[95]. It is likely that oxygen desaturation has a more vital role than haemoglobin in white matter viability of frontal lobe white matter.

7.3.2 Neuropsychology

The results from this sample indicate no significant differences in IQ between children with SCA without SCI compared to controls. Previous reports from the CSSCD[106,220] have shown that children with normal MRI findings have deficits in IQ, but the control group used were age-, gender- and race-matched controls from a normative database, whereas a sibling control group matched for socioeconomic status would have been ideal[216,264]. A meta-analysis[114] of cognitive studies in SCA, including comparison between children without SCI and controls, showed a small effect size in IQ measures, with patients approximately 4-5 points lower than controls. Results from the present study, using mainly siblings but also age- and race-matched controls concurrently tested with patients, did not provide any evidence to suggest marked differences in IQ, or that IQ of patients was outside the average range. It is possible that the 2-subtest WASI, which does not give verbal or performance IQ, may not be specific enough for more subtle discrepancies in cognition between patients and controls. Performance IQ, made up for perceptual organisation and processing speed, has been associated with cerebral blood flow[254] and basal ganglia and thalamus volume[331] and may also be associated with white matter integrity.

Results from multiple executive functioning tasks are also reported, also showing no differences between patients and controls in attention, visual processing speed, or cognitive flexibility. Executive functioning deficits are often reported in children with SCI compared to those without SCI[115], but none have yet reported executive dysfunction in those without SCI compared to healthy controls.

No information about socioeconomic status was available for these subjects, although 10 of 14 controls (71%) were siblings of patients, and all were of the same ethnic background. Although socioeconomic status and parental education are both relevant factors in a child's cognitive profile[252], it is unlikely these factors are so different between patient and control groups to mediate a statistically significant effect in white matter microstructure.

The observed differences in white matter microstructure seen in our patient group do not appear to be related to any specific underlying cognitive deficits detectable by the administered neuropsychological battery. However, changes in white matter microstructure may be indicative of future cognitive difficulties in general measures such as academic achievement, as one study reported 27% of children with SCA without SCI experienced poor academic achievement compared to only 6% of healthy siblings[227]. With this sample, future work is needed to investigate academic performance and cognitive functioning longitudinally and to elucidate the effects of chronic oxygen saturation on white matter microstructure and general cognitive function.

7.3.3 Implications for treatment

Nocturnal oxygen desaturation in children with SCA has been reported to predict central nervous system events[94], and to be associated with poorer performance on the D-KEFS Tower test[162]. The present study establishes a link between daytime oxygen saturation and white matter microstructural abnormality, which may be potentially ameliorated with interventions to reduce hypoxic exposure, most practically overnight[279]. Studies examining the effect of altitude exposure suggest that longer-term experience of hypoxia is associated with widespread decreases in FA[332], but the thresholds for chronic hypoxic exposure and whether these changes are reversible remains uncertain. These DTI metrics may serve as biomarkers for future randomised controlled trials in SCA to investigate white matter microstructure before and after a period of overnight respiratory support or other experimental or standard treatments such as chronic blood transfusion or hydroxycarbamide.

7.3.4 Conclusion

In a cohort of children and adolescents with SCA with no evidence of SCI, markers of physiological disease severity (*i.e.* daytime oxygen saturation) are significantly correlated with white matter microstructure in anterior inter-hemispheric pathways. These results underline the importance of maintaining high levels of oxygen saturation in SCA to avoid damage to inter-hemispheric white matter and potentially set DTI metrics as a biomarker for monitoring potential therapeutic effects.

Chapter 8. General Discussion

This thesis overviewed SCD in respect to the principal medical complications, epidemiology, public health and treatments, as well as the neurological and neuropsychological sequelae of the disease. Ischaemic events secondary to chronic anaemia in childhood are discussed with neuroimaging and neurocognitive findings. The aim of this thesis was to incorporate new quantitative MRI analyses and neuropsychological testing results to bridge a gap in the existing literature, and to determine neuroimaging biomarkers of sickle cell disease severity.

8.1 Main Findings

First, this thesis summarises the IQ literature in SCD, in those studies that used MRI-defined groups based on presence or absence of SCI. There is a commonly reported trend in the SCD cognitive literature corresponding to a step-wise trend with lesion burden[199,216,217]: those with evidence of SCI perform worse than those patients with normal MRI, and those with normal MRI perform worse than controls. The current findings from a sample of previously unreported patients showed SCD patients, regardless of abnormality seen on T2-weighted MRI, have significantly lowered full-scale IQ than appropriately matched controls. Patients with SCI had lower mean full-scale IQ than patients without, although not significantly lower. These results imply cognitive dysfunction may not be exclusively a result of visible ischaemic injury (*i.e.* SCI), but may be due to the chronic disease process.

The following three chapters discuss quantitative neuroimaging biomarkers of the disease process, including volumetric differences, longitudinal whole-brain atrophy and diffusion characteristics.

After expanding on a previously published report (see Appendix B), patients in a larger cohort were found to have decreased volumes of specific, subcortical structures, in groups corresponding to lesion burden, mirroring the step-wise trend seen in the cognitive literature. Similar to the results found in the full-scale IQ chapter, both patient groups, with and without SCI, had significantly lower mean volumes than controls for the bilateral cerebellar cortices, left amygdala and total subcortical grey matter volume. This chapter also showed significant negative correlations with age in patients without evidence of SCI comparable to controls, while no correlations were found in patients with evidence of SCI; this may indicate differential patterns of brain maturation from childhood to adulthood.

From the SIT trial, a subset of those randomised to transfusion treatment or standard care had high-resolution T1-weighted data in which the percentage of brain volume change over three years of the trial could be assessed. There was evidence of atrophy in total brain volume over 3 years in all SCD patients, with rates of atrophy similar to those seen in older people with small vessel disease or traumatic brain injury. These findings also revealed no protective effect of transfusion treatment, in contrast to the main hypothesis.

The final chapter showed marked differences in diffusion characteristics between those patients without evidence of SCI compared to controls. There was evidence of reduced fractional anisotropy, as well as increased diffusivity in widespread areas across the brain. Radial diffusivity, a marker of reduced myelination and membrane permeability (*i.e.* reduced white matter integrity) correlated significantly with haematological markers of disease severity (*i.e.* oxygen saturation and haemoglobin). This result underlines the importance of maintaining high levels of oxygen saturation to avoid white matter damage, and sets these DTI metrics as a biomarker for monitoring potential therapeutic effects.

These findings are consistent with the hypothesis of a global diffuse pattern of brain injury, related to the effects of chronic illness (*i.e.* chronic anaemia and chronic intermittent hypoxia). These four chapters extend the neuroimaging literature, further defining the extent of neurological injury in children with SCD.

8.2 Future work

SCD has been called a developmental disorder[296], with a range of neurological complications resulting from chronic anaemia and oxygen desaturation from a very young age. Clinical neuroimaging has long been used to routinely diagnose cerebral infarction during hospitalisation after a suspected event, or for screening in clinical trials, such as SIT. Only in the last 10 years has MRI been systematically applied in research settings. As MR systems, software and analysis techniques become more advanced, there is much promise for the future in SCD neuroimaging research.

In SCD, the deep white matter in the centrum semiovale is vulnerable tissue where SCI frequently occur. DTI results from Chapter 7 of this thesis showed marked diffusion abnormalities in normal-appearing white matter, compared to controls. There are some limitations to DTI and tractography: multiple fibre orientations within the same voxel can skew results and DTI indices can lack of specificity[333]. Although DTI processing in this thesis used a model-dependent approach to fit two fibre orientations per voxel, there are more advanced, model-free approaches such as spherical deconvolution[334], which can extract directly the underlying fibre orientation, and neurite orientation dispersion and

density imaging (NODDI)[335], which can measure density and orientation dispersion properties of axons in white matter and dendrites in grey matter. Spherical deconvolution may be able to give more reliable tractography results especially in areas of crossing fibres, while NODDI may be able to disentangle the factors that make up fractional anisotropy for more specific interpretation of pathology.

Cerebral blood flow (CBF) studies have shown areas of decreased perfusion corresponding to areas of structural abnormality (*i.e.* stroke-like lesions)[93,336], while elevated values were found in patients with no MRI abnormality[259,260,337,338] Elevated CBF appears to be a compensatory measure caused by vasodilation secondary to chronic anaemia[91]. Whether areas of decreased perfusion can predict localised ischaemic events remains to be determined. Arterial spin labelling perfusion MRI can non-invasively measure CBF in children with SCD[254,259–261,277]. Dynamic ASL acquisitions are assocated with haemodynamic parameters, such as arrival time and dispersion of the bolus of labelled blood, which may give useful information about the underlying vasculature.

Task-based and resting-state functional MRI (fMRI) tasks rely on a normal arterial input function, and detection of blood-oxygen level dependent (BOLD) activation in SCD patients may be compromised due to anaemia and abnormal haemodynamics[92,339], even if underlying neuronal activity was intact. A previous task-based fMRI study looking at visual stimuli showed BOLD effect activation was not strongly associated with resting CBF, but there was strong association with full-scale IQ[340]. The authors suggest the inability to mount an appropriate haemodynamic response to support increased neural activity[341] underpins potential cognitive dysfunction in SCD. Further work is needed to first calculate a potential abnormal haemodynamic response function using task-based fMRI in treated and untreated children with SCD, then to use that information in resting-state fMRI, which can allow for analysis of connectivity networks underlying attention, mentalising, and thought processing.

8.3 Post-doctoral research position

The quantitative neuroimaging experiments discussed in this thesis provide a base to explore the effect of chronic oxygen desaturation on the brain. In 2014, funding was secured from Great Ormond Street Hospital Children's Charity for a post-doctoral research position to start in early 2015, in which there are two parallel studies to take place.

8.3.1 POMS II

First, the project includes neuroimaging analysis for a proof-of-concept clinical trial, funded by the National Institutes for Health Research/Research for Patient Benefit stream. The trial is an extension of POMS[163], in which 30 adult patients and 30 paediatric patients will receive either auto-adjusting continuous positive pressure therapy or oxygen therapy for six months. The choice of intervention is based on patient preference during a 30-day pilot that will complete in December 2014. The main trial aim is that the intervention will reduce frequency and severity of pain symptoms, improve quality of life and cognition. There is some evidence in adults with obstructive sleep apnoea that treatment may potentially reverse acute hypoxic damage to the brain[279]. All patients will undergo MRI before randomisation and after trial exit, with advanced sequences on a 3T MRI scanner. Detailed neuropsychological testing will be performed at randomisation to the trial, and tests sensitive to processing speed, visuomotor coordination, attention and concentration will be performed at trial exit.

8.3.2 SAC follow-up

Second, the project is to recruit up to 84 patients with SCD who have participated in Sleep Asthma Cohort (SAC) study[161], which investigated nocturnal hypoxaemia between 2005-2014. The objectives of SAC were to assess asthma risk factors associated with pain episodes and hospitalisations and to define the relationship between sleep-disordered breathing and pulmonary complications. The aim of the follow-up project to begin in early 2015 is to determine neuroimaging and neurocognitive biomarkers specifically for chronic oxygen saturation on the brain by applying advanced sequences on a 3T MRI scanner and detailed neuropsychological testing. A previous study in this cohort of children has linked poor executive function performance on the D-KEFS Tower task with nocturnal haemoglobin oxygen saturation[162]. The main hypothesis of the study is that subtle brain insults due to chronic nocturnal hypoxia have a profound effect on structural abnormality of the brain as well as short-term and working memory, cognitive flexibility and processing speed.

8.3.3 MSc projects

In 2015, two students doing their research project as part of the Applied Paediatric Neuropsychology MSc will be linked to the SAC follow-up study.

- **“White matter lesions and cognitive profiles in children and adults with SCD”**

The aim of this project is to establish a link between size and location of SCI, cognitive ability and school performance. Using high-resolution T2-weighted MRI, SCI will be identified by a neuroradiologist and the student will manually trace lesion volume. The hypothesis is that children and adults will have differing neuropsychological profiles correlated with the number of lesions, total lesion size and location of infarcted tissue.

- **“Structural and neuropsychological correlates of nocturnal hypoxaemia in children and adults with SCD”**

The aim of this project is to investigate brain structures that are susceptible to hypoxia, such as the hippocampus, as well as white matter pathways connecting the hippocampus with cortical regions. This project will apply high-resolution T1-weighted images to manually trace hippocampal volume and diffusion tensor imaging to virtually dissect medial temporal lobe pathways, along with neuropsychological testing aimed at memory function. The hypothesis is that hippocampal volumetric deficits and altered white matter pathways are related to poorer performance on learning and memory tasks.

Appendix A: Selected Neuropsychological Tests

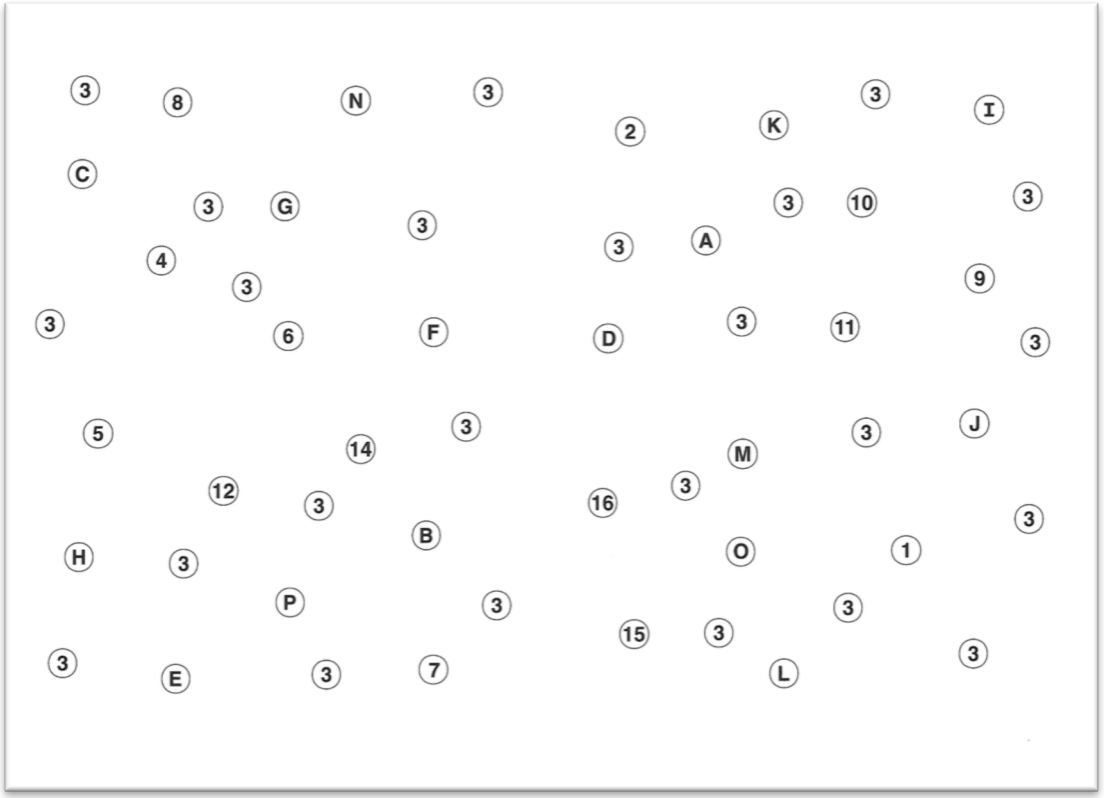

Appendix Figure 1. The Trail-making test – visual scanning condition (Scanning) measures visuomotor processing speed and attention. In this task, the subject is presented with this A3 landscape page with various circles of different numbers and letters, and asked to make a single mark through all the circles with the number "3", as fast as possible without making mistakes Completion time is recorded.

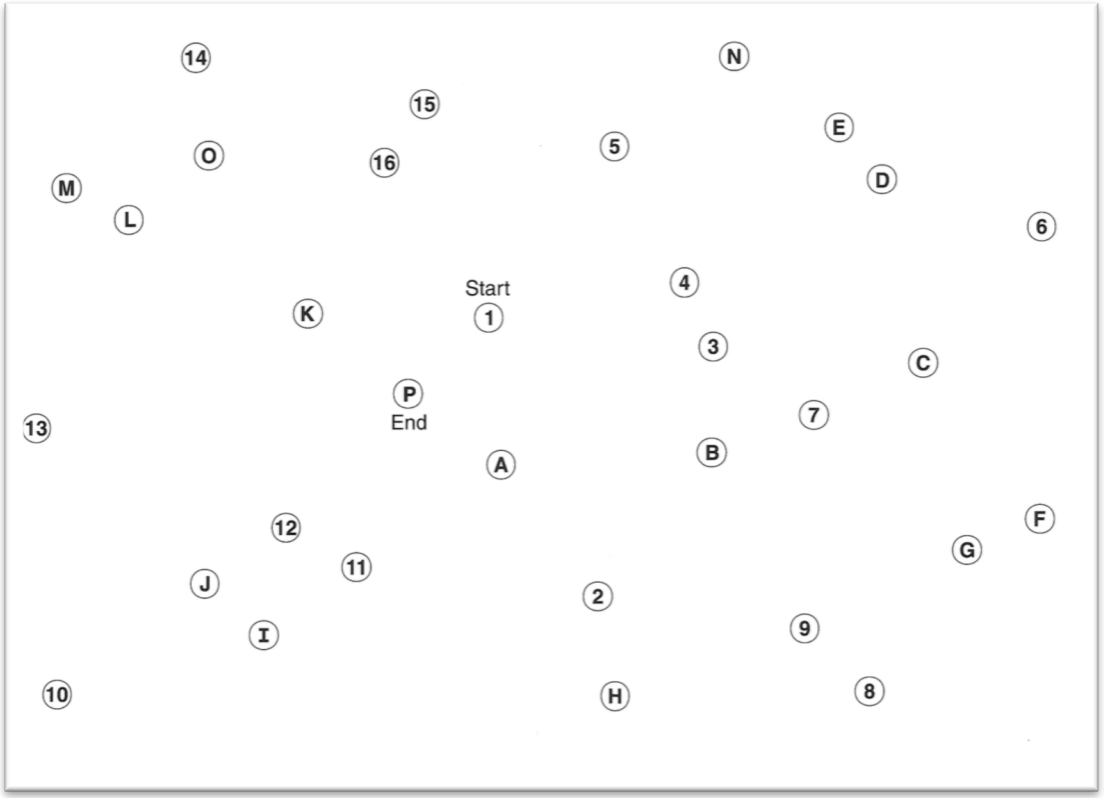

Appendix Figure 2. The Trailmaking test – number-letter switching condition (Switching) requires cognitive flexibility, attentional-set shifting and motor speed. In this task, the subject is presented with this A3 landscape page with various circles of different numbers and letters, and asked to draw lines to connect circles with letters and numbers, in the order of “1-A-2-B-3-C” etc. Completion time is recorded.

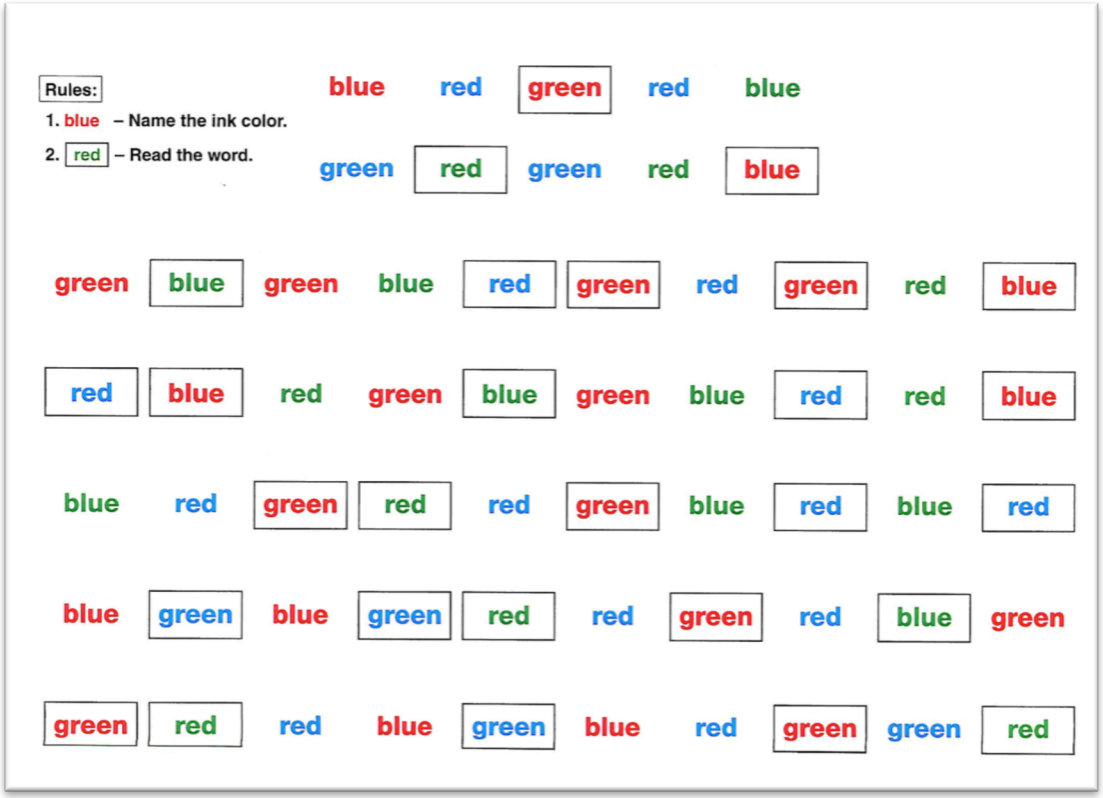

Appendix Figure 3. The Colour-Word Interference – inhibition/switching condition (CWI), a version of the commonly known Stroop test, measures naming speed, reading speed, verbal inhibition and cognitive flexibility. The subject is given this page with names of colours written in the same ink colour to the words that are printed, and words written in dissonant ink colours to the words that are printed. In this condition, the subject is asked to switch back and forth between naming the dissonant ink colours and reading the words that are in the black boxes. Completion time is recorded.

BRIEF®

Behavior Rating Inventory of Executive Function®

PARENT FORM

Gerard A. Gioia, PhD, Peter K. Isquith, PhD, Steven C. Guy, PhD, and Lauren Kenworthy, PhD

Instructions

On the following pages is a list of statements that describe children. We would like to know if your child has had problems with these behaviors over the past 6 months. Please answer all the items the best that you can. Please DO NOT SKIP ANY ITEMS. Think about your child as you read each statement and circle your response:

N	if the behavior is	**Never** a problem
S	if the behavior is	**Sometimes** a problem
O	if the behavior is	**Often** a problem

For example, if your child **never** has trouble completing homework on time, you would circle **N** for this item:

Has trouble completing homework on time (N) S O

If you make a mistake or want to change your answer, DO NOT ERASE. Draw an "X" through the answer you want to change, and then circle the correct answer:

Has trouble completing homework on time (X) (S) O

Before you begin answering the items, please fill in your child's name, gender, grade, age, birth date, your name, your relationship to the child, and today's date in the spaces provided at the top of the next page.

PAR • 16204 N. Florida Ave. • Lutz, FL 33549 • 1.800.331.8378 • www.parinc.com

9 8 7 6 5 4 3 Reorder #RO-4467 Printed in the U.S.A.

Child's Name _____ Gender _____ Grade _____ Age _____ Birth Date ___/___/___

Your Name _____ Relationship to Child _____ Today's Date ___/___/___

N = Never S = Sometimes O = Often

1.	Overreacts to small problems	N	S	O
2.	When given three things to do, remembers only the first or last	N	S	O
3.	Is not a self-starter	N	S	O
4.	Leaves playroom a mess	N	S	O
5.	Resists or has trouble accepting a different way to solve a problem with schoolwork, friends, chores, etc.	N	S	O
6.	Becomes upset with new situations	N	S	O
7.	Has explosive, angry outbursts	N	S	O
8.	Tries the same approach to a problem over and over even when it does not work	N	S	O
9.	Has a short attention span	N	S	O
10.	Needs to be told to begin a task even when willing	N	S	O
11.	Does not bring home homework, assignment sheets, materials, etc.	N	S	O
12.	Acts upset by a change in plans	N	S	O
13.	Is disturbed by change of teacher or class	N	S	O
14.	Does not check work for mistakes	N	S	O
15.	Has good ideas but cannot get them on paper	N	S	O
16.	Has trouble coming up with ideas for what to do in play or free time	N	S	O
17.	Has trouble concentrating on chores, schoolwork, etc.	N	S	O
18.	Does not connect doing tonight's homework with grades	N	S	O
19.	Is easily distracted by noises, activity, sights, etc.	N	S	O
20.	Becomes tearful easily	N	S	O
21.	Makes careless errors	N	S	O
22.	Forgets to hand in homework, even when completed	N	S	O
23.	Resists change of routine, foods, places, etc.	N	S	O
24.	Has trouble with chores or tasks that have more than one step	N	S	O
25.	Has outbursts for little reason	N	S	O
26.	Mood changes frequently	N	S	O
27.	Needs help from an adult to stay on task	N	S	O
28.	Gets caught up in details and misses the big picture	N	S	O
29.	Keeps room messy	N	S	O
30.	Has trouble getting used to new situations (classes, groups, friends)	N	S	O
31.	Has poor handwriting	N	S	O
32.	Forgets what he/she was doing	N	S	O
33.	When sent to get something, forgets what he/she is supposed to get	N	S	O
34.	Is unaware of how his/her behavior affects or bothers others	N	S	O
35.	Has good ideas but does not get job done (lacks follow-through)	N	S	O
36.	Becomes overwhelmed by large assignments	N	S	O
37.	Has trouble finishing tasks (chores, homework)	N	S	O
38.	Acts wilder or sillier than others in groups (birthday parties, recess)	N	S	O
39.	Thinks too much about the same topic	N	S	O
40.	Underestimates time needed to finish tasks	N	S	O
41.	Interrupts others	N	S	O
42.	Does not notice when his/her behavior causes negative reactions	N	S	O
43.	Gets out of seat at the wrong times	N	S	O
44.	Gets out of control more than friends	N	S	O

N = Never S = Sometimes O = Often			
45. Reacts more strongly to situations than other children	N	S	O
46. Starts assignments or chores at the last minute	N	S	O
47. Has trouble getting started on homework or chores	N	S	O
48. Has trouble organizing activities with friends	N	S	O
49. Blurts things out	N	S	O
50. Mood is easily influenced by the situation	N	S	O
51. Does not plan ahead for school assignments	N	S	O
52. Has poor understanding of own strengths and weaknesses	N	S	O
53. Written work is poorly organized	N	S	O
54. Acts too wild or "out of control"	N	S	O
55. Has trouble putting the brakes on his/her actions	N	S	O
56. Gets in trouble if not supervised by an adult	N	S	O
57. Has trouble remembering things, even for a few minutes	N	S	O
58. Has trouble carrying out the actions needed to reach goals (saving money for special item, studying to get a good grade)	N	S	O
59. Becomes too silly	N	S	O
60. Work is sloppy	N	S	O
61. Does not take initiative	N	S	O
62. Angry or tearful outbursts are intense but end suddenly	N	S	O
63. Does not realize that certain actions bother others	N	S	O
64. Small events trigger big reactions	N	S	O
65. Talks at the wrong time	N	S	O
66. Complains there is nothing to do	N	S	O
67. Cannot find things in room or school desk	N	S	O
68. Leaves a trail of belongings wherever he/she goes	N	S	O
69. Leaves messes that others have to clean up	N	S	O
70. Becomes upset too easily	N	S	O
71. Lies around the house a lot ("couch potato")	N	S	O
72. Has a messy closet	N	S	O
73. Has trouble waiting for turn	N	S	O
74. Loses lunch box, lunch money, permission slips, homework, etc.	N	S	O
75. Cannot find clothes, glasses, shoes, toys, books, pencils, etc.	N	S	O
76. Tests poorly even when knows correct answers	N	S	O
77. Does not finish long-term projects	N	S	O
78. Has to be closely supervised	N	S	O
79. Does not think before doing	N	S	O
80. Has trouble moving from one activity to another	N	S	O
81. Is fidgety	N	S	O
82. Is impulsive	N	S	O
83. Cannot stay on the same topic when talking	N	S	O
84. Gets stuck on one topic or activity	N	S	O
85. Says the same things over and over	N	S	O
86. Has trouble getting through morning routine in getting ready for school	N	S	O

Appendix Figure 4. The Behaviour Rating Inventory of Executive Functions (BRIEF) is a parent questionnaire for children younger than 18, consisting of 86 items in eight non-overlapping behavioural regulation and metacognition clinical scales. The Global Executive Composite score takes into account all the clinical scales and represents the child's overall executive function.

Appendix C: Presentations attributed to this thesis

Oral Presentations

Kawadler JM, Kirkham FJ, Barker S & Clark CA. White matter abnormalities in asymptomatic children with sickle cell anaemia. 19th Annual meeting of the British Chapter of ISMRM. York, UK, 24-25 September 2013.

Kawadler JM, Kirkham FJ, Barker S & Clark CA. White matter abnormalities in asymptomatic children with sickle cell anaemia. Sickle Cell in Focus - 7th Annual Meeting. London, UK. 6-8 June 2013.

Kawadler JM, Clayden JD, Kirkham FJ, Cox TC, Saunders DE, Clark CA. Subcortical and Cerebellar Volumetric Deficits in Pediatric Sickle Cell Anemia. International Society for Magnetic Resonance in Medicine - 21st Annual Meeting. Salt Lake City, USA, 20-26 April 2013.

Kawadler JM, Clayden JD, Kirkham FJ, Cox TC, Saunders DE, Clark CA. Subcortical and Cerebellar Volumetric Deficits in Paediatric Sickle Cell Anaemia. British Society of Haematology - 53rd Annual Meeting. Liverpool, UK, 15-17 April 2013.

Kawadler JM, Clayden JD, Kirkham FJ, Cox TC, Saunders DE, Clark CA. Subcortical volumetric differences in children with sickle cell disease. 18th Annual Meeting of the British Chapter of ISMRM. Cambridge, UK, 11-13 September 2012.

Poster Presentations

Kawadler JM, Kirkham FJ, Barker S, Cox TC, Clark, CA. White matter abnormalities in children with sickle cell anemia: Potential link with oxygen desaturation. International Society for Magnetic Resonance in Medicine – 22nd Annual Meeting. Milan, Italy, 10-16 May 2014.

References

1. Serjeant, G. R. & Serjeant, B. E. *Sickle Cell Disease*. (Oxford University Press, 2001).

2. Seakins, M., Gibbs, W. N., Milner, P. F. & Bertles, J. F. Erythrocyte Hb-S concentration. An important factor in the low oxygen affinity of blood in sickle cell anemia. *J. Clin. Invest.* **52,** 422–32 (1973).

3. Herrick, J. B. Peculiar elongated and sickle-shaped red blood corpuscles in a case of severe anemia. 1910. *Yale J. Biol. Med.* **74,** 179–84 (2001).

4. Embury, S. H., Hebbel, R. P., Steinberg, M. H. & Mohandas, N. in *Sickle Cell Disease: Basic Principles and Clinical Practice* (eds. Embury, S., Hebbel, R. P., Mohandas, N. & Steinberg, M. H.) 311–326 (Raven Press, Ltd, 1994).

5. Stockman, J. A., Nigro, M. A., Mishkin, M. M. & Oski, F. A. Occlusion of large cerebral vessels in sickle-cell anemia. *N. Engl. J. Med.* **287,** 846–9 (1972).

6. Hebbel, R. P., Osarogiagbon, R. & Kaul, D. The endothelial biology of sickle cell disease: inflammation and a chronic vasculopathy. *Microcirculation* **11,** 129–51 (2004).

7. Klug, P. P., Kaye, N. & Jensen, W. N. Endothelial cell and vascular damage in the sickle cell disorders. *Blood Cells* **8,** 175–84 (1982).

8. De Chadarévian, J. P., Balarezo, F. S., Heggere, M. & Dampier, C. Splenic arteries and veins in pediatric sickle cell disease. *Pediatr. Dev. Pathol.* **4,** 538–44 (2001).

9. Decastel, M., Leborgne-Samuel, Y., Alexandre, L., Merault, G. & Berchel, C. Morphological features of the human umbilical vein in normal, sickle cell trait, and sickle cell disease pregnancies. *Hum. Pathol.* **30,** 13–20 (1999).

10. Haque, A. K. *et al.* Pulmonary hypertension in sickle cell hemoglobinopathy: a clinicopathologic study of 20 cases. *Hum. Pathol.* **33,** 1037–43 (2002).

11. Hillery, C. A. & Panepinto, J. A. Pathophysiology of stroke in sickle cell disease. *Microcirculation* **11,** 195–208 (2004).

12. Yam, L. T. & Li, C.-Y. in *Sickle Cell Disease: Basic Principles and Clinical Practice* (eds. Embury, S. H., Hebbel, R. P., Steinberg, M. H. & Mohandas, N.) 555 (Raven Press, Ltd, 1994).

13. Koshey, M. & Burd, L. in *Sickle Cell Disease: Basic Principles and Clinical Practice* (eds. Embury, S. H., Hebbel, R. P., Steinberg, M. H. & Mohandas, N.) 689 (Raven Press, Ltd, 1994).

14. Castro, O., Hoque, M. & Brown, B. D. Pulmonary hypertension in sickle cell disease: cardiac catheterization results and survival. *Blood* **101,** 1257–61 (2003).

15. Adams, R. J. in *Sickle Cell Disease: Basic Principles and Clinical Practice* (eds. Embury, S. H., Hebbel, R. P., Mohandas, N. & Steinberg, M. H.) 599–621 (Raven Press, Ltd, 1994).

16. Hayes, R. J., Condon, P. I. & Serjeant, G. R. Haematological factors associated with proliferative retinopathy in homozygous sickle cell disease. *Br. J. Ophthalmol.* **65,** 29–35 (1981).

17. Milner, P. F. *et al.* Sickle cell disease as a cause of osteonecrosis of the femoral head. *N. Engl. J. Med.* **325,** 1476–81 (1991).

18. Milner, P. F. *et al.* Osteonecrosis of the humeral head in sickle cell disease. *Clin. Orthop. Relat. Res.* 136–43 (1993).

19. Platt, O. S. *et al.* Pain in sickle cell disease. Rates and risk factors. *N. Engl. J. Med.* **325,** 11–6 (1991).

20. Bensinger, T. A. & Gillette, P. N. Hemolysis in sickle cell disease. *Arch. Intern. Med.* **133,** 624–31 (1974).

21. Steinberg, M. H. & Hebbel, R. P. Clinical diversity of sickle cell anemia: genetic and cellular modulation of disease severity. *Am. J. Hematol.* **14,** 405–16 (1983).

22. Brittenham, G. M., Schechter, A. N. & Noguchi, C. T. Hemoglobin S polymerization: primary determinant of the hemolytic and clinical severity of the sickling syndromes. *Blood* **65,** 183–9 (1985).

23. Serjeant, G. R., Serjeant, B. E. & Milner, P. F. The irreversibly sickled cell; a determinant of haemolysis in sickle cell anaemia. *Br. J. Haematol.* **17,** 527–33 (1969).

24. McCurdy, P. R. & Sherman, A. S. Irreversibly sickled cells and red cell survival in sickle cell anemia: a study with both DF32P and 51CR. *Am. J. Med.* **64,** 253–8 (1978).

25. Glader, B. E. in *Sickle Cell Disease: Basic Principles and Clinical Practice* (eds. Embury, S. H., Hebbel, R. P., Mohandas, N. & Steinberg, M. H.) 545–553 (Raven Press, Ltd, 1994).

26. Serjeant, G. R. *et al.* The development of haematological changes in homozygous sickle cell disease: a cohort study from birth to 6 years. *Br. J. Haematol.* **48,** 533–43 (1981).

27. Shapiro, B. S. & Ballas, S. K. in *Sickle Cell Disease: Basic Principles and Clinical Practice* (eds. Embury, S. H., Hebbel, R. P., Steinberg, M. H. & Mohandas, N.) 531 (Raven Press, Ltd, 1994).

28. Shapiro, B., Dinges, D. F. & Orne, E. D. in *Advances in pain research and therapy* (eds. Tyler, D. & Krane, E.) 313–321 (Raven Press, Ltd, 1990).

29. Davies, S. C. The hospital management of patients with sickle cell disease. *Haematologica* **75 Suppl 5,** 96–106 (1990).

30. Benjamin, L. J. in *Advances in pain research and therapy* (eds. Max, M., Portenoy, R. & Laska, E.) (Raven Press, Ltd, 1991).

31. Hargrave, D. R., Wade, A., Evans, J. P. M., Hewes, D. K. M. & Kirkham, F. J. Nocturnal oxygen saturation and painful sickle cell crises in children. *Blood* **101,** 846–8 (2003).

32. Ballas, S. K., Gupta, K. & Adams-Graves, P. Sickle cell pain: a critical reappraisal. *Blood* 3647–3656 (2012). doi:10.1182/blood-2012-04-383430

33. Ballas, S. K. *Sickle Cell Pain: Second Edition*. (IASP Press, 2014).

34. Schatz, J. Brief report: Academic attainment in children with sickle cell disease. *J. Pediatr. Psychol.* **29,** 627–33 (2004).

35. Hofmann, M., de Montalembert, M., Beauquier-Maccotta, B., de Villartay, P. & Golse, B. Posttraumatic stress disorder in children affected by sickle-cell disease and their parents. *Am. J. Hematol.* **82,** 171–2 (2007).

36. Wang, W. C. *et al.* Hydroxycarbamide in very young children with sickle-cell anaemia: a multicentre, randomised, controlled trial (BABY HUG). *Lancet* **377,** 1663–72 (2011).

37. Charache, S. *et al.* Effect of hydroxyurea on the frequency of painful crises in sickle cell anemia. Investigators of the Multicenter Study of Hydroxyurea in Sickle Cell Anemia. *N. Engl. J. Med.* **332,** 1317–22 (1995).

38. Gil, K. M. *et al.* Daily coping practice predicts treatment effects in children with sickle cell disease. *J. Pediatr. Psychol.* **26,** 163–73 (2001).

39. Quinn, C. T., Rogers, Z. R., McCavit, T. L. & Buchanan, G. R. Improved survival of children and adolescents with sickle cell disease. *Blood* **115,** 3447–52 (2010).

40. Makani, J. *et al.* Mortality in sickle cell anemia in Africa: a prospective cohort study in Tanzania. *PLoS One* **6,** e14699 (2011).

41. Telfer, P. *et al.* Clinical outcomes in children with sickle cell disease living in England: a neonatal cohort in East London. *Haematologica* **92,** 905–12 (2007).

42. Dowling, M. M. *et al.* Acute silent cerebral ischemia and infarction during acute anemia in children with and without sickle cell disease. *Blood* **120,** 3891–7 (2012).

43. Powars, D. R. *et al.* Chronic renal failure in sickle cell disease: risk factors, clinical course, and mortality. *Ann. Intern. Med.* **115,** 614–20 (1991).

44. Hernández, P., Dorticós, E., Espinosa, E., González, X. & Svarch, E. Clinical features of hepatic sequestration in sickle cell anaemia. *Haematologia (Budap).* **22,** 169–74 (1989).

45. Haynes, J. & Kirkpatrick, M. B. The acute chest syndrome of sickle cell disease. *Am. J. Med. Sci.* **305,** 326–30 (1993).

46. Powars, D., Weidman, J. A., Odom-Maryon, T., Niland, J. C. & Johnson, C. Sickle cell chronic lung disease: prior morbidity and the risk of pulmonary failure. *Medicine (Baltimore).* **67,** 66–76 (1988).

47. Hamre, M. R., Harmon, E. P., Kirkpatrick, D. V, Stern, M. J. & Humbert, J. R. Priapism as a complication of sickle cell disease. *J. Urol.* **145,** 1–5 (1991).

48. Miller, S. T. *et al.* Prediction of adverse outcomes in children with sickle cell disease. *N. Engl. J. Med.* **342,** 1612–3 (2000).

49. Quinn, C. T. & Miller, S. T. Risk factors and prediction of outcomes in children and adolescents who have sickle cell anemia. *Hematol. Oncol. Clin. North Am.* **18,** 1339–54, ix (2004).

50. Diggs, L. W. Bone and joint lesions in sickle-cell disease. *Clin. Orthop. Relat. Res.* **52,** 119–43 (1967).

51. Bohrer, S. *Bone ischemia and infarction in sickle cell disease*. (Warren H. Green, 1981).

52. Serjeant, G. R. *Sickle Cell Disease*. (Oxford University Press, 1985).

53. Konotey-Ahulu, F. I. The sickle cell diseases. Clinical manifestations including the "sickle crisis". *Arch. Intern. Med.* **133,** 611–9 (1974).

54. Diallo, D. & Tchernia, G. Sickle cell disease in Africa. *Curr. Opin. Hematol.* **9,** 111–116 (2002).

55. Onwubalili, J. Sickle-cell anaemia: an explanation for the ancient myth of reincarnation in Nigeria. *Lancet* 503–505 (1983).

56. Pauling, L. & Itano, H. A. Sickle cell anemia a molecular disease. *Science* **110,** 543–8 (1949).

57. Neel, J. V. The Inheritance of Sickle Cell Anemia. *Science* **110,** 64–6 (1949).

58. Ingram, V. M. Gene mutations in human haemoglobin: the chemical difference between normal and sickle cell haemoglobin. *Nature* **180,** 326–8 (1957).

59. Nagel, R. L., Fabry, M. E. & Steinberg, M. H. The paradox of hemoglobin SC disease. *Blood Rev.* **17,** 167–78 (2003).

60. Allison, A. C. The sickle-cell and haemoglobin C genes in some African populations. *Ann. Hum. Genet.* **21,** 67–89 (1956).

61. Lehmann, H. & Raper, A. B. Maintenance of high sickling rate in an African community. *Br. Med. J.* **2,** 333–6 (1956).

62. Allison, A. C. Notes on sickle-cell polymorphism. *Ann. Hum. Genet.* **19,** 39–51 (1954).

63. Piel, F. B. *et al.* Global distribution of the sickle cell gene and geographical confirmation of the malaria hypothesis. *Nat. Commun.* **1,** 104 (2010).

64. Williams, T. N. *et al.* Sickle cell trait and the risk of Plasmodium falciparum malaria and other childhood diseases. *J. Infect. Dis.* **192,** 178–86 (2005).

65. May, J. *et al.* Hemoglobin variants and disease manifestations in severe falciparum malaria. *JAMA* **297,** 2220–6 (2007).

66. Friedman, M. J. Erythrocytic mechanism of sickle cell resistance to malaria. *Proc. Natl. Acad. Sci. U. S. A.* **75,** 1994–7 (1978).

67. Pasvol, G., Weatherall, D. J. & Wilson, R. J. Cellular mechanism for the protective effect of haemoglobin S against P. falciparum malaria. *Nature* **274,** 701–3 (1978).

68. Hay, S. I., Guerra, C. A., Tatem, A. J., Noor, A. M. & Snow, R. W. The global distribution and population at risk of malaria: past, present, and future. *Lancet Infect. Dis.* **4,** 327–36 (2004).

69. *Manson's Tropical Diseases*. (W. B. Saunders, 2003).

70. Weatherall, D. J., Akinyanju, O., Fucharoen, S., Oliveri, N. & Musgrove, P. in *Disease Control Priorities in Developing Countries* (eds. Jamison, D. T., Breman, J. G. & Measham, A. R.) 663–680 (World Bank, 2006).

71. Ohene-Frempong, K. & Nkrumah, F. in *Sickle Cell Disease: Basic Principles and Clinical Practice* (eds. Embury, S., Hebbel, R. & Mohandas, N.) 423–435 (Raven Press, Ltd, 1994).

72. Fleming, A. F. The presentation, management and prevention of crisis in sickle cell disease in Africa. *Blood Rev.* **3,** 18–28 (1989).

73. in (ed. Modell, B.) (World Health Organization Publications, 1994).

74. Ashley-Koch, A., Yang, Q. & Olney, R. S. Sickle hemoglobin (HbS) allele and sickle cell disease: a HuGE review. *Am. J. Epidemiol.* **151,** 839–45 (2000).

75. Motulsky, A. G. Frequency of Sickling Disorders in U.S. Blacks. *N Engl J Med* **288,** 31–33 (1973).

76. Streetly, A., Latinovic, R., Hall, K. & Henthorn, J. Implementation of universal newborn bloodspot screening for sickle cell disease and other clinically significant haemoglobinopathies in England: screening results for 2005-7. *J. Clin. Pathol.* **62,** 26–30 (2009).

77. Lindsay, P., Furie, K. L., Davis, S. M., Donnan, G. A. & Norrving, B. World stroke organization global stroke services guidelines and action plan. *Int. J. Stroke* **9 Suppl A1,** 4–13 (2014).

78. Pegelow, C. H. Longitudinal changes in brain magnetic resonance imaging findings in children with sickle cell disease. *Blood* **99,** 3014–3018 (2002).

79. Ohene-Frempong, K. *et al.* Cerebrovascular accidents in sickle cell disease: rates and risk factors. *Blood* **91,** 288–94 (1998).

80. Tarazi, R. a, Grant, M. L., Ely, E. & Barakat, L. P. Neuropsychological functioning in preschool-age children with sickle cell disease: the role of illness-related and psychosocial factors. *Child Neuropsychol.* **13,** 155–72 (2007).

81. Balkaran, B. *et al.* Stroke in a cohort of patients with homozygous sickle cell disease. *J. Pediatr.* **120,** 360–6 (1992).

82. Moser, F. G. *et al.* The spectrum of brain MR abnormalities in sickle-cell disease: a report from the Cooperative Study of Sickle Cell Disease. *AJNR. Am. J. Neuroradiol.* **17,** 965–72 (1996).

83. Powars, D. R. & Schroeder, W. A. in *Biochemical and Clinical Aspects of Hemoglobin Abnormalities* (ed. Caughey, W. A.) 151–164 (Academic Press, 1978).

84. Ohene-Frempong, K. Stroke in sickle cell disease: demographic, clinical, and therapeutic considerations. *Semin. Hematol.* **28,** 213–9 (1991).

85. Russell, M. O. *et al.* Effect of transfusion therapy on arteriographic abnormalities and on recurrence of stroke in sickle cell disease. *Blood* **63,** 162–9 (1984).

86. Gerald, B., Sebes, J. I. & Langston, J. W. Cerebral infarction secondary to sickle cell disease: arteriographic findings. *AJR. Am. J. Roentgenol.* **134,** 1209–12 (1980).

87. Dobson, S. R. *et al.* Moyamoya syndrome in childhood sickle cell disease: a predictive factor for recurrent cerebrovascular events. *Blood* **99,** 3144–50 (2002).

88. Sébire, G. *et al.* Cerebral venous sinus thrombosis in children: risk factors, presentation, diagnosis and outcome. *Brain* **128,** 477–89 (2005).

89. Hess, D. C., Adams, R. J. & Nichols, F. T. Sickle cell anemia and other hemoglobinopathies. *Semin. Neurol.* **11,** 314–28 (1991).

90. Pavlakis, S. G., Prohovnik, I., Piomelli, S. & DeVivo, D. C. Neurologic complications of sickle cell disease. *Adv. Pediatr.* **36,** 247–76 (1989).

91. Prohovnik, I. *et al.* Cerebral hyperemia, stroke, and transfusion in sickle cell disease. *Neurology* **39,** 344–348 (1989).

92. Prohovnik, I., Hurlet-Jensen, A., Adams, R., De Vivo, D. & Pavlakis, S. G. Hemodynamic etiology of elevated flow velocity and stroke in sickle-cell disease. *J. Cereb. Blood Flow Metab.* **29,** 803–10 (2009).

93. Kirkham, F. J. *et al.* Perfusion magnetic resonance abnormalities in patients with sickle cell disease. *Ann. Neurol.* **49,** 477–85 (2001).

94. Kirkham, F. J. *et al.* Nocturnal hypoxaemia and central-nervous-system events in sickle-cell disease. *Lancet* **357,** 1656–9 (2001).

95. Quinn, C. T. & Ahmad, N. Clinical correlates of steady-state oxyhaemoglobin desaturation in children who have sickle cell disease. *Br. J. Haematol.* **131,** 129–34 (2005).

96. Quinn, C. T., Variste, J. & Dowling, M. M. Haemoglobin oxygen saturation is a determinant of cerebral artery blood flow velocity in children with sickle cell anaemia. *Br. J. Haematol.* **145,** 500–5 (2009).

97. Wood, D. H. Cerebrovascular complications of sickle cell anemia. *Stroke* **9,** 73–5 (1978).

98. Robertson, P. L., Aldrich, M. S., Hanash, S. M. & Goldstein, G. W. Stroke associated with obstructive sleep apnea in a child with sickle cell anemia. *Ann. Neurol.* **23,** 614–6 (1988).

99. Powars, D., Wilson, B., Imbus, C., Pegelow, C. & Allen, J. The natural history of stroke in sickle cell disease. *Am. J. Med.* **65,** 461–71 (1978).

100. Sarnaik, S. A. & Lusher, J. M. Neurological complications of sickle cell anemia. *Am. J. Pediatr. Hematol. Oncol.* **4,** 386–94 (1982).

101. Mercuri, E. *et al.* Neurological “soft” signs may identify children with sickle cell disease who are at risk for stroke. *Eur. J. Pediatr.* **154,** 150–6 (1995).

102. Hariman, L. M., Griffith, E. R., Hurtig, A. L. & Keehn, M. T. Functional outcomes of children with sickle-cell disease affected by stroke. *Arch. Phys. Med. Rehabil.* **72,** 498–502 (1991).

103. Cohen, M. J., Branch, W. B., McKie, V. C. & Adams, R. J. Neuropsychological impairment in children with sickle cell anemia and cerebrovascular accidents. *Clin. Pediatr. (Phila).* **33,** 517–24 (1994).

104. Armstrong, F. D. *et al.* Cognitive Functioning and Brain Magnetic Resonance Imaging in Children With Sickle Cell Disease. *Pediatrics* **97,** 864–870 (1996).

105. DeBaun, M. R. *et al.* Silent cerebral infarcts: a review on a prevalent and progressive cause of neurologic injury in sickle cell anemia. *Blood* **119,** 4587–96 (2012).

106. Steen, R. G. *et al.* Cognitive Deficits in Children With Sickle Cell Disease. *J. Child Neurol.* **20,** 102–107 (2005).

107. Wang, W. C. *et al.* Abnormalities of the central nervous system in very young children with sickle cell anemia. *J. Pediatr.* **132,** 994–8 (1998).

108. Miller, S. T. *et al.* Impact of chronic transfusion on incidence of pain and acute chest syndrome during the Stroke Prevention Trial (STOP) in sickle-cell anemia. *J. Pediatr.* **139,** 785–9 (2001).

109. Pegelow, C. H. *et al.* Silent infarcts in children with sickle cell anemia and abnormal cerebral artery velocity. *Arch. Neurol.* **58,** 2017–21 (2001).

110. Kinney, T. R. *et al.* Silent Cerebral Infarcts in Sickle Cell Anemia: A Risk Factor Analysis. *Pediatrics* **103,** 640–645 (1999).

111. DeBaun, M. R. *et al.* Associated risk factors for silent cerebral infarcts in sickle cell anemia: low baseline hemoglobin, sex, and relative high systolic blood pressure. *Blood* **119,** 3684–90 (2012).

112. Quinn, C. T. *et al.* Acute Silent Cerebral Ischemic Events in Children with Sickle Cell Anemia. *Arch. Neurol.* 1–8 (2012). doi:10.1001/jamaneurol.2013.576

113. Brown, R. T., Armstrong, F. D. & Eckman, J. R. Neurocognitive Aspects of Pediatric Sickle Cell Disease. *J. Learn. Disabil.* **26,** 33–45 (1993).

114. Schatz, J., Finke, R. L., Kellett, J. M. & Kramer, J. H. Cognitive functioning in children with sickle cell disease: a meta-analysis. *J. Pediatr. Psychol.* **27,** 739–48 (2002).

115. Berkelhammer, L. D. *et al.* Neurocognitive sequelae of pediatric sickle cell disease: a review of the literature. *Child Neuropsychol.* **13,** 120–31 (2007).

116. Platt, O. *et al.* Mortality in Sickle Cell Disease Life Expectancy and Risk Factors for Early Death. *N. Engl. J. Med.* **330,** 1639–44 (1994).

117. Gaston, M. H. *et al.* Prophylaxis with oral penicillin in children with sickle cell anemia. A randomized trial. *N. Engl. J. Med.* **314,** 1593–9 (1986).

118. Vichinsky, E. & Lubin, B. H. Suggested guidelines for the treatment of children with sickle cell anemia. *Hematol. Oncol. Clin. North Am.* **1,** 483–501 (1987).

119. Wierenga, K. J., Hambleton, I. R. & Lewis, N. A. Survival estimates for patients with homozygous sickle-cell disease in Jamaica: a clinic-based population study. *Lancet* **357,** 680–3 (2001).

120. Steinberg, B. Sickle Cell Anemia. *Arch. Pathol.* **9,** 876–897 . (1930).

121. Russell, M. O. *et al.* Transfusion therapy for cerebrovascular abnormalities in sickle cell disease. *J. Pediatr.* **88,** 382–7 (1976).

122. Lusher, J. M., Haghighat, H. & Khalifa, A. S. A prophylactic transfusion program for children with sickle cell anemia complicated by CNS infarction. *Am. J. Hematol.* **1,** 265–73 (1976).

123. Adams, R. J. *et al.* Prevention of a first stroke by transfusions in children with sickle cell anemia and abnormal results on transcranial Doppler ultrasonography. *N. Engl. J. Med.* **339,** 5–11 (1998).

124. Cohen, A. R. *et al.* A modified transfusion program for prevention of stroke in sickle cell disease. *Blood* **79,** 1657–61 (1992).

125. Miller, S. T., Jensen, D. & Rao, S. P. Less intensive long-term transfusion therapy for sickle cell anemia and cerebrovascular accident. *J. Pediatr.* **120,** 54–7 (1992).

126. Wayne, A. S., Kevy, S. V & Nathan, D. G. Transfusion management in sickle cell disease. *Blood* **81,** 1109–1123 (1993).

127. Ballas, S. K. Iron overload is a determinant of morbidity and mortality in adult patients with sickle cell disease. *Semin. Hematol.* **38,** 30–6 (2001).

128. Junqueira, F. P. *et al.* Right and left ventricular function and myocardial scarring in adult patients with sickle cell disease: a comprehensive magnetic resonance assessment of hepatic and myocardial iron overload. *J. Cardiovasc. Magn. Reson.* **15,** 83 (2013).

129. St Pierre, T. G. *et al.* Noninvasive measurement and imaging of liver iron concentrations using proton magnetic resonance. *Blood* **105,** 855–61 (2005).

130. Meloni, A. *et al.* Cardiac iron overload in sickle-cell disease. *Am. J. Hematol.* **89,** 678–83 (2014).

131. Qiu, D. *et al.* MR Quantitative Susceptibility Imaging for the Evaluation of Iron Loading in the Brains of Patients with β-Thalassemia Major. *AJNR. Am. J. Neuroradiol.* **35,** 1085–90 (2014).

132. Wang, W. & Dwan, K. Blood transfusion for preventing primary and secondary stroke in people with sickle cell disease (Review). *Cochrane Database Syst. Rev.* 1–30 (2013).

133. Smith-Whitley, K. & Thompson, A. A. Indications and complications of transfusions in sickle cell disease. *Pediatr. Blood Cancer* **59,** 358–64 (2012).

134. Lanzkron, S. *et al.* Systematic review: Hydroxyurea for the treatment of adults with sickle cell disease. *Ann. Intern. Med.* **148,** 939–55 (2008).

135. Charache, S. *et al.* Hydroxyurea and sickle cell anemia. Clinical utility of a myelosuppressive "switching" agent. The Multicenter Study of Hydroxyurea in Sickle Cell Anemia. *Medicine (Baltimore).* **75,** 300–26 (1996).

136. Ballas, S. K., Marcolina, M. J., Dover, G. J. & Barton, F. B. Erythropoietic activity in patients with sickle cell anaemia before and after treatment with hydroxyurea. *Br. J. Haematol.* **105,** 491–6 (1999).

137. Powars, D. R., Weiss, J. N., Chan, L. S. & Schroeder, W. A. Is there a threshold level of fetal hemoglobin that ameliorates morbidity in sickle cell anemia? *Blood* **63,** 921–6 (1984).

138. Adekile, A. D. *et al.* Silent brain infarcts are rare in Kuwaiti children with sickle cell disease and high Hb F. *Am. J. Hematol.* **70,** 228–31 (2002).

139. Benkerrou, M. *et al.* Hydroxyurea corrects the dysregulated L-selectin expression and increased H(2)O(2) production of polymorphonuclear neutrophils from patients with sickle cell anemia. *Blood* **99,** 2297–303 (2002).

140. Ware, R. E., Zimmerman, S. a & Schultz, W. H. Hydroxyurea as an alternative to blood transfusions for the prevention of recurrent stroke in children with sickle cell disease. *Blood* **94,** 3022–6 (1999).

141. Strouse, J. J. *et al.* Hydroxyurea for sickle cell disease: a systematic review for efficacy and toxicity in children. *Pediatrics* **122,** 1332–42 (2008).

142. Lagunju, I. A., Brown, B. J. & Sodeinde, O. O. Stroke recurrence in Nigerian children with sickle cell disease treated with hydroxyurea. *Niger. Postgrad. Med. J.* **20,** 181–7 (2013).

143. Johnson, F. L. *et al.* Bone-marrow transplantation in a patient with sickle-cell anemia. *N. Engl. J. Med.* **311,** 780–3 (1984).

144. Walters, M. C. *et al.* Bone marrow transplantation for sickle cell disease. *N. Engl. J. Med.* **335,** 369–76 (1996).

145. Bhatia, M. & Walters, M. C. Hematopoietic cell transplantation for thalassemia and sickle cell disease: past, present and future. *Bone Marrow Transplant.* **41,** 109–17 (2008).

146. Hanna, J. *et al.* Treatment of sickle cell anemia mouse model with iPS cells generated from autologous skin. *Science* **318,** 1920–3 (2007).

147. Pawliuk, R. *et al.* Correction of sickle cell disease in transgenic mouse models by gene therapy. *Science* **294,** 2368–71 (2001).

148. Persons, D. A. Hematopoietic stem cell gene transfer for the treatment of hemoglobin disorders. *Hematology Am. Soc. Hematol. Educ. Program* 690–7 (2009). doi:10.1182/asheducation-2009.1.690

149. Rees, D. C., Williams, T. N. & Gladwin, M. T. Sickle-cell disease. *Lancet* **376,** 2018–31 (2010).

150. Jordan, L., Swerdlow, P. & Coates, T. D. Systematic review of transition from adolescent to adult care in patients with sickle cell disease. *J. Pediatr. Hematol. Oncol.* **35,** 165–9 (2013).

151. Doulton, D. M. From cradle to commencement: transitioning pediatric sickle cell disease patients to adult providers. *J. Pediatr. Oncol. Nurs.* **27,** 119–23 (2010).

152. Telfair, J., Ehiri, J. E., Loosier, P. S. & Baskin, M. L. Transition to adult care for adolescents with sickle cell disease: results of a national survey. *Int. J. Adolesc. Med. Health* **16,** 47–64 (2004).

153. Treadwell, M., Telfair, J., Gibson, R. W., Johnson, S. & Osunkwo, I. Transition from pediatric to adult care in sickle cell disease: establishing evidence-based practice and directions for research. *Am. J. Hematol.* **86,** 116–20 (2011).

154. Adams, R. J., Nichols, F. T., Figueroa, R., McKie, V. & Lott, T. Transcranial Doppler correlation with cerebral angiography in sickle cell disease. *Stroke* **23,** 1073–1077 (1992).

155. Adams, R. J. *et al.* Long-term stroke risk in children with sickle cell disease screened with transcranial Doppler. *Ann. Neurol.* **42,** 699–704 (1997).

156. Wang, W. C. *et al.* High risk of recurrent stroke after discontinuance of five to twelve years of transfusion therapy in patients with sickle cell disease. *J. Pediatr.* **118,** 377–82 (1991).

157. Scothorn, D. J. *et al.* Risk of recurrent stroke in children with sickle cell disease receiving blood transfusion therapy for at least five years after initial stroke. *J. Pediatr.* **140,** 348–54 (2002).

158. Smith, E. R., McClain, C. D., Heeney, M. & Scott, R. M. Pial synangiosis in patients with moyamoya syndrome and sickle cell anemia: perioperative management and surgical outcome. *Neurosurg. Focus* **26,** E10 (2009).

159. Goldstein, L. B. *et al.* Primary prevention of ischemic stroke: A statement for healthcare professionals from the Stroke Council of the American Heart Association. *Stroke.* **32,** 280–99 (2001).

160. DeBaun, M. R. *et al.* Controlled Trial of Transfusions for Silent Cerebral Infarcts in Sickle Cell Anemia. *N. Engl. J. Med.* **371,** 699–710 (2014).

161. Rosen, C. L. *et al.* Obstructive Sleep Apnea and Sickle Cell Anemia. *Pediatrics* **134,** 273–81 (2014).

162. Hollocks, M. J. *et al.* Nocturnal oxygen desaturation and disordered sleep as a potential factor in executive dysfunction in sickle cell anemia. *J. Int. Neuropsychol. Soc.* **18,** 168–73 (2012).

163. Marshall, M. J. *et al.* Auto-adjusting positive airway pressure in children with sickle cell anemia: results of a phase I randomized controlled trial. *Haematologica* **94,** 4–8 (2009).

164. McRobbie, D., Moore, E. A., Graves, M. J. & Prince, M. R. *MRI from Picture to Proton*. (Cambridge University Press, 2007).

165. Kuperman, V. *Magnetic Resonance Imaging: Physical Principles and Applications.* (2000).

166. Akkerman, E. M. *Introduction to MRI*. (AMC, 2001).

167. Le Bihan, D. *et al.* MR imaging of intravoxel incoherent motions: application to diffusion and perfusion in neurologic disorders. *Radiology* **161,** 401–7 (1986).

168. Tanner, J. E. Transient diffusion in a system partitioned by permeable barriers. Application to NMR measurements with a pulsed field gradient. *J. Chem. Phys.* **69,** 1748 (1978).

169. Beaulieu, C. The basis of anisotropic water diffusion in the nervous system - a technical review. *NMR Biomed.* **15,** 435–55 (2002).

170. Muir, K. W., Buchan, A., von Kummer, R., Rother, J. & Baron, J.-C. Imaging of acute stroke. *Lancet Neurol.* **5,** 755–68 (2006).

171. Sevick, R. J. *et al.* Cytotoxic brain edema: assessment with diffusion-weighted MR imaging. *Radiology* **185,** 687–90 (1992).

172. Basser, P. J., Mattiello, J. & LeBihan, D. MR diffusion tensor spectroscopy and imaging. *Biophys. J.* **66,** 259–67 (1994).

173. Wiegell, M., Larsson, H. & Wedeen, V. Fiber Crossing in Human Brain Depicted with Diffusion Tensor MR Imaging. *Radiology* 897–903 (2000).

174. Ciccarelli, O., Catani, M. & Johansen-Berg, H. Diffusion-based tractography in neurological disorders: concepts , applications, and future developments. *Lancet Neurol.* **7,** 715–727 (2008).

175. Song, S.-K. *et al.* Dysmyelination revealed through MRI as increased radial (but unchanged axial) diffusion of water. *Neuroimage* **17,** 1429–36 (2002).

176. Pajevic, S. & Pierpaoli, C. Color schemes to represent the orientation of anisotropic tissues from diffusion tensor data: application to white matter fiber tract mapping in the human brain. *Magn. Reson. Med.* **42,** 526–40 (1999).

177. Basser, P. J., Pajevic, S., Pierpaoli, C., Duda, J. & Aldroubi, A. In vivo fiber tractography using DT-MRI data. *Magn. Reson. Med.* **44,** 625–32 (2000).

178. Catani, M. & Thiebaut de Schotten, M. A diffusion tensor imaging tractography atlas for virtual in vivo dissections. *Cortex* **44,** 1105–32 (2008).

179. Rothman, S. M., Fulling, K. H. & Nelson, J. S. Sickle cell anemia and central nervous system infarction: a neuropathological study. *Ann. Neurol.* **20,** 684–90 (1986).

180. Adams, R. J. *et al.* Cerebral infarction in sickle cell anemia: Mechanism based on CT and MRI. *Neurology* **38,** 1012– (1988).

181. Pavlakis, S. G. *et al.* Brain infarction in sickle cell anemia: Magnetic resonance imaging correlates. *Ann. Neurol.* **23,** 125–30 (1988).

182. Wang, W. C. *et al.* MRI Abnormalities of the Brain in One-Year-Old Children With Sickle Cell Anemia. *Pediatr. Blood Cancer* **51,** 643–646 (2008).

183. Kwiatkowski, J. L. *et al.* Silent infarcts in young children with sickle cell disease. *Br. J. Haematol.* **146,** 300–5 (2009).

184. Bernaudin, F. *et al.* Long-term follow-up of pediatric sickle cell disease patients with abnormal high velocities on transcranial Doppler. *Pediatr. Radiol.* **35,** 242–8 (2005).

185. Hindmarsh, P. C., Brozovic, M., Brook, C. G. & Davies, S. C. Incidence of overt and covert neurological damage in children with sickle cell disease. *Postgrad. Med. J.* **63,** 751–3 (1987).

186. Casella, J. F. *et al.* Design of the silent cerebral infarct transfusion (SIT) trial. *Pediatr. Hematol. Oncol.* **27,** 69–89 (2010).

187. Glauser, T. A., Siegel, M. J., Lee, B. C. & DeBaun, M. R. Accuracy of neurologic examination and history in detecting evidence of MRI-diagnosed cerebral infarctions in children with sickle cell hemoglobinopathy. *J. Child Neurol.* **10,** 88–92 (1995).

188. Kral, M. C. *et al.* Radiographic Predictors of Neurocognitive Functioning in Pediatric Sickle Cell Disease. *J. Child Neurol.* **21,** 37–44 (2006).

189. Steen, R. G., Xiong, X., Langston, J. W. & Helton, K. J. Brain injury in children with sickle cell disease: Prevalence and etiology. *Ann. Neurol.* **54,** 564–572 (2003).

190. Moritani, T. *et al.* Sickle cell cerebrovascular disease: usual and unusual findings on MR imaging and MR angiography. *Clin. Imaging* **28,** 173–86 (2004).

191. Seibert, J. J. *et al.* Transcranial Doppler, MRA, and MRI as a screening examination for cerebrovascular disease in patients with sickle cell anemia: an 8-year study. *Pediatr. Radiol.* **28,** 138–42 (1998).

192. Emam, A. T., Ali, A. M. & Babikr, M. A. Magnetic resonance spectroscopy of the brain in children with sickle cell disease. *Neurosciences (Riyadh).* **14,** 364–7 (2009).

193. Steen, R. G. & Ogg, R. J. Abnormally high levels of brain N-acetylaspartate in children with sickle cell disease. *AJNR. Am. J. Neuroradiol.* **26,** 463–8 (2005).

194. Steen, R. G., Xiong, X., Mulhern, R. K., Langston, J. W. & Wang, W. C. Subtle brain abnormalities in children with sickle cell disease: relationship to blood hematocrit. *Ann. Neurol.* **45,** 279–86 (1999).

195. Steen, R., Langston, J., Ogg, R. & Xiong, X. Diffuse T1 Reduction in Gray Matter of Sickle Cell Disease Patients: Evidence of a selective vulnerability to damage? *Magn. Reson. Imaging* **17,** 503–515 (1999).

196. Dowling, M. M., Quinn, C. T., Rogers, Z. R. & Buchanan, G. R. Acute Silent Cerebral Infarction in Children with Sickle Cell Anemia. *Pediatr. Blood Cancer* **54,** 461–464 (2010).

197. Steen, R. G. *et al.* Brain Imaging Findings in Pediatric Patients with Sickle Cell Disease. *Radiology* **228,** 216–225 (2003).

198. Enninful-Eghan, H., Moore, R. H., Ichord, R., Smith-Whitley, K. & Kwiatkowski, J. L. Transcranial Doppler ultrasonography and prophylactic transfusion program is effective in preventing overt stroke in children with sickle cell disease. *J. Pediatr.* **157,** 479–84 (2010).

199. Baldeweg, T. *et al.* Detecting white matter injury in sickle cell disease using voxel-based morphometry. *Ann. Neurol.* **59,** 662–72 (2006).

200. Steen, R. G. *et al.* Brain volume in pediatric patients with sickle cell disease: Evidence of volumetric growth delay? *AJNR. Am. J. Neuroradiol.* **26,** 455–62 (2005).

201. Chen, R. *et al.* Brain morphometry and intelligence quotient measurements in children with sickle cell disease. *J. Dev. Behav. Pediatr.* **30,** 509–17 (2009).

202. Kirk, G. R. *et al.* Regionally specific cortical thinning in children with sickle cell disease. *Cereb. Cortex* **19,** 1549–56 (2009).

203. Scantlebury, N. *et al.* White matter integrity and core cognitive function in children diagnosed with sickle cell disease. *J. Pediatr. Hematol. Oncol.* **33,** 163–71 (2011).

204. Helton, K. J. *et al.* Arterial Spin-Labeled Perfusion Combined With Segmentation Techniques to Evaluate Cerebral Blood Flow in White and Gray Matter of Children With Sickle Cell Anemia. *Pediatr. Blood Cancer* **52,** 85–91 (2009).

205. Sun, B. *et al.* White Matter Damage in Asymptomatic Patients with Sickle Cell Anemia: Screening with DIffusion Tensor Imaging. *AJNR. Am. J. Neuroradiol.* 1–7 (2012).

206. Balci, A. *et al.* Quantitative brain diffusion-tensor MRI findings in patients with sickle cell disease. *AJR. Am. J. Roentgenol.* **198,** 1167–74 (2012).

207. Chapar, G. N. Chronic diseases of children and neuropsychologic dysfunction. *J. Dev. Behav. Pediatr.* **9,** 221–2 (1988).

208. Logothetis, J. *et al.* Intelligence and behavioral patterns in patients with Cooley's anemia (homozygous beta-thalassemia); a study based on 138 consecutive cases. *Pediatrics* **48,** 740–4 (1971).

209. Chodorkoff, J. & Whitten, C. F. Intellectual status of children with sickle cell anemia. *J. Pediatr.* **63,** 29–35 (1963).

210. Fowler, M. *et al.* Neuropsychologic and Academic Functioning of Children with Sickle Cell Anemia. *Dev. Behav. Pediatr.* **9,** 213–20 (1988).

211. Goonan, B. T., Goonan, L. J., Brown, R. T., Buchanan, I. & Eckman, J. R. Sustained attention and inhibitory control in children with sickle cell syndrome. *Arch. Clin. Neuropsychol.* **9,** 89–104 (1994).

212. Midence, K., McManus, C., Fuggle, P. & Davies, S. Psychological adjustment and family functioning in a group of British children with sickle cell disease: preliminary empirical findings and a meta-analysis. *Br. J. Clin. Psychol.* **35,** 439–50 (1996).

213. Swift, A. V *et al.* Neuropsychologic impairment in children with sickle cell anemia. *Pediatrics* **84,** 1077–85 (1989).

214. Wasserman, A. L. *et al.* Subtle neuropsychological deficits in children with sickle cell disease. *Am. J. Pediatr. Hematol. Oncol.* **13,** 14–20 (1991).

215. Knight, S., Singhal, A., Thomas, P. & Serjeant, G. Factors associated with lowered intelligence in homozygous sickle cell disease. *Arch. Dis. Child.* **73,** 316–320 (1995).

216. Steen, R. G. *et al.* Quantitative MRI of the brain in children with sickle cell disease reveals abnormalities unseen by conventional MRI. *J. Magn. Reson. Imaging* **8,** 535–43 (1998).

217. Watkins, K. E. *et al.* Cognitive deficits associated with frontal-lobe infarction in children with sickle cell disease. *Dev. Med. Child Neurol.* **40,** 536–43 (1998).

218. Bernaudin, F. *et al.* Multicenter Prospective Study of Children With Sickle Cell Disease: Radiographic and Psychometric Correlation. *J. Child Neurol.* **15,** 333–343 (2000).

219. Brown, R. T. *et al.* Neurocognitive functioning and magnetic resonance imaging in children with sickle cell disease. *J. Pediatr. Psychol.* **25,** 503–13 (2000).

220. Wang, W. *et al.* Neuropsychologic performance in school-aged children with sickle cell disease: a report from the Cooperative Study of Sickle Cell Disease. *J. Pediatr.* **139,** 391–7 (2001).

221. Schatz, J. & Buzan, R. Decreased corpus callosum size in sickle cell disease: relationship with cerebral infarcts and cognitive functioning. *J. Int. Neuropsychol. Soc.* **12,** 24–33 (2006).

222. Gold, J. I., Johnson, C. B., Treadwell, M. J., Hans, N. & Vichinsky, E. Detection and assessment of stroke in patients with sickle cell disease: neuropsychological functioning and magnetic resonance imaging. *Pediatr. Hematol. Oncol.* **25,** 409–21 (2008).

223. Steen, R. G. *et al.* Cognitive impairment in children with hemoglobin SS sickle cell disease: relationship to MR imaging findings and hematocrit. *AJNR. Am. J. Neuroradiol.* **24,** 382–9 (2003).

224. Schatz, J., White, D. A., Moinuddin, A., Armstrong, M. & DeBaun, M. R. Lesion burden and cognitive morbidity in children with sickle cell disease. *J. Child Neurol.* **17,** 891–5 (2002).

225. Van der Land, V. *et al.* Volume of white matter hyperintensities is an independent predictor of intelligence quotient and processing speed in children with sickle cell disease. *Br. J. Haematol.* 1–4 (2014). doi:10.1111/bjh.13179

226. Craft, S., Schatz, J., Glauser, T. a, Lee, B. & DeBaun, M. R. Neuropsychologic effects of stroke in children with sickle cell anemia. *J. Pediatr.* **123,** 712–7 (1993).

227. Schatz, J., Brown, R. T., Pascual, J. M., Hsu, L. & Debaun, M. R. Poor school performance and cognitive functioning with silent cerebral infarcts and sickle cell disease. *Neurology* **56,** 1109–1111 (2001).

228. Berg, C., Edwards, D. F. & King, A. Executive function performance on the children's kitchen task assessment with children with sickle cell disease and matched controls. *Child Neuropsychol.* **18,** 432–48 (2012).

229. White, D. A., Salorio, C. F., Schatz, J. & Debaun, M. Preliminary Study of Working Memory in Children with Stroke Related to Sickle Cell Disease. *J. Clin. Exp. Neuropsychol.* **22,** 257–264 (2000).

230. Brandling-Bennett, E. M., White, D. A., Armstrong, M. M. & Christ, S. E. Developmental Neuropsychology Patterns of Verbal Long- Term and Working Memory Performance Reveal Deficits in Strategic Processing in Children With Frontal Infarcts Related to Sickle Cell Disease. *Dev. Neuropsychol.* **24,** 423–434 (2003).

231. Hijmans, C. T., Grootenhuis, M. A., Oosterlaan, J., Peters, M. & Fijnvandraat, K. Neurocognitive Deficits in Children With Sickle Cell Disease Are Associated With the Severity of Anemia. *Pediatr. Blood Cancer* 297–302 (2011). doi:10.1002/pbc

232. Christ, S. E., Moinuddin, A., McKinstry, R. C., DeBaun, M. & White, D. a. Inhibitory control in children with frontal infarcts related to sickle cell disease. *Child Neuropsychol.* **13,** 132–41 (2007).

233. DeBaun, M. R. *et al.* Cognitive screening examinations for silent cerebral infarcts in sickle cell disease. *Neurology* **50,** 1678–82 (1998).

234. Vichinsky, E., Neumayr, L. & Gold, J. Neuropsychological dysfunction and neuroimaging abnormalities in neurologically intact adults with sickle cell anemia. *JAMA J.* **303,** 1823–1831 (2010).

235. Thompson, R. J., Gustafson, K. E., Bonner, M. J. & Ware, R. E. Neurocognitive development of young children with sickle cell disease through three years of age. *J. Pediatr. Psychol.* **27,** 235–44 (2002).

236. Schatz, J., Finke, R. & Roberts, C. W. Interactions of biomedical and environmental risk factors for cognitive development: a preliminary study of sickle cell disease. *J. Dev. Behav. Pediatr.* **25,** 303–10 (2004).

237. Kral, M. C. *et al.* Transcranial Doppler ultrasonography and neurocognitive functioning in children with sickle cell disease. *Pediatrics* **112,** 324–331 (2003).

238. Kral, M. C. & Brown, R. T. Transcranial Doppler Ultrasonography and Executive Dysfunction in Children with Sickle Cell Disease. *J. Pediatr. Psychol.* **29,** 185–195 (2004).

239. Hogan, A. M. *et al.* An exploratory study of physiological correlates of neurodevelopmental delay in infants with sickle cell anaemia. *Br. J. Haematol.* **132,** 99–107 (2006).

240. Hogan, A. M., Telfer, P. T., Kirkham, F. J. & de Haan, M. Precursors of Executive Function in Infants With Sickle Cell Anemia. *J. Child Neurol.* **10,** 1197–202 (2013).

241. Hogan, A. M., Vargha-Khadem, F., Saunders, D. E., Kirkham, F. J. & Baldeweg, T. Impact of frontal white matter lesions on performance monitoring: ERP evidence for cortical disconnection. *Brain* **129,** 2177–88 (2006).

242. Smith, S. M. *et al.* Advances in functional and structural MR image analysis and implementation as FSL. *Neuroimage* **23 Suppl 1,** S208–19 (2004).

243. Wechsler, D. *Wechsler abbreviated scale of intelligence*. (Psychological Corporation, 1999).

244. Delis, D., Kaplan, E. & Kramer, J. *Delis-Kaplan executive function system (D-KEFS)*. (Psychological Corporation, 2001).

245. Shunk, A. W., Davis, A. S. & Dean, R. S. TEST REVIEW: Dean C. Dlis, Edith Kaplan & Joel H. Kramer, Delis Kaplan Executive Function System (D-KEFS), The Psychological Corporation, San Antonio, TX, 2001. $415.00 (complete kit). *Appl. Neuropsychol.* **13,** 275–279 (2006).

246. Homack, S., Lee, D. & Riccio, C. a. Test review: Delis-Kaplan executive function system. *J. Clin. Exp. Neuropsychol.* **27,** 599–609 (2005).

247. Noll, R. B. *et al.* Neuropsychological functioning of youths with sickle cell disease: comparison with non-chronically ill peers. *J. Pediatr. Psychol.* **26,** 69–78 (2001).

248. Hijmans, C. T. *et al.* Neurocognitive deficits in children with sickle cell disease: a comprehensive profile. *Pediatr. Blood Cancer* **56,** 783–8 (2011).

249. Schatz, J. *et al.* Neuropsychologic Deficits in Children with Sickle Cell Disease and Cerebral Infarction : Role of Lesion Site and Volume Neuropsychologic Deficits in Children. *Child Neuropsychol.* **5,** 92–103 (1999).

250. Armstrong, F. D. Neurocognitive function in sickle cell disease: have we been missing something? *Expert Rev. Hematol.* **3,** 519–21 (2010).

251. King, A. *et al.* Silent Cerebral Infarction, Income and Grade Retention among Students with Sickle Cell. *Am. J. Hematol.* 2–28 (2014).

252. King, A. A. *et al.* Parent education and biologic factors influence on cognition in sickle cell anemia. *Am. J. Hematol.* **89,** 162–7 (2014).

253. Hogan, A. M., Pit-ten Cate, I. M., Vargha-Khadem, F., Prengler, M. & Kirkham, F. J. Physiological correlates of intellectual function in children with sickle cell disease: hypoxaemia, hyperaemia and brain infarction. *Dev. Sci.* **9,** 379–87 (2006).

254. Strouse, J. J. *et al.* Inverse correlation between cerebral blood flow measured by continuous arterial spin-labeling (CASL) MRI and neurocognitive function in children with sickle cell anemia (SCA). *Blood* **108,** 379–81 (2006).

255. Pollitt, E. Iron deficiency and cognitive function. *Annu. Rev. Nutr.* **13,** 521–37 (1993).

256. Otero, G. A., Aguirre, D. M., Porcayo, R. & Fernández, T. Psychological and electroencephalographic study in school children with iron deficiency. *Int. J. Neurosci.* **99,** 113–21 (1999).

257. Weiskopf, R. B. *et al.* Fresh blood and aged stored blood are equally efficacious in immediately reversing anemia-induced brain oxygenation deficits in humans. *Anesthesiology* **104,** 911–20 (2006).

258. Steen, R. G. *et al.* Ectasia of the basilar artery in children with sickle cell disease: relationship to hematocrit and psychometric measures. *J. Stroke Cerebrovasc. Dis.* **7,** 32–43 (1998).

259. Oguz, K. K. *et al.* Sickle cell disease: continuous arterial spin-labeling perfusion MR imaging in children. *Radiology* **227,** 567–74 (2003).

260. Gevers, S. *et al.* Arterial spin labeling measurement of cerebral perfusion in children with sickle cell disease. *J. Magn. Reson. Imaging* **35,** 119–787 (2011).

261. Hales, P. W., Kawadler, J. M., Aylett, S. E., Kirkham, F. J. & Clark, C. a. Arterial spin labeling characterization of cerebral perfusion during normal maturation from late childhood into adulthood: normal “reference range” values and their use in clinical studies. *J. Cereb. blood flow Metab.* 1–9 (2014). doi:10.1038/jcbfm.2014.17

262. Kirkham, F. & Datta, A. Hypoxic adaptation during development: relation to pattern of neurological presentation and cognitive disability. *Dev. Sci.* **9,** 411–427 (2006).

263. Platt, O. S., Rosenstock, W. & Espeland, M. A. Influence of sickle hemoglobinopathies on growth and development. *N. Engl. J. Med.* **311,** 7–12 (1984).

264. White, D. & DeBaun, M. Cognitive and behavioral function in children with sickle cell disease: a review and discussion of methodological issues. *J. Pediatr. Hematol. Oncol.* **20,** 458–462 (1998).

265. Kugler, S. *et al.* Abnormal Cranial Magnetic Resonance Imaging Scans in Sickle-cell Disease: Neurological Correlates and Clinical Implications. *Arch. Neurol.* **50,** 629–635 (1993).

266. Cho, E. R. *et al.* Obstructive sleep apnea as a risk factor for silent cerebral infarction. *J. Sleep Res.* **22,** 452–8 (2013).

267. Aloia, M. S., Arnedt, J. T., Davis, J. D., Riggs, R. L. & Byrd, D. Neuropsychological sequelae of obstructive sleep apnea-hypopnea syndrome: a critical review. *J. Int. Neuropsychol. Soc.* **10,** 772–85 (2004).

268. Beebe, D. W., Groesz, L., Wells, C., Nichols, A. & McGee, K. The neuropsychological effects of obstructive sleep apnea: a meta-analysis of norm-referenced and case-controlled data. *Sleep* **26,** 298–307 (2003).

269. Virués-Ortega, J. *et al.* Changing patterns of neuropsychological functioning in children living at high altitude above and below 4000 m: a report from the Bolivian Children Living at Altitude (BoCLA) study. *Dev. Sci.* **14,** 1185–93 (2011).

270. Rosen, C. L. *et al.* Obstructive Sleep Apnea Syndrome in a Sickle Cell Disease Cohort: Prevalence and Risk Factors. *Pediatrics* **in press.,** (2014).

271. Kaleyias, J., Mostofi, N. & Grant, M. Severity of obstructive sleep apnea in children with sickle cell disease. *J. Pediatr. Hematol. Oncol.* **30,** 659–665 (2008).

272. Peng, W. *et al.* [Correlation between cognitive function and hippocampal atrophy and cerebral white matter lesions in patients with obstructive sleep apnea hypopnea syndrome]. *Zhonghua Yi Xue Za Zhi* **94,** 724–8 (2014).

273. Burgess, P. W. *et al.* The case for the development and use of “ecologically valid” measures of executive function in experimental and clinical neuropsychology. *J. Int. Neuropsychol. Soc.* **12,** 194–209 (2006).

274. Boulet, S. L., Yanni, E. A., Creary, M. S. & Olney, R. S. Health status and healthcare use in a national sample of children with sickle cell disease. *Am. J. Prev. Med.* **38,** S528–35 (2010).

275. Gil, K. M. *et al.* Daily Stress and Mood and Their Association With Pain , Health-Care Use , and School Activity in Adolescents With Sickle Cell Disease. (2001).

276. Vichinsky, E., Neumayr, L. & Gold, J. Neuropsychological Dysfunction and Neuroimaging Abnormalities in Neurologically Intact Adults With Sickle Cell Anemia. *JAMA* **303,** 1823–1831 (2010).

277. Van den Tweel, X. W. *et al.* Cerebral blood flow measurement in children with sickle cell disease using continuous arterial spin labeling at 3.0-Tesla MRI. *Stroke* **40,** 795–800 (2009).

278. Zhou, D., Wang, J., Zapala, M. & Xue, J. Gene expression in mouse brain following chronic hypoxia: role of sarcospan in glial cell death. *Physiol. Genomics* 370–379 (2008). doi:10.1152/physiolgenomics.00147.2007.

279. Canessa, N. *et al.* Obstructive sleep apnea: brain structural changes and neurocognitive function before and after treatment. *Am. J. Respir. Crit. Care Med.* **183,** 1419–26 (2011).

280. Kawadler, J. M. *et al.* Subcortical and cerebellar volumetric deficits in paediatric sickle cell anaemia. *Br. J. Haematol.* **163,** 373–6 (2013).

281. Fischl, B., Liu, A. & Dale, A. M. Automated manifold surgery: constructing geometrically accurate and topologically correct models of the human cerebral cortex. *IEEE Trans. Med. Imaging* **20,** 70–80 (2001).

282. Fischl, B. *et al.* Whole brain segmentation: automated labeling of neuroanatomical structures in the human brain. *Neuron* **33,** 341–55 (2002).

283. Fischl, B. *et al.* Sequence-independent segmentation of magnetic resonance images. *Neuroimage* **23 Suppl 1,** S69–84 (2004).

284. Fischl, B. *et al.* Automatically parcellating the human cerebral cortex. *Cereb. Cortex* **14,** 11–22 (2004).

285. Jovicich, J. *et al.* Reliability in multi-site structural MRI studies: effects of gradient non-linearity correction on phantom and human data. *Neuroimage* **30,** 436–43 (2006).

286. Han, X. *et al.* Reliability of MRI-derived measurements of human cerebral cortical thickness: the effects of field strength, scanner upgrade and manufacturer. *Neuroimage* **32,** 180–94 (2006).

287. Ségonne, F. *et al.* A hybrid approach to the skull stripping problem in MRI. *Neuroimage* **22,** 1060–75 (2004).

288. Reuter, M., Rosas, H. D. & Fischl, B. Highly accurate inverse consistent registration: a robust approach. *Neuroimage* **53,** 1181–96 (2010).

289. Sled, J. G., Zijdenbos, A. P. & Evans, A. C. A nonparametric method for automatic correction of intensity nonuniformity in MRI data. *IEEE Trans. Med. Imaging* **17,** 87–97 (1998).

290. Brain Development Group. Total and regional brain volumes in a population-based normative sample from 4 to 18 years: the NIH MRI Study of Normal Brain Development. *Cereb. Cortex* **22,** 1–12 (2012).

291. Dennison, M. *et al.* Mapping subcortical brain maturation during adolescence: evidence of hemisphere- and sex-specific longitudinal changes. *Dev. Sci.* **16,** 772–91 (2013).

292. Schoonheim, M. M. *et al.* Subcortical atrophy and cognition: sex effects in multiple sclerosis. *Neurology* **79,** 1754–61 (2012).

293. Batista, S. *et al.* Basal ganglia, thalamus and neocortical atrophy predicting slowed cognitive processing in multiple sclerosis. *J. Neurol.* **259,** 139–46 (2012).

294. De Jong, L. W. *et al.* Ventral striatal volume is associated with cognitive decline in older people: a population based MR-study. *Neurobiol. Aging* **33,** 424.e1–10 (2012).

295. Singhal, a, Thomas, P., Cook, R., Wierenga, K. & Serjeant, G. Delayed adolescent growth in homozygous sickle cell disease. *Arch. Dis. Child.* **71,** 404–8 (1994).

296. Schatz, J. & Mcclellan, C. B. Sickle Cell Disease as a Neurodevelopmental Disorder. *Ment. Retard. Dev. Disabil. Res. Rev.* **12,** 200–207 (2006).

297. Bernaudin, F. *et al.* Impact of early transcranial Doppler screening and intensive therapy on cerebral vasculopathy outcome in a newborn sickle cell anemia cohort. *Blood* **117,** 1130–40; quiz 1436 (2011).

298. Giedd, J. N. *et al.* Brain development during childhood and adolescence: a longitudinal MRI study. *Nat. Neurosci.* **2,** 861–3 (1999).

299. Gogtay, N. *et al.* Dynamic mapping of human cortical development during childhood through early adulthood. **101,** (2004).

300. Wonderlick, J. S. *et al.* Reliability of MRI-derived cortical and subcortical morphometric measures: effects of pulse sequence, voxel geometry, and parallel imaging. *Neuroimage* **44,** 1324–33 (2009).

301. Zafeiriou, D. I. *et al.* Central Nervous System Abnormalities in Asymptomatic Young Patients with SB-Thalassemia. *Ann. Neurol.* **1,** 835–839 (2004).

302. Smith, S. M. *et al.* Accurate, robust, and automated longitudinal and cross-sectional brain change analysis. *Neuroimage* **17,** 479–89 (2002).

303. De Stefano, N. *et al.* Assessing brain atrophy rates in a large population of untreated multiple sclerosis subtypes. *Neurology* **74,** 1868–76 (2010).

304. Peters, N. *et al.* Brain volume changes in CADASIL: A serial MRI study in pure subcortical ischemic subcortical ischemic vascular disease. *Neurology* **66,** 1517–1522 (2006).

305. Nitkunan, A., Lanfranconi, S., Charlton, R. A., Barrick, T. R. & Markus, H. S. Brain Atrophy and Cerebral Small Vessel Disease A Prospective Follow-Up Study. *Stroke* **42,** 133–138 (2011).

306. Trivedi, M. A. *et al.* Longitudinal changes in global brain volume between 79 and 409 days after traumatic brain injury: relationship with duration of coma. *J Neurotrauma* **24,** 766–771 (2007).

307. Sidaros, A. *et al.* Long-term global and regional brain volume changes following severe traumatic brain injury: a longitudinal study with clinical correlates. *Neuroimage* **44,** 1–8 (2009).

308. Enzinger, C. *et al.* Risk factors for progression of brain atrophy in aging: six-year follow-up of normal subjects. *Neurology* **64,** 1704–11 (2005).

309. Takao, H., Hayashi, N. & Ohtomo, K. A longitudinal study of brain volume changes in normal aging. *Eur. J. Radiol.* **81,** 2801–4 (2012).

310. Battaglini, M., Smith, S. M., Brogi, S. & Stefano, N. De. Enhanced brain extraction improves the accuracy of brain atrophy estimation. *Neuroimage* **40,** 583–589 (2008).

311. Takao, H., Hayashi, N. & Ohtomo, K. Effect of Scanner in Longitudinal Studies of Brain Volume Changes. *J. Magn. Reson. Imaging* **34,** 438–444 (2011).

312. Prengler, M., Pavlakis, S. G., Prohovnik, I. & Adams, R. J. Sickle cell disease: the neurological complications. *Ann. Neurol.* **51,** 543–52 (2002).

313. Quinn, C. T. & Sargent, J. W. Daytime steady-state haemoglobin desaturation is a risk factor for overt stroke in children with sickle cell anaemia. *Br. J. Haematol.* **140,** 336–9 (2008).

314. Safo, M. K. & Kato, G. J. Therapeutic Strategies to Alter the Oxygen Affinity of Sickle Hemoglobin. *Hematol. Oncol. Clin. North Am.* **28,** 217–231 (2014).

315. Setty, B., Stuart, M., Dampier, C., Brodecki, D. & Allen, J. Hypoxaemia in sickle cell disease: biomarker modulation and relevance to pathophysiology. *Lancet* **362,** 1450–1455 (2003).

316. Halbower, A. C. & Mahone, E. M. Neuropsychological morbidity linked to childhood sleep-disordered breathing. *Sleep Med. Rev.* **10,** 97–107 (2006).

317. Halbower, A. C. *et al.* Childhood obstructive sleep apnea associates with neuropsychological deficits and neuronal brain injury. *PLoS Med.* **3,** e301 (2006).

318. Feng, J., Wu, Q., Zhang, D. & Chen, B. Hippocampal impairments are associated with intermittent hypoxia of obstructive sleep apnea. *Chin. Med. J. (Engl).* **125,** 696–701 (2012).

319. Xie, H. & Yung, W. Chronic intermittent hypoxia-induced deficits in synaptic plasticity and neurocognitive functions: a role for brain-derived neurotrophic factor. *Acta Pharmacol. Sin.* **33,** 5–10 (2012).

320. Clayden, J. D. *et al.* TractoR : Magnetic Resonance Imaging and Tractography with R. *J. Stat. Softw.* **44,** (2011).

321. Smith, S. M. Fast robust automated brain extraction. *Hum. Brain Mapp.* **17,** 143–55 (2002).

322. Gallichan, D. *et al.* Addressing a systematic vibration artifact in diffusion-weighted MRI. *Hum. Brain Mapp.* **31,** 193–202 (2010).

323. Cox, S. E., Makani, J., Newton, C. R., Prentice, A. M. & Kirkham, F. J. Hematological and Genetic Predictors of Daytime Hemoglobin Saturation in Tanzanian Children with and without Sickle Cell Anemia. *ISRN Hematol.* **2013,** 472909 (2013).

324. Takahashi, M. *et al.* Magnetic resonance microimaging of intraaxonal water diffusion in live excised lamprey spinal cord. *Proc. Natl. Acad. Sci. U. S. A.* **99,** 16192–6 (2002).

325. Song, S.-K. *et al.* Diffusion tensor imaging detects and differentiates axon and myelin degeneration in mouse optic nerve after retinal ischemia. *Neuroimage* **20,** 1714–22 (2003).

326. Davies, E. H., Seunarine, K. K., Banks, T., Clark, C. a & Vellodi, A. Brain white matter abnormalities in paediatric Gaucher Type I and Type III using diffusion tensor imaging. *J. Inherit. Metab. Dis.* **34,** 549–53 (2011).

327. Shukla, D. K., Keehn, B. & Müller, R.-A. Tract-specific analyses of diffusion tensor imaging show widespread white matter compromise in autism spectrum disorder. *J. Child Psychol. Psychiatry.* **52,** 286–95 (2011).

328. LeWinn, K. Z. *et al.* White matter correlates of adolescent depression: structural evidence for frontolimbic disconnectivity. *J. Am. Acad. Child Adolesc. Psychiatry* **53,** 899–909, 909.e1–7 (2014).

329. Quinn, C. & Dowling, M. Cerebral tissue hemoglobin saturation in children with sickle cell disease. *Pediatr. Blood Cancer* 881–887 (2012). doi:10.1002/pbc

330. Homi, J., Levee, L., Higgs, D., Thomas, P. & Serjeant, G. Pulse oximetry in a cohort study of sickle cell disease. *Clin. Lab. Haematol.* **19,** 17–22 (1997).

331. Mackin, R. S. *et al.* Neuroimaging abnormalities in adults with sickle cell anemia: Associations with cognition. *Neurology* **82,** 835–41 (2014).

332. Zhang, H. *et al.* Compromised white matter microstructural integrity after mountain climbing: evidence from diffusion tensor imaging. *High Alt. Med. Biol.* **13,** 118–25 (2012).

333. Wheeler-Kingshott, C. a M. & Cercignani, M. About “axial” and “radial” diffusivities. *Magn. Reson. Med.* **61,** 1255–60 (2009).

334. Tournier, J.-D., Calamante, F., Gadian, D. G. & Connelly, A. Direct estimation of the fiber orientation density function from diffusion-weighted MRI data using spherical deconvolution. *Neuroimage* **23,** 1176–85 (2004).

335. Zhang, H., Schneider, T., Wheeler-Kingshott, C. A. & Alexander, D. C. NODDI: practical in vivo neurite orientation dispersion and density imaging of the human brain. *Neuroimage* **61,** 1000–16 (2012).

336. Tzika, A. A. *et al.* Cerebral perfusion in children: detection with dynamic contrast-enhanced T2*-weighted MR images. *Radiology* **187,** 449–58 (1993).

337. Reed, W., Jagust, W., Al-Mateen, M. & Vichinsky, E. Role of positron emission tomography in determining the extent of CNS ischemia in patients with sickle cell disease. *Am. J. Hematol.* **60,** 268–72 (1999).

338. Al-Kandari, F. a *et al.* Regional cerebral blood flow in patients with sickle cell disease: study with single photon emission computed tomography. *Ann. Nucl. Med.* **21,** 439–45 (2007).

339. D'Esposito, M., Deouell, L. Y. & Gazzaley, A. Alterations in the BOLD fMRI signal with ageing and disease: a challenge for neuroimaging. *Nat. Rev. Neurosci.* **4,** 863–72 (2003).

340. Zou, P. *et al.* Hemodynamic responses to visual stimulation in children with sickle cell anemia. *Brain Imaging Behav.* **5,** 295–306 (2011).

341. Moore, C. I. & Cao, R. The hemo-neural hypothesis: on the role of blood flow in information processing. *J. Neurophysiol.* **99,** 2035–47 (2008).